

HELERIN MARGUS

Characterization of
cell-penetrating peptide/nucleic acid
nanocomplexes and their
cell-entry mechanisms



HELERIN MARGUS

Characterization of
cell-penetrating peptide/nucleic acid
nanocomplexes and their
cell-entry mechanisms



Department of Developmental Biology, Institute of Molecular and Cell Biology,
University of Tartu, Estonia

Dissertation is accepted for commencement of the degree of Doctor of Philosophy in Cell Biology on April 25th, 2016 by the Council of the Institute of Molecular and Cell Biology, University of Tartu

Supervisors: Prof. Margus Pooga, Ph.D
Department of Developmental Biology
Institute of Molecular and Cell Biology
University of Tartu
23 Riia Street, Tartu, Estonia

Dr. Kärt Padari, Ph.D
Department of Developmental Biology
Institute of Molecular and Cell Biology
University of Tartu
23 Riia Street, Tartu, Estonia

Opponent: Prof. Ines Neundorf, Ph.D
Department of Chemistry
Institute of Biochemistry
University of Cologne
Zuelpicher Street 47, Cologne, Germany

Commencement: Room No 105, 23B Riia Street, Tartu, Estonia, at 10:15 on
June 15th, 2016

Publication of this dissertation is granted by the University of Tartu, Estonia

ISSN 1024-6479
ISBN 978-9949-77-104-2 (print)
ISBN 978-9949-77-105-9 (pdf)

Copyright: Helerin Margus, 2016

University of Tartu Press
www.tyk.ee

TABLE OF CONTENTS

| | |
|---|----|
| LIST OF ORIGINAL PUBLICATIONS | 7 |
| ABBREVIATIONS | 8 |
| INTRODUCTION | 10 |
| 1. LITERATURE OVERVIEW | 11 |
| 1.1. Cell-penetrating peptides (CPPs) | 11 |
| 1.1.1. Classification of CPPs | 11 |
| 1.1.2. Coupling of cargo to CPP | 12 |
| 1.2. Cellular delivery of nucleic acids by CPPs using non-covalent strategy | 13 |
| 1.2.1. Plasmid DNA (pDNA) | 13 |
| 1.2.2. Splicing switching oligonucleotides (SSOs) | 15 |
| 1.2.3. Short interfering RNA (siRNA) | 17 |
| 1.2.4. Antisense oligonucleotides (ASOs) | 19 |
| 1.3. Characterization of CPP/nucleic acid nanocomplexes and their cell-surface association | 20 |
| 1.3.1. Characterization of nanocomplexes | 20 |
| 1.3.2. Cell-surface interactions of CPP/nucleic acid nanocomplexes | 22 |
| 1.4. Cell entry mechanisms and intracellular trafficking of CPP/nucleic acid nanocomplexes | 23 |
| 1.4.1. Endocytosis | 23 |
| 1.4.1.1. Clathrin-mediated endocytosis | 24 |
| 1.4.1.2. Caveolin-mediated endocytosis | 25 |
| 1.4.1.3. Macropinocytosis | 27 |
| 1.4.1.4. Other endocytic pathways | 28 |
| 1.4.2. Direct translocation | 30 |
| 1.4.3. Intracellular trafficking | 31 |
| 1.4.4. Endosomal release of CPP/nucleic acid nanocomplexes | 32 |
| 2. AIMS OF THE STUDY | 35 |
| 3. METHODOLOGICAL CONSIDERATIONS | 36 |
| 3.1. Cell lines | 36 |
| 3.2. CPPs | 36 |
| 3.3. CPPs and their complexes with nucleic acids | 38 |
| 3.4. Characterization of CPP/nucleic acid nanocomplexes | 38 |
| 3.4.1. Dynamic light scattering (DLS) | 38 |
| 3.4.2. Transmission electron microscopy (TEM) | 39 |
| 3.5. Cellular uptake and intracellular trafficking of CPP/nucleic acid nanocomplexes | 40 |
| 3.5.1. Confocal laser scanning microscopy (CLSM) | 40 |
| 3.5.2. TEM | 40 |
| 4. RESULTS | 42 |

| | |
|---|-----|
| 4.1. Cell-entry mechanisms and intracellular trafficking of PepFect14/pDNA NPs (Paper I) | 42 |
| 4.1.1. PF14 forms stable NPs with pDNA..... | 42 |
| 4.1.2. PF14/pDNA NPs internalize to cells via caveolin-mediated endocytosis and macropinocytosis | 43 |
| 4.1.3. Scavenger receptors are involved in the cellular uptake of PF14/pDNA nanocomplexes | 45 |
| 4.2. NickFect 51 mediates the cellular uptake of SSO using endocytosis (Paper II) | 46 |
| 4.2.1. NFs form nanoparticles with nucleic acids | 46 |
| 4.2.2. NF51 efficiently delivers different types of nucleic acids into cells | 46 |
| 4.2.3. NF51/SSO NPs are released from endosomes | 47 |
| 4.3. NickFects deliver nucleic acids into cells using different endocytic mechanisms (Paper III) | 48 |
| 4.3.1. Characterization of NF/pDNA NPs | 48 |
| 4.3.2. Cell-entry mechanisms of NF/pDNA NPs | 49 |
| 4.3.3. Intracellular trafficking of NF/pDNA NPs | 50 |
| 4.3.4. Scavenger receptors are involved in the uptake of NF/pDNA NPs | 51 |
| 4.4. Characteristics of Cell-Penetrating Peptide/Nucleic Acid Nanoparticles (Paper IV)..... | 51 |
| 4.4.1. CPPs pack pDNA to nanoparticles which have similar size and morphology | 52 |
| 4.4.2. CPPs form smaller nanoparticles with SSO and siRNA compared to pDNA | 52 |
| 4.4.3. Dynamic light scattering overestimates the size of CPP/nucleic acid NPs | 53 |
| 4.4.4. The fluorescent or (nano)-gold label on nucleic acid does not affect the gross-characteristics of CPP/nucleic acid nanoparticles | 54 |
| 5. DISCUSSION | 56 |
| SUMMARY | 64 |
| SUMMARY IN ESTONIAN | 66 |
| REFERENCES | 70 |
| ACKNOWLEDGMENTS | 86 |
| PUBLICATIONS | 87 |
| CURRICULUM VITAE | 155 |
| ELULOOKIRJELDUS | 157 |

LIST OF ORIGINAL PUBLICATIONS

The current thesis is based on the following original publications, which will be referred in the text by their Roman numerals.

- I Veiman, K.-L., Mäger, I., Ezzat, K., **Margus, H.**, Lehto, T., Langel, K., Kurrikoff, K., Arukuusk, P., Suhorutšenko, J., Padari, K., Pooga, M., Lehto, T., Langel, Ü. (2012) PepFect14 peptide vector for efficient gene delivery in cell cultures. *Molecular Pharmaceutics* 10: 199–210.
- II Arukuusk, P., Pärnaste, L., Oskolkov, N., Copolovici, D.-M., **Margus, H.**, Padari, K., Möll, K., Maslovskaja, J., Tegova, R., Kivi, G., Tover, A., Pooga, M., Ustav, M., Langel, Ü. (2013) New generation of efficient peptide-based vectors, NickFects, for the delivery of nucleic acids. *Biochimica et. Biophysica Acta* 1828: 1365–73.
- III Arukuusk, P., Pärnaste, L., **Margus, H.**, Eriksson, N.K.J., Vasconcelos, L., Padari, K., Pooga, M., Langel, Ü. (2013) Differential endosomal pathways for radically modified peptide vectors. *Bioconjugate chemistry* 24: 1721–32.
- IV **Margus, H.**, Arukuusk, P., Langel, Ü., Pooga, M. (2015) Characteristics of cell-penetrating peptide/nucleic acid nanoparticles. *Molecular Pharmaceutics* 13(1): 172–9

The articles listed above have been reprinted with the permission of the copyright owners.

My contribution to the articles referred to in this study is following:

- Paper I Designed and performed electron microscopy experiments, participated in data analysis and writing the manuscript.
- Paper II Designed and performed electron microscopy experiments, participated in data analysis and writing the manuscript.
- Paper III Designed and performed fluorescence microscopy and electron microscopy experiments, participated in data analysis and writing the manuscript.
- Paper IV Conceived and designed the study, performed all experiments except peptide synthesis, analysed the data and wrote the manuscript.

ABBREVIATIONS

| | |
|--------------------------|--|
| AP2 | adaptor protein 2 |
| Arf | adenosine diphosphate-ribosylation factor |
| ASO | antisense oligonucleotide |
| CAM | cell-adhesion molecule |
| CCP | clathrin-coated pit |
| CCV | clathrin coated vesicle |
| Cdc 42 | cell division cycle protein 42 |
| CLIC | clathrin independent carrier |
| CLSM | confocal laser scanning microscopy |
| CME | clathrin-mediated endocytosis |
| CPP | cell-penetrating peptide |
| EGF | epidermal growth factor |
| EGFR | epidermal growth factor receptor |
| EtBr | ethidium bromide |
| GEEC | glycophosphatidylinositol-anchored protein-enriched early endosome |
| GPI | glycosylphosphatidylinositol |
| LF2000 | LipoFectamine 2000 TM |
| MEF | mouse embryonic fibroblast |
| miRNA | micro RNA |
| MR | molar ratio |
| NF | NickFect |
| NG | Nanogold TM |
| NLS | nuclear localization signal |
| NP | nanoparticle |
| ns-PF14 | non-stearylated PF14 |
| ns-TP10 | non-stearylated TP10 |
| Pak1 | p21-activated kinase 1 |
| PdIns(4,5)P ₂ | phosphatidylinositol-4,5-bisphosphate |
| pDNA | plasmid DNA |
| PEG | polyethylene glycol |
| PF | PepFect |
| Poly C | polycytidylic acid |
| Poly I | polyinosinic acid |
| RTK | Receptor tyrosine kinase |
| RT-PCR | real-time PCR |
| RVG | rabies virus glycoprotein |
| SA-NG | streptavidin-Nanogold TM |
| SCARA | scavenger receptor class A |
| siRNA | short interfering RNA |
| SNA | spherical nucleic acid |
| SSO | splice switching oligonucleotide |

| | |
|---------|---|
| SSO-NG | splice-switching oligonucleotide-Nanogold TM |
| st-TP10 | stearylated TP10 |
| Tat | transcription activating protein |
| TEM | transmission electron microscopy |
| TP | transportan |
| TP-10 | transportan 10 |
| VEGF | vascular endothelial growth factor |

INTRODUCTION

Nucleic acids such as plasmid DNA, splice correction oligonucleotides, short interfering RNA and antisense oligonucleotides are highly promising candidates for the treatment of genetic disorders. To achieve biological functionality, nucleic acids need to be internalized by cells and reach their action site in cytoplasm or nucleus. However, due to the large size and negative charge, naked nucleic acids are not capable of traversing the plasma membrane of cells. A wide variety of delivery vectors have been designed to facilitate the cellular uptake of nucleic acids. One class of such vectors are cell-penetrating peptides (CPPs), short sequences of 5–40 amino acid residues, which are capable of gaining access to the interior of cells, and importantly, mediate the internalization of coupled cargo molecules.

CPPs can be coupled to nucleic acids via a covalent bond or by complex formation, i.e. simple co-incubation of peptide and cargo. In case of co-incubation or non-covalent strategy CPPs associate with nucleic acids through electrostatic and hydrophobic interactions. This strategy is simpler, less money- and time-consuming than covalent conjugation. Moreover, co-incubation of CPPs and nucleic acids requires lower concentration of peptide and cargo to trigger bioactivity compared to covalent conjugation. In addition, for certain types of nucleic acids such as plasmid DNA and miRNA only non-covalent coupling can be employed for transfection by CPPs. One of the major weaknesses of the co-incubation strategy is the complicated physicochemical characterization of the forming nanocomplexes. However, in order to be considered for implementation in biomedicine the properties of CPP/nucleic acid complexes such as size, morphology and charge need to be characterized in detail. Another bottleneck which impedes the implementation of non-covalent strategy for nucleic acid delivery is the poor knowledge of the cellular uptake mechanisms and intracellular trafficking of the CPP/nucleic acid nanocomplexes. However, detailed characterization of the cell internalization pathways and cellular trafficking of CPP/cargo complexes are essential to avoid undesired side effects and to refine their properties to yield higher activities of delivered cargo.

The main objectives of the current thesis were to characterize the physicochemical properties of CPP/nucleic acid nanocomplexes, and to examine their cellular uptake mechanisms and intracellular trafficking. All studied peptides are analogues of transportan-10, which have been specifically developed for the cellular delivery of nucleic acids.

1. LITERATURE OVERVIEW

1.1. Cell-penetrating peptides (CPPs)

Cell-penetrating peptides (CPPs) are a large class of short (5–40 amino acid residues) cationic and/or amphipathic peptides which are capable of gaining access to the interior of cells and, importantly, facilitating the cellular internalization of various covalently or non-covalently coupled cargos (Langel 2011) such as small molecules, fluorophores, proteins, peptides, plasmid DNA (pDNA), oligonucleotides (ONs), nanoparticles and liposomes (reviewed in Ramsey and Flynn 2015). CPPs are highly promising candidates for drug delivery applications due to low cytotoxicity and minimal risk of triggering immune response.

The capacity of certain proteins to overcome plasma membrane barrier was discovered more than 25 years ago when transcription-transactivating (Tat) protein of HIV-1 was shown to bypass the plasma membrane and translocate into the nuclei of cells (Frankel and Pabo 1988). Soon after, the cellular uptake of *Drosophila* Antennapedia homeodomain was reported (Joliot et al. 1991), and a few years later the domains being responsible for the cellular internalization of the two named proteins were identified (Derossi et al. 1994, Vives et al. 1997).

To date, there are more than 1800 CPPs and their chemically modified analogues characterized according to CPPsite 2.0, and the number is still increasing (Agrawal et al. 2016). Although different in their origin and primary structure, CPPs have several common properties. For example, CPPs are typically linear and possess a positive net charge at physiological pH.

1.1.1. Classification of CPPs

There is no uniform system developed for the classification of CPPs. Most commonly, CPPs are divided by their origin into protein derived, chimeric or synthetic peptides. However, this classification does not provide information about their chemical and physical properties. Alternatively, CPPs can be classified into primary amphipathic, secondary amphipathic and non-amphipathic CPPs. This classification is based on the membrane interaction properties of CPPs with model cell membranes, which differ in lipid affinities, structural conformations during membrane binding, and internalization efficacies (reviewed in Ziegler 2008).

Primary amphipathic CPPs contain sequential cationic and hydrophobic regions in their primary structure. Typically, primary amphipathic CPPs are composed of more than 20 amino acid residues, enough to reach the hydrophobic core of the lipid bilayer of the plasma membrane (Wimley 1994). Primary amphipathic peptides strongly associate with both neutral and anionic membrane lipids (Magzoub et al. 2001, Deshayes et al. 2004), mainly through hydrophobic interactions (Magzoub et al. 2001). The presence of anionic lipids in membrane does not affect the membrane affinity of these peptides (Barany-Wallje et al. 2007, Yandek et al. 2007) and several primary amphipathic pep-

tides such as transportan (TP) and MPG can be internalized by cells at sub-micromolar concentrations (Barany-Wallje et al. 2007). Other well-known peptides belonging to this group are Pep-1 (Morris et al. 2001) and transportan 10 (TP10) analogues PepFects (PFs) and NickFects (NFs) (El-Andaloussi et al. 2011, Ezzat et al. 2011, Oskolkov et al. 2011).

Secondary amphipathic peptides contain alternately hydrophobic and cationic amino acid residues and gain amphipathicity through association with membrane lipids and glycosaminoglycans, resulting the separation of uncharged amino acid residues from charged ones, and acquisition of alpha-helix (Dathe et al. 1996, Lamaziere et al. 2007, Crombez et al. 2009) or beta-sheet (Oehlke et al. 1997) conformation. Secondary amphipathic CPPs have low affinity to electrically neutral membranes, but the affinity increases significantly in the presence of anionic lipids in the plasma membrane (Dathe et al. 1996, Magzoub et al. 2001). Some of the well-known secondary amphipathic CPPs are penetratin (Derossi et al. 1994), CADY (Crombez et al. 2009) and MAP (KLAL) (Oehlke et al. 1998).

Non-amphipathic CPPs are typically shorter than amphipathic CPPs and are composed of mainly cationic amino acids. Non-amphipathic CPPs associate only with membranes which have high excess of anionic lipids (Magzoub et al. 2001) and in line with secondary amphipathic CPPs, these are not able to internalize into cells at low (sub-micromolar) concentrations (Ziegler et al. 2003, Tiriveedhi and Butko 2007). The most well-known non-amphipathic CPPs are Tat peptide and oligoarginines. The efficacy of arginine-rich CPPs comes from the guanidine group of arginine which forms hydrogen bonds with anionic membrane lipids (Mitchell et al. 2000).

1.1.2. Coupling of cargo to CPP

In principle, two distinct approaches can be employed for coupling CPPs to molecules to be delivered into cells – covalent and non-covalent strategy. In case of covalent conjugation, CPP is attached to the cargo by formation of covalent (often disulfide) bond. Disulfide bond is dissociated in the reducing environment of cytoplasm, thereby releasing the cargo (Muratovska and Eccles 2004). This approach leads to the formation of well-defined CPP-cargo conjugates. In case of non-covalent strategy, the association of CPP to cargo occurs mainly through electrostatic and hydrophobic interactions. The non-covalent strategy has numerous advantages over covalent conjugation. Firstly, co-incubation is simpler and less time- and money-consuming than covalent coupling. Secondly, since lower CPP and cargo concentrations are needed for yielding high bioactivity of cargo, non-covalent coupling could less probably lead to undesired side effects. Moreover, for some bioactive molecules (e.g. pDNA), only co-incubation can be used for coupling the cargo to CPP. Nevertheless, there are obstacles that impede the implementation of non-covalent strategy in biomedicine. One of the biggest challenges is the complicated characterization of the forming CPP/cargo nanocomplexes/nanoparticles (NPs). Yet, for implementation in biomedicine, the

production of NPs of defined properties, precise dimensions, and high mono-dispersity need to be ensured.

1.2. Cellular delivery of nucleic acids by CPPs using non-covalent strategy

1.2.1. Plasmid DNA (pDNA)

The delivery of recombinant plasmid DNA (pDNA) which contains a therapeutic gene is the most comprehensively examined approach for gene regulation. Fermentation of bacterial cultures enables the production of pDNA in large quantities. More importantly, the transfection of cells with recombinant plasmid enables high and long-term expression of properly folded and post-translationally modified proteins.

For the expression of therapeutic genes from pDNA the cellular uptake, endosomal release, dissociation from the carrier molecule, and translocation into the nuclei of cells need to be ensured. pDNA can only be coupled to CPP via co-incubation strategy. There are numerous reports of efficient delivery of pDNA (Table 1) or pDNA-loaded nanoparticles (Huang et al. 2007) by CPPs, yielding high levels of gene expression in cells and/or in animals. In 1999, Morris *et al.* provided the first data of efficient cellular delivery of pDNA by CPPs (Morris et al. 2001). In these experiments primary amphipathic MPG peptide which contains a nuclear localization signal (NLS) in its primary sequence mediated the internalization of pDNA into various cell-lines including HS-68 and NIH 3T3 fibroblasts, C2C12 myoblasts, HeLa and Cos-7 cells, and importantly, yielded high expression levels of delivered gene without decreasing the viability of cells even at 10 μ M peptide concentration.

Table 1. Examples of CPP-mediated plasmid DNA delivery using co-incubation strategy.

| CPP/delivery system | Cells/tissue | Reference |
|---------------------------------|--|---------------------|
| Primary amphipathic CPPs | | |
| MPG | HS-68 and NIH 3T3 fibroblasts, C2C12 myoblasts, COS-7 cells, human CEM-SS lymphoblasts | Morris et al. 1999 |
| MPG | Human fibroblasts HS-68, HeLa | Simeoni et al. 2003 |
| Pep-3 | HeLa, HUVEC, Jurkat T, PC3, MCF-7, athymic nude mice | Morris et al. 2007 |
| PF14 | CHO, HEK293, U87, U2OS, MEF, THP-1 | Paper I |
| NF51, NF1 | HeLa | Paper III |

| CPP/delivery system | Cells/tissue | Reference |
|---|--|------------------------|
| Arginine-rich CPPs | | |
| Stearyl-R8, Stearyl-Tat, Stearyl-FHV | Cos-7 | Futaki et al. 2001 |
| Branched Tat peptide (8Tat) | Cos-1, PC-3, 9L, 3T3, murine cardiac endothelial cells | Tung et al. 2002 |
| Tat ⁴⁸⁻⁶⁰ (C-terminal cysteinamide) | CHO-K1, pgsA-745, pgsB-618, human embryonic lung fibroblasts (HFL-1) | Sandgren et al. 2002 |
| Tat ⁴⁷⁻⁵⁷ | Human hepatoma cells HepG2, CHO1, buffalo green monkey cells | Ignatovich et al. 2003 |
| Tat ₂₋₄ complexed with DNA followed by addition of cationic polymer (e.g. PEI) | Human bronchoepithelial cells 16HBE14o ⁺ , Cos-7 | Rudolph et al. 2003 |
| MEND-Stearyl-R8 | NIH3T3 | Kogure et al. 2004 |
| Stearyl-R8 | NIH3T3 | Khalil et al. 2004 |
| Tat-PEG-PEI | Mouse lungs | Kleemann et al. 2005 |
| (RxR) ₄ , Stearyl-(RxR) ₄ | CHO, HEK | Lehto et al. 2010 |

Several arginine-rich CPPs such as Tat peptide and oligoarginines have been employed for the delivery of pDNA into cells. Futaki *et al.* demonstrated that stearylation of oligoarginines, Tat and FHV peptide induces high expression of delivered luciferase encoding pDNA in Cos-7 cells (Futaki et al. 2001). The obtained expression level was similar to that of commercial transfection reagent LipofectamineTM 2000 (LF2000). Efficient transfection of cells by modified (e.g. branched) or cationic polymer-conjugated Tat peptide complexed with pDNA has been later reported in several studies (Sandgren et al. 2002, Tung et al. 2002, Ignatovich et al. 2003, Rudolph et al. 2003, Kleemann et al. 2005). However, in contrary to promising *in vitro* experiments, Ignatovich *et al.* found that Tat⁴⁷⁻⁵⁷/pDNA complexes induced significantly lower gene expression level of transferred gene after systemic administration of mice compared to the injection of naked pDNA (Ignatovich et al. 2003). The low gene expression level was probably caused by the inactivation of pDNA/Tat complexes in blood-stream due to interactions with serum albumin. Kleemann *et al.* used PEGylated (PEG) Tat peptide conjugated to polyethyleneimine (PEI) (Tat-PEG-PEI) to deliver pDNA into human lung epithelial cell line A549 and lungs of C57BL/6 mice (Kleemann et al. 2005). Interestingly, Tat-PEG-PEI mediated pDNA delivery led to significantly lower gene expression levels in A549 cells compared to PEI-mediated pDNA. The lower level of gene expression was probably obtained due to aggregation of PEI/pDNA complexes in presence of sodium chloride which sedimented on the surface of cells, and in turn, increased the cellular uptake of complexes. Tat-PEG-PEI forms smaller and more stable

complexes with pDNA which do not aggregate, and thus, reach the bottom of the well plates, resulting in lower cellular uptake and lower gene expression compared to PEI-pDNA (Kleemann et al. 2005). The *in vivo* experiments, however, proved the opposite, and intratracheal instillation of Tat-PEG-PEI/pDNA complexes led to more than 600% higher transfection efficiency in mice lungs compared to PEI or Tat/PEI. Tat-PEG-PEI/pDNA complexes were detected in epithelial cells of the bronchi and alveoli of mice. Thus, covalent coupling of Tat to PEI via PEG is advantageous in gene delivery applications into lung epithelial cells of living mice (Kleemann et al. 2005).

1.2.2. Splicing switching oligonucleotides (SSOs)

In eukaryotes, pre-mRNA splicing is an important gene regulation mechanism. More than 90% of human protein-coding genes undergo alternative splicing, a process in which particular exons can be either included into or excluded from the final mature mRNA (Pan et al. 2008, Wang et al. 2008). Alternative splicing tremendously increases the biodiversity of transcriptome which in turn enables the synthesis of wide variety of protein isoforms from a single gene. Disruptions of alternative splicing can lead to disease. According to Human Gene Mutation Database about 10% of all mutations causing human inherited diseases are caused by single-base pair substitutions in splice-sites (Stenson et al. 2014). Importantly, the modulation of pre-mRNA towards correct aberrant splicing can be achieved by the intracellular delivery of short antisense oligonucleotides, termed splice switching oligonucleotides (SSOs).

In 1998, Kang and Kole introduced HeLa pLuc 705 cell-line to enable quantitative evaluation of efficacies of transfection reagents developed for the delivery of SSOs (Kang et al. 1998). HeLa pLuc 705 cells are stably transfected with a recombinant plasmid which contains luciferase-coding gene interrupted by a mutated intron 2 of β -globin gene. The mutant intron of β -globin causes aberrant splicing of luciferase pre-mRNA which results the synthesis of non-functional luciferase. Luciferase activity can be restored using SSOs which bind to the aberrant splicing site.

Most of the studies using CPPs for the cellular delivery of SSOs have employed HeLa pLuc 705 cells (Table 2). The first report of efficient delivery of SSO/CPP complexes was published by Ülo Langels group in 2009 (Mäe et al. 2009). In this study SSO delivery into cells by TP10, stearyl-TP10 (st-TP10), nona-arginine and penetratin was examined. Despite effective intracellular delivery of SSOs by TP10 and penetratin the observed splice correction activity was only slightly higher compared to the activity of naked SSO. Using st-TP10 the splice correction activity increased by approximately a factor thirty. Similar luciferase expression level was achieved using LF2000. However, co-incubation of st-TP10 with endosomotropic agent chloroquine led to even higher splice correction activity than that of LF2000. Stearylation did not have significant impact on the splice correction activity of nona-arginine or penetratin (Mäe et

al. 2009), although stearyl-oligoarginines have been earlier shown as efficient transfection reagents (Futaki et al. 2001, Tönges et al. 2006).

Table 2. Examples of CPP-mediated SSO delivery.

| CPP/delivery system | Cells/tissues | Reference |
|--|-----------------------------------|----------------------|
| <i>Non-covalent strategy</i> | | |
| St-TP10 | HeLa pLuc 705 | Mäe et al. 2009 |
| St-(RxR) ₄ | HeLa pLuc 705 | Lehto et al. 2010 |
| S4 ₁₃ -PV complexed with cationic liposomes | HeLa pLuc 705 | Trabulo et al. 2010 |
| PF14 | HeLa pLuc 705, mouse mdx myotubes | Ezzat et al. 2011 |
| NF1, NF2 | HeLa pLuc 705 | Oskolkov et al. 2011 |
| NF51 | HeLa pLuc 705 | Paper III |
| <i>Covalent strategy</i> | | |
| R ₆ -penetratin | HeLa pLuc 705 | Abes et al. 2007 |
| Pip5c, 6a-h | Mdx mouse myotubes, mdx mice | Betts et al. 2012 |

Recently, chemically modified st-TP10 analogues, PepFects (PFs) and NickFects (NFs) were designed to enhance the cellular uptake and endosomal release of nucleic acids (El-Andaloussi et al. 2011, Ezzat et al. 2011, Oskolkov et al. 2011). NickFect 1 (NF1) and NickFect 2 (NF2) were modified by the addition of phosphoryl group to the primary sequence of the CPPs. It was hypothesized that phosphoryl group could on one hand induce better endosomal release due to pH-responsiveness, and on the other, change the properties of the NF/SSO nanocomplexes which could enhance the dissociation of the cargo from CPP in cytoplasm of cells. Indeed, phosphorylation significantly increased the splice correction efficacy. Remarkably, NF1 and NF2 were at least 3 times more efficient compared to LF2000. Moreover, the addition of chloroquine increased the splice correction activity only about 20–30% (Oskolkov et al. 2011). Another st-TP10 analogue PepFect14 (PF14), which has ornithines and leucines instead of lysines and isoleucines in the primary structure, is also an efficient delivery vector for SSOs (Ezzat et al. 2011). PF14-mediated SSO delivery yielded >85% of splice correction in HeLa pLuc 705 cells after 24 h of transfection as evaluated by the measurement of corrected mRNA levels after conducting RT-PCR analysis. The splice correction activity was also measured in H2K mdx mouse myotubes which is a commonly used cell-model for the examination of drug candidates and drug delivery systems for the treatment of Duchenne muscular dystrophy. H2K mdx mouse myotubes carry a point mutation in exon 23 of the dystrophin gene which results the synthesis of non-functional protein. Importantly, PF14/SSO nanocomplexes yielded high level of splicing correction in both serum-free and serum-containing tissue culture medium.

The cellular delivery of SSOs by CPPs using noncovalent strategy has been seldom applied for splicing redirection, and vast majority of studies have focused on the application of CPP-SSO covalent conjugates. The groups of M.J. Gait and B. Lebleu have made a strong contribution to the field by developing a series of R₆-penetratin-derived CPPs, termed PiP peptides for the delivery of covalently coupled SSOs (Abes et al. 2007, Betts et al. 2012). PiP-SSO conjugates were specifically developed for the treatment of Duchenne muscular dystrophy. The most promising of the designed peptides is Pip6a which currently undergoes comprehensive preclinical research (Betts et al. 2012). Pip6a-SSO triggered high level of exon skipping in both cell based assays (Lehto et al. 2014) and in *mdx* mice (Betts et al. 2012, Betts et al. 2015). In addition to skeletal muscle, significant splice correction was measured in cardiac muscle of *mdx* mice after systemic administration (Betts et al. 2012).

1.2.3. Short interfering RNA (siRNA)

RNA interference (RNAi) is a powerful technology for gene silencing by degrading target mRNAs which are complementary to antisense strands of administered double-stranded short interfering RNAs (siRNAs). The RNAi approach has various advantages over small molecule drugs. RNAi enables the suppression of one or more transcripts with high selectivity, and importantly, the approach is applicable for almost all transcripts of the genome.

The first peptide vector employed for the delivery of siRNA by co-incubation strategy was MPG (Simeoni et al. 2003). MPG/luc-siRNA complexes induced 80–85% of luciferase downregulation in HeLa and Cos-7 cells which had previously been transfected with luciferase-encoding plasmid (Table 3). Using MPG peptide without NLS (MPG Δ^{NLS}) the suppression of luciferase was even stronger, and reached to 90%. Later, MPG-8, a shorter version of MPG efficiently mediated the delivery of cyclin B1 siRNA into prostate carcinoma cell PC3-xenografted mice (Crombez et al. 2009). Reduction of tumour growth by 75% was observed using 0.05 mg/kg of siRNA, and complete removal of tumour was observed by using 0.25 mg/kg of siRNA. The inhibition of tumour growth was sequence-dependent since mutated form of cyclin B1 was unable to impair tumour growth. siRNA delivery by PF6 has also been evaluated in animals (El-Andaloussi et al. 2011). In this study mice stably expressing luciferase in liver were treated with PF6/luc-siRNA (1 mg/kg) and assayed over 15 days. PF6/siRNA treatment diminished luciferase expression for 2 weeks, reaching the maximum suppression (about 75%) by day 5.

Oligoarginines have also been used for the siRNA delivery by co-incubation strategy (Kim et al. 2006, Tönges et al. 2006, Kumar et al. 2007, Nakamura et al. 2007). For example, Tönges *et. al* demonstrated an effective downregulation of EGFP reporter gene in EGFP-expressing hippocampal neurons by st-R8/EGFP-siRNA nanocomplexes. Later, Cholesteryl-R9 was used to deliver vascular endothelial growth factor (VEGF) siRNA into tumour-bearing mice.

Impairing the function of VEGF has been previously suggested to inhibit tumour growth and metastasis by preventing its vascularization (Holash et al. 1999, Brekken and Thorpe 2001). Indeed, cholesteryl-R9/VEGF-siRNA significantly decreased tumour growth due to the antiangiogenic effect of VEGF-siRNA (Leung et al. 1989, Kim et al. 2006). Another study showing the high potency of CPP-mediated siRNA delivery *in vivo* used rabies virus glycoprotein (RVG) added to the carboxy-terminus of nona-arginine (Kumar et al. 2007). RVG is a short peptide which enables the transvascular delivery of siRNAs into brain. GFP-transgenic mice were injected with nanocomplexes on three consecutive days and two days after the last administration GFP expression was measured in their brain, spleen and liver. The GFP expression decreased about 50% in the brains of GFP-siRNA/R9-RVG treated mice, whereas no significant reduction was detected in liver or spleen. These results indicate that R9-RVG peptide enables transvascular delivery of siRNA to the central nervous system with high specificity.

Table 3. Examples of CPP-mediated siRNA delivery using co-incubation strategy.

| CPP/delivery system | Cells/tissues | Reference |
|-----------------------------------|--|---------------------------|
| Primary amphipathic CPPs | | |
| MPG, MPG Δ^{NLS} | HeLa, Cos-7, HS-68 | Simeoni et al. 2003 |
| MPG α | HeLa-TetOff, 293T cells, ECV304, ECV-GFP-Nuc | Veldhoen et al. 2006 |
| MPG-8 | HeLa, PC3 xenografted mice | Crombez et al. 2009 |
| PF6 | Hepatoma, MEF, HUVEC, mESC, mice | El-Andaloussi et al. 2011 |
| Secondary amphipathic CPPs | | |
| CADY | HUVEC, THP1, mouse 3T3 cells | Crombez et al. 2009 |
| Arginine-rich CPPs | | |
| Stearyl-R8 | EGFP-expressing hippocampal neurons | Tönges et al. 2006 |
| Chol-R9 | Tumor-bearing mice | Kim et al. 2006 |
| R8-MEND | HeLa | Nakamura et al. 2007 |
| RVG-9R | GFP-transgenic mice | Kumar et al. 2007 |
| EB1 | HeLa, HepG2 | Lundberg et al. 2007 |
| Tat-DRBD | H1299, HUVEC, Jurkat T, hESC | Eguchi et al. 2009 |

In 2009, the group of S. Dowdy introduced Tat-DRBD fusion protein for intracellular delivery of siRNA (Eguchi et al. 2009). The constructed fusion protein contained a single double-stranded RNA binding site with high affinity to siRNA (Bevilacqua and Cech 1996, Ryter and Schultz 1998, Tian et al. 2004). Tat-DRBD induced high RNAi response in various cell-types including hard-to-

transfect primary T-cells, HUVEC and hES cells. To evaluate the *in vivo* potency of Tat-DRBD-mediated siRNA delivery, ROSA 26 mice expressing luciferase in the nasal and tracheal passages (Safran et al. 2003) were used. The transfection of Tat-DRBD/Luc-siRNA led to about 50% of reduction of luciferase expression already at the first day of experiment. The luciferase expression was recovered by day 15 (Eguchi et al. 2009).

1.2.4. Antisense oligonucleotides (ASOs)

Antisense oligonucleotides (ASOs) are short (15–20 bases) single-stranded oligonucleotides which bind to their complementary mRNA or miRNA sequences in cells' cytoplasm. The downregulation of target RNA can be caused by either sterically hindering the binding of ribosomal subunits on the RNA molecule or by recruiting of ubiquitous enzyme RNaseH which degrades the RNA strand from the RNA-DNA duplex (reviewed in Bennett and Swayze 2010).

The application of ASOs for gene regulation is a popular approach in the field of CPPs, but the number of studies using non-covalent strategy has remained very limited. The first report dates back to 1997, when the group of G. Divita and F. Heitz reported the cellular uptake of primary amphipathic peptide MPG/ASO noncovalent complexes (Morris et al. 1997) (Table 4). Peptides from the Pep family of CPPs have perhaps proved to be most promising candidates in this field. Pep-2 and Pep-3 are primary amphipathic peptides which have shown to induce significant downregulation of target gene by intracellular delivery of antisense oligonucleotides (Morris et al. 2004, Morris et al. 2007). Importantly, the intratumoural injection of 5 µg of anti-cyclin B1 HypNA-pPNA/Pep-3 nanocomplexes into tumour-bearing mice inhibited tumour growth >92%. In contrast, intravenous administration of the nanocomplexes suppressed tumour growth only by 20%. However, modification of the N-terminus of Pep-3 with PEG increased tumour inhibition upon systemic administration to >90% (Morris et al. 2007). Regrettably, this delivery system has not yet found widespread application.

Table 4. Examples of CPP-mediated delivery of ASOs using co-incubation strategy.

| CPP/delivery system | Cells/tissues | Reference |
|---------------------|---|--------------------|
| MPG | HS68, NIH-3T3 | Morris et al. 1997 |
| Pep-2 | HeLa, HS68, HEK293 | Morris et al. 2004 |
| Pep-3 | HUVEC, Jurkat T, MCF-7, PC3, PC3 xenografted mice | Morris et al. 2007 |

1.3. Characterization of CPP/nucleic acid nanocomplexes and their cell-surface association

1.3.1. Characterization of nanocomplexes

The non-covalent strategy of coupling CPPs to nucleic acid molecules relies mostly on electrostatic and hydrophobic interactions between positively charged CPP and negatively charged cargo which result the formation of nanocomplexes/nanoparticles (NP). In order to be considered for implementation in biomedical research and medicine the characteristics of CPP/nucleic acid NPs such as size, shape and charge need to be characterized in detail.

One of the most important characteristics of nanoparticles designed for drug delivery is their size. Size determines the cellular uptake efficacy of NPs. Various studies have demonstrated that smaller nanoparticles are internalized by cells more efficiently compared to larger particles (Prabha et al. 2002). For example, transfection of Cos-7 cells with luc-pDNA-loaded nanoparticles with a diameter of 70 nm yielded 27-fold higher luciferase expression compared to larger (d=200 nm) nanoparticles (Prabha et al. 2002). The size limit of nanoparticles that can be engulfed varies by cell type. While some cell types (e.g. HUVEC, ECV 304, HNX 14C) are able to internalize nanoparticles with large size range (20 nm–1 μ m), others (e.g. Hepa 1–6 and HepG2) are not capable of engulfing larger particles than 100 nm in diameter (Zauner et al. 2001). The optimal diameter for receptor-mediated endocytosis is 50–60 nm (Chithrani et al. 2006, Chithrani and Chan 2007, Zhang et al. 2009) and the upper limit is about 200 nm in diameter. Larger nanoparticles can be internalized by macropinocytosis, which is typically a signal-dependent process, but in some cells such as antigen-presenting cells occurs constitutively (Norbury et al. 1995, Sallusto et al. 1995, Norbury et al. 1997).

The size of NPs plays an important role in dictating the circulation half-life and biodistribution of NPs *in vivo*. For example, smaller (d= 10–15 nm) nanoparticles show higher distribution in tissues compared to larger (d= 50–200 nm) NPs (De Jong et al. 2008, Sonavane et al. 2008).

Interestingly, shape can also influence the cellular uptake efficacy of nanoparticles. Chithrani *et. al* showed that spherical gold-nanoparticles were internalized by HeLa cells more effectively compared to their rod-shaped counterparts (Chithrani et al. 2006). One reason behind this could be that rod-shaped NPs bind more cell-surface receptors when the longitudinal axis of the NP interacts with the cell surface, which could result in less available binding sites (Chithrani et al. 2006). However, these differences could have been caused by the different amounts of coating material on the surface of NPs. Shape may have an impact on the circulation half-life of NPs. Geng *et al.*, showed that filamentous polymer micelle assemblies (filomicelles) persist in vascular circulation of rodents up to one week – about ten times longer compared to their spherical counterparts (Geng et al. 2007).

Zeta (ζ) potential, the electrical potential between ions bound to a particle and ions which remain in the surrounding solution, is another important parameter which influences the cell association and cellular uptake mechanism of nanoparticles. ζ -potential of NPs depends on the surrounding solution, and therefore it is important to measure it in relevant medium. Positively charged nanoparticles are believed to interact with the plasma membrane of cells via cell-surface proteoglycans, and internalized by various mechanisms (Padari et al. 2010). Negatively charged nanoparticles, however, can be internalized via binding to specific cell-surface receptors (Ezzat et al. 2012, Juks et al. 2015) as to be discussed in the next chapter. Neutral and negatively charged NPs show lower adsorption of serum proteins, resulting in longer circulation times (Alexis et al. 2008). In contrast, cationic nanoparticles can be more easily released from endosomes compared to anionic or neutral NPs (Nel et al. 2009).

In tissue culture medium or in blood colloidal particles typically absorb some amount of proteins to their surface, forming a “protein corona”. The composition of the protein coat depends on the properties of NPs, for example their surface chemistry, charge and size (Nel et al. 2009). “Protein corona” plays an important role in the association of NPs with the plasma membrane, their cellular uptake and intracellular trafficking (Walkey et al. 2014). Moreover, the binding of specific proteins can dictate the biodistribution or clearance of NPs. For example, attached plasma proteins (e.g. complement factors, coagulation proteins, immunoglobulins) can be recognized by phagocytes, which could result the engulfment of NPs and their degradation (reviewed in Owens and Peppas 2006).

Stability of nanoparticles is also an important parameter which defines the efficiency of a drug delivery vehicle. Nanoparticles should be stable in blood circulation in order to protect the encapsulated cargo from degradation and to be able to mediate their cellular uptake. However, once in cytoplasm, the release of cargo from carrier is essential for triggering the bioactivity of delivered molecule.

The group of R. Brock recently performed a detailed analysis of the molecular and physicochemical properties of CPP/siRNA nanoparticles (van Asbeck et al. 2013). Interestingly, the dynamic light scattering (DLS) analysis revealed that in case of some peptides (TP10, Tat, PF6, hLF) the size of nanocomplexes depended on the used molar ratio (MR) of CPP and siRNA, whereas others (R9, r9-hLF, PF14) did not show such correlation. In the former case, individual peptides had different behaviours. For example, TP10 did not form NPs beneath MR 20, but aggregated at high (MR 30 and beyond) molar ratios. PF6, however, formed largest particles (about 200 nm) at MR 15 and at lower (MR 5) or higher (MR 30–40) molar ratios smaller (about 100 nm) particles were formed. In the latter case, the nanocomplexes had a size ranging from 150–200 nm. In addition, the analysis revealed that the size of CPP/siRNA nanocomplexes increased 2–3 fold when the complexes were incubated in physiological salt solution or in a tissue culture media, whereas the addition of serum yielded smaller complexes that were comparable with the ones obtained in salt-free conditions. All studied

CPP/siRNA nanocomplexes had a positive ζ -potential when formed in water, but obtained slightly negative charge after addition of serum-containing media, probably due to association with negatively charged serum proteins. Moreover, the stability of CPP/siRNA NPs was analysed using heparin replacement assay. Heparin is highly anionic compound which resembles anionic cell-surface heparan sulfate proteoglycans. The addition of heparin could disintegrate the CPP/siRNA NPs due to strong affinity to CPP. There was a strong correlation between the charge of CPP and the stability of complexes in the presence of heparin, and higher charge of CPP led to higher resistance to heparin replacement. In addition, the stability of CPP/siRNA NPs in the presence of serum was analysed by gel retardation assay. The analysis revealed the disintegration of complexes formed with cationic CPPs Tat, R9 and hLF already after 1 h of incubation with serum as indicated the free siRNA fraction. TP10/siRNA complexes were slightly more resistant compared to cationic CPPs, and PF6 and PF14 nanoparticles with siRNA were highly stable in the presence of serum even after 20 h of incubation (van Asbeck et al. 2013).

1.3.2. Cell-surface interactions of CPP/nucleic acid nanocomplexes

The initial associations of CPPs and CPP/cargo complexes with cells have been proposed to occur through anionic disaccharide units of glycosaminoglycans (GAGs). Various studies have shown that in cells which lack all GAGs or heparan sulfates the cellular uptake of CPPs is drastically decreased or completely abolished (Tyagi et al. 2001, Richard et al. 2005, Nakase et al. 2007, Padari et al. 2010). For arginine-rich CPPs the association with GAGs only at high peptide concentrations (above 1 μ M) has been proposed (Jiao et al. 2009). The association of CPPs with GAGs can activate cell signalling cascades. For example, the association of MPG/oligonucleotide complexes with GAGs has been demonstrated to activate Rho/Rac GTPase, leading to cytoskeletal remodelling and triggering of macropinocytosis (Gerbal-Chaloin et al. 2007, Nakase et al. 2007). Although it is well-established that GAGs are the first contact site for CPPs and CPP/cargo complexes, recent studies have found that the initial cell-surface associations can involve diverse mechanisms, and simple electrostatic interactions of CPP or CPP/cargo with cell surface proteoglycans do not necessarily apply invariably. For example, Gump *et al.* demonstrated that the cellular uptake of TAT peptide occurs via macropinocytosis, and the uptake is not abolished in cells which lack heparan sulfates and sialic acid, indicating that these plasma membrane components are not required for Tat peptide cellular uptake (Gump et al. 2010). Instead, they proposed that a protein is needed for Tat internalization, because removal of cell-surface proteins with proteinase significantly decreased the cellular uptake of Tat peptide.

The association of CPP/nucleic acid NPs with cell-surface proteoglycans presumes that the nanoparticles possess a positive surface charge. This might apply to CPP/nucleic acid NPs which are formed in water, however, recent observations revealed that in a biorelevant media the nanocomplexes obtain negative ζ -potential (Oskolkov et al. 2011, van Asbeck et al. 2013). Thus, the association of CPP/nucleic acid NPs with the cell surface could not be explained simply by electrostatic interactions with negatively charged components of extracellular matrix.

Scavenger receptors, a large class of cell-surface glycoproteins are receptors for various ligands. To date, there are 10 classes (class A-J) of scavenger receptors identified (reviewed in Prabhudas et al. 2014). Two members of these, scavenger receptor class A (SCARA) receptors SCARA3 and SCARA5 have been shown to be involved in the cellular uptake of nucleic acids (Pearson et al. 1993, Limmon et al. 2008, DeWitte-Orr et al. 2010) and nucleotide-functionalized gold nanoparticles (Patel et al. 2010). Recently, Ezzat *et al.* demonstrated that SCARA3 and SCARA5 also serve as cell-surface receptors for negatively charged CPP/oligonucleotide nanocomplexes (Ezzat et al. 2012). The biological activity of PF14-delivered SSOs was drastically decreased in HeLa pLuc 705 cells where SCARA3 and SCARA 5 were downregulated using inhibitory ligands or RNAi approach. Furthermore, SCARA3 and SCARA5 co-localized with PF14/SSO nanocomplexes at the plasma membrane as revealed by TEM analysis.

1.4. Cell entry mechanisms and intracellular trafficking of CPP/nucleic acid nanocomplexes

1.4.1. Endocytosis

Endocytosis is a process of cellular uptake of membrane components, fluids, solutes and macromolecules which cannot passively diffuse through the plasma membrane. Endocytosis is divided into phagocytosis and pinocytosis. Phagocytosis occurs only in specialized cells and involves the uptake of large particles. Pinocytosis is divided into clathrin-dependent endocytosis (CME), caveolin-dependent endocytosis, clathrin- and caveolin-independent endocytosis, and macropinocytosis (Fig. 1).

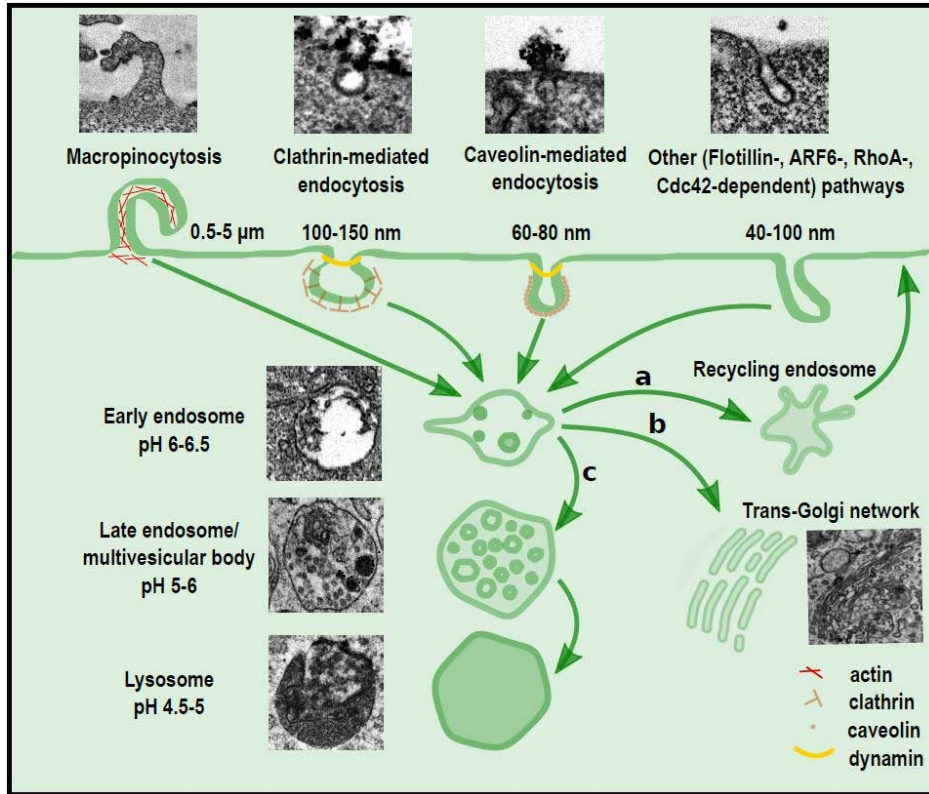


Figure 1. Schematic illustration of main endocytic pathways and intracellular trafficking routes of endocytosed material. A, b, c refer to trafficking from early endosomes to recycling endosomes (a), trans-golgi network (b) or late endosomes (c). TEM images from different cell-lines were captured by the author of the thesis.

1.4.1.1. Clathrin-mediated endocytosis

Clathrin-mediated endocytosis (CME) is the most thoroughly examined endocytic pathway, and it is active in all mammalian cells. In CME, the coat protein clathrin polymerizes at the plasma membrane and forms a clathrin-coated pit (CCP) which can ultrastructurally be identified by basket-like morphology and thick protein coat (Fig. 1). The size of CCPs in mammalian cells depends on cell type, but typically ranges from 100–150 nm in diameter.

CME is multifaceted endocytic pathway which is involved in the cellular internalization of various different cargos using numerous adaptor and accessory proteins. The initiation of CME is not yet fully understood, but recent studies suggest the formation of nucleation module at the plasma membrane (Schmid et al. 2006). The nucleation module is formed by the binding of membrane sculpting Fps/Fes/Fer/CIP4 homology (FCH) domain only proteins, epi-

dermal growth factor (EGF) pathway substrate 15 and intersectins to phosphatidyl-4,5-bisphosphate (PtdIns(4,5)P₂)-rich plasma membrane regions followed by binding of several other proteins (Stimpson et al. 2009, Henne et al. 2010). Subsequently, adaptor protein 2 (AP2) is recruited to the nucleation site where it binds directly to PtdIns(4,5)P₂ and cell-surface receptors, and indirectly to cargo through association with accessory proteins (Collins et al. 2002, Kelly et al. 2008). Additionally, various cargo-specific accessory proteins can be involved, and these are always bound to AP2 (Edeling et al. 2006, Schmid et al. 2006). Thereafter, clathrin triskelia are recruited to the plasma membrane, bind to AP2 and polymerize, forming a basket-like invagination (reviewed in Kirchhausen 2000). The budding of clathrin-coated vesicle (CCV) relies on the activity of large GTPase dynamin which is recruited to the CCP neck-region by BAR-domain containing proteins. Dynamin forms a helical polymer around the CCPs neck, and after GTP hydrolysis CCV is released (Herskovits et al. 1993, van der Bliek et al. 1993). Quickly after CCV is released, the clathrin lattice-structure is disassembled by ATPase heat shock cognate 70 and its cofactor auxillin releasing clathrin to cytoplasm for reuse (Rothnie et al. 2011). The uncoated vesicle fuses with early endosomes and the cargo can be either recycled back to the plasma membrane or targeted to late endosomes and/or lysosomes (Fig. 1a,c).

CME is considered as the most significant contributor to the total endocytic flux in cultured cells (Bitsikas et al. 2014). CME is the internalization pathway for the majority of cell surface receptors and integral membrane proteins. In addition, several viruses exploit the pathway to gain entry to the cell (Lecot et al. 2005, Blanchard et al. 2006, van der Schaar et al. 2008). Besides controlling cellular uptake of numerous cell surface receptors, CME has other biological functions such as the maintenance of cellular homeostasis, growth control, cell differentiation and signal transduction regulation (reviewed in McMahon and Boucrot 2011).

The involvement of CME in CPP-mediated nucleic acid delivery has been mainly examined using pharmacological inhibitors of this pathway, chlorpromazine or potassium depletion in cells. Chlorpromazine leads to the translocation of AP2 and clathrin to endosomal membranes, depleting it from the cell surface. Potassium depletion causes the aggregation of clathrin in cytoplasm, and thus, prevents the formation of clathrin-coated pits at the plasma membrane (Larkin et al. 1983). Using these methods, CME was shown to be the main cell-entry pathway for PF6/SSO nanocomplexes (Hassane et al. 2011).

1.4.1.2. Caveolin-mediated endocytosis

Caveolin-mediated endocytosis occurs in most vertebrates. Caveolae are small (60–80 nm) flask-shaped invaginations. Two protein families are required for the formation of caveolae: caveolins and cavins. The morphology of caveolae can be distinguished from CCPs by smaller size, elongated shape and lack of thick protein coat (Palade 1953, Yamada 1955, Richter et al. 2008) (Fig. 1).

Caveolae form by oligomerization of caveolin at the cholesterol and sphingolipid rich regions (“lipid rafts”) at the plasma membrane, and cholesterol is essential for maintaining their structure (Rothberg et al. 1992). The concentration of cholesterol and certain glycosphingolipids and sphingomyelin is much higher in caveolae compared to other plasma membrane regions (Ortegren et al. 2004). Cytoplasmic cavin proteins oligomerize before associating with the plasma membrane where they function as stabilizers of caveolae. In addition to stabilization, cavin proteins modulate the morphology and functions of caveolae (reviewed in Nassar and Parat 2015). Mammalian cells express three different types of caveolin proteins: caveolin-1, caveolin-2 and caveolin-3. Caveolin-1 and caveolin-2 are expressed in all cell types except in neurons and leukocytes, and particularly high expression of these has been observed in adipocytes, endothelial cells, smooth muscle cells and fibroblasts (Scherer et al. 1996, Scherer et al. 1997). Caveolin-3 is specific to cardiac and skeletal muscle cells (Way and Parton 1995, Song et al. 1996, Tang et al. 1996).

Caveolae play an important role in various cellular functions such as cholesterol and lipid homeostasis, cellular signalling, transcytosis and endocytosis (reviewed in Parton and Simons 2007). In contrary to highly dynamic clathrin coated pits, caveolae are static structures, which can remain at the cell surface for long periods of time (Thomsen et al. 2002), however, their internalization can be induced by stimulation. Caveolin-mediated endocytosis plays an integral part in the cellular uptake of various growth factor receptors, viruses (e.g. Simi-ani virus 40, Papilloma virus, polyoma virus, echovirus) and cholera toxin β subunit (CTx β) (Kartenbeck et al. 1989, Anderson et al. 1996, Stang et al. 1997, Richterova et al. 2001).

In endothelial cells, caveolae are involved in transcytosis of internalized cargo to the underlying tissues (Palade and Bruns 1968, Ghitescu et al. 1986, Ge et al. 2008). In non-endothelial cells, however, the fate of internalized caveolae is less clear. For a long time it was suggested that internalized caveolae can fuse with pH-neutral caveosomes in Rab5-independent manner or with early endosomes in Rab5-dependent manner. However, recently, a comprehensive analysis of caveolin-1 trafficking revealed that endogenous caveolin is directly directed to early endosomes (Hayer et al. 2010, Parton and Howes 2010). This finding put the existence of caveosomes as distinct organelles under debate. Currently, it seems that in non-endothelial cells the cargoes internalized by caveolin-mediated endocytosis are destined to the classical endolysosomal pathway (Hayer et al. 2010, Parton and Howes 2010) (Fig 1c). Still, for example cholera toxin has been shown by TEM to enter endosomes and trans-Golgi network instead of lysosomes of host cells (Joseph et al. 1979) (Fig 1b).

Using immunofluorescence microscopy, TEM and depletion of cholesterol from the plasma membrane, Choi *et al.* showed that spherical nucleic acids (SNAs) associate with the cell surface of C166 endothelial cells in lipid raft domains (Choi et al. 2013). Two common classes of molecules employing caveolin-mediated endocytosis for internalization into cells are cholera toxin β subunit and glycosylphosphatidylinositol (GPI)- anchored proteins. Pretreat-

ment of cells with phosphatidylinositolphospholipase C which enzymatically cleaves GPI-anchored proteins from the cell-surface reduced the uptake of SNAs about 50%, indicating the role of caveolar endocytosis in the uptake of SNAs. The importance of caveolar endocytosis was further confirmed by using caveolin-1 deficient cells, which showed 60% reduction of SNA cellular uptake compared to control cells (Choi et al. 2013). Very recently, we found that the transfection activity of PF14/SCO nanocomplexes was reduced about 80% in HeLa cells pretreated with amiloride (inhibits macropinocytosis), and about 30% in cells pretreated with nystatin (inhibits caveolin-mediated endocytosis) (Juks et al. 2015). Chlorpromazine which impedes CME did not affect the transfection activity of PF14/SCO NPs. PF14/SCO NPs often co-localized with fluid-phase marker dextran at the cell surface. Inside cells the complexes were detected together with dextran in punctuate structures resembling endosomes, confirming the importance of macropinocytosis in the cellular uptake of PF14/SCO NPs. A fraction of PF14/SCO NPs also co-localized with caveolin-1 at the plasma membrane within 30 min of incubation. In addition, suppression of caveolin-1 reduced the uptake of the complexes by about 40% compared to control cells.

1.4.1.3. Macropinocytosis

Macropinocytosis is an endocytic process which leads to the internalization of fluid and membranes in large vacuoles called macropinosomes. Constitutive macropinocytosis occurs only in specialized cells (e.g. dendritic cells) (Sallusto et al. 1995, Norbury et al. 1997, West et al. 2000, Bohdanowicz et al. 2013) but it can be induced by growth factors or other stimulants in the vast majority of cells (Haigler et al. 1979, Swanson 1989, Dowrick et al. 1993, Racoosin and Swanson 1993, Anton et al. 2003). Macropinocytosis is highly active in many types of cancer cells. An estimated 20% of all known types of cancer cells over-express oncogenic Ras or Src proteins (Bos 1989) which induce macropinocytotic uptake of extracellular fluid, and thus, ensure the constant influx of nutrients (Bar-Sagi and Feramisco 1986, Bar-Sagi et al. 1987, Amyere et al. 2000, Kasahara et al. 2007, Commisso et al. 2013).

Macropinocytosis is dependent on actin cytoskeleton which triggers structural changes in the plasma membrane resulting the formation of protrusions (lamellipodes or ruffles) at the cell surface which can fall back to the plasma membrane forming a large ($d = 0.5\text{--}5\text{ }\mu\text{m}$) fluid-filled macropinosome (Lewis 1931) (Fig 1). Typically, macropinocytosis is initiated by the activation of receptor tyrosine kinases (RTKs) after external stimulation (Mercer and Helenius 2009). RTKs, in turn, activate Ras GTPases which initiate several signalling cascades involving Rac1, Rab5, Arf6 and phosphatidylinositol-3-kinase (Bar-Sagi and Feramisco 1986, Bar-Sagi et al. 1987), resulting the formation of lamellipodes and closure of macropinosome. P21-activated kinase 1 (Pak1) regulates the dynamics and motility of cytoskeleton, and is also required in all stages of macropinocytosis (Dharmawardhane et al. 2000, Parrini et al.

2005, Liberali et al. 2008). Pak1 translocates to the plasma membrane after initiation of macropinocytosis, where it activates various effectors required for the formation of macropinosome (Galisteo et al. 1996, Even-Faitelson et al. 2005, Mercer and Helenius 2008, Dharmawardhane et al. 1999). Protein kinase C and c-Src promote ruffling and macropinosome formation (Miyata et al. 1989, Amyere et al. 2000, Kasahara et al. 2007). Other factors such as Na^+/H^+ exchangers and cholesterol play a role in macropinocytosis. Inhibition of Na^+/H^+ exchangers by amiloride or its analogue ethylisopropylamiloride (EIPA) impairs macropinocytosis and are commonly used for the inhibition of the pathway (Koivusalo et al. 2010).

Typically, macropinocytosis is a degradative endocytic pathway and after formation, macropinosomes acidify, acquire early endosomal markers Rab5 and/or EEA1 followed by further acidification and acquiring late endosomal marker Rab7 (Fig. 1c). Eventually, macropinosomes fuse with lysosomes where internalized cargo is degraded (Racoosin and Swanson 1993). Thus, the cellular fate of macropinosomes is similar to classical endolysosomal pathway. Although in vast majority of cell types, internalized cargo is destined to degradation, in some cells (e.g. A531 human carcinoma cells) the recycling of cargo from macropinosomes to plasma membrane has been demonstrated (Hewlett et al. 1994). Thus, the intracellular fate of macropinosomes depends on cell-type.

Numerous viruses e.g. vaccinia virus, herpes simplex virus 1, HIV-1 utilize macropinocytosis to gain entry into cells (Marechal et al. 2001, Mercer and Helenius 2008, Devadas et al. 2014). While some viruses use macropinocytosis to enter cells, others use diverse endocytic mechanisms but require macropinocytosis to promote internalization (Meier et al. 2002). It is well-established that macropinocytosis plays an important role in the uptake of arginine-rich CPPs and their conjugates with nucleic acids (Nakase et al. 2004, Wadia et al. 2004, Kaplan et al. 2005, Nakase et al. 2007). However, its involvement in the internalization of CPP/nucleic acid non-covalent complexes is far less examined. In one study, R8-MEND, oligoarginine-modified liposomes encapsulating pDNA was shown to internalize cells via macropinocytosis. Interestingly, the cellular uptake route of R8-MEND/pDNA was dependent on the concentration of R8 used for the formation of liposomes, and clathrin-mediated endocytosis was employed at lower amounts of the peptide (Khalil et al. 2007). Recently, Nakase *et al.* demonstrated that by stimulating EGFR which activates macropinocytosis significantly improves the cellular uptake of exosomes (Nakase et al. 2015). Macropinosomes are more leaky compared to other endosomes (Meier et al. 2002), and thus, this cellular uptake pathway is suggested to be advantageous for drug delivery applications.

1.4.1.4. Other endocytic pathways

In addition to extensively studied clathrin- and caveolin-mediated endocytosis and macropinocytosis less common endocytic pathways are used by cells to

internalize extracellular material. Some examples of these comprise flotillin-, GRAF1-, ARF6- and RhoA-dependent endocytosis. Commonly, these endocytic pathways occur in cholesterol-rich lipid raft membrane domains of cells, and involve the formation of small (40–100 nm) flask shaped or tubular invaginations (for a review see Doherty and McMahon 2009) (Fig 1).

Clathrin-independent carriers (CLICs) which deliver endocytosed material into GPI-anchored protein-enriched early endosomes (GEEC) have become an interesting topic in the research of endocytosis. This endocytic pathway was discovered in 2002 by Sabharanjak *et al.* who showed that GPI-anchored proteins regulated by Cdc42 are taken up by cells in a dynamin-independent manner, and the internalized small ($d=50\text{--}80\text{ nm}$) tubular and ring-like vesicles lack clathrin coat and are not enriched with caveolin (Sabharanjak *et al.* 2002). CLICs locate in lipid rafts, are sensitive to cholesterol depletion and require actin polymerization (Kirkham *et al.* 2005). CLICs mature into GEECs which can then fuse with early endosomes Rab-5 dependently or can be directly targeted to other compartments such as Golgi complex (Kirkham *et al.* 2005). CLIC/GEEC pathway is involved in the uptake of GPI-anchored proteins, bacterial toxins and extracellular fluid (Lundmark *et al.* 2008). GRAF1 is a CLIC-associating protein, which stabilizes the membrane curvature and can be used as a protein marker for this endocytic pathway (Lundmark *et al.* 2008). It is established that small G-proteins from the Rho, ADP-ribosylation factor (ARF) and Rab families regulate the endocytic uptake by CLICs (Lamaze *et al.* 2001, Kirkham *et al.* 2005). Rho and Rac1 induce the cellular uptake of the interleukin-2 receptor (Lamaze *et al.* 2001, Grassart *et al.* 2008), and cell division cycle 42 (Cdc42) is required for the cellular uptake of GPI-anchored proteins (Sabharanjak *et al.* 2002). CTx β and *Helicobacter pylori* vacuolating cytotoxin A are internalized by cells using CLIC/GEEC pathway (Gauthier *et al.* 2005). To date, there is no evidence that non-viral gene delivery vectors employ CLIC/GEEC pathway to gain access to the interior of cells.

Flotillin-mediated endocytosis was demonstrated when flotillin-1 was shown to mediate the cellular uptake of GPI-anchored proteins in Cos-7 cells by phosphorylation of Fyn kinase (Glebov *et al.* 2006, Riento *et al.* 2009). Later, Ait-Slimane *et al.* found that in HepG2 cells the uptake of GPI-anchored proteins occurs through the activity of flotillin-2 (Ait-Slimane *et al.* 2009). However, the latter finding could be associated with GRAF1 associated endocytosis. Flotillin-1 (reggie 2) and flotillin-2 (reggie 1) predominantly localize at cholesterol-rich lipid membrane microdomains (“lipid rafts”), but also in intracellular compartments such as late endosomes, recycling endosomes and exosomes (Salzer and Prohaska 2001, de Gassart *et al.* 2003, Kokubo *et al.* 2003, Santamaria *et al.* 2005). Flotillin-induced membrane invaginations are small and typically flask-shaped, morphologically similar to caveolar invaginations, except that these do not contain caveolin (Frick *et al.* 2007). The importance of dynamin in flotillin-mediated endocytosis is still argued, and the data is often controversial (Glebov *et al.* 2006, Payne *et al.* 2007). In addition to endocytosis, flotillins have various other cellular functions, such as cell adhesion, signal transduction through

RTKs and cellular trafficking (reviewed in Zhao et al. 2011). Flotillins have been shown to be involved in the cellular internalization of polyplexes (Vercauteren et al. 2011), proteoglycans and their ligands (Payne et al. 2007), and proteins (Glebov et al. 2006, Ait-Slimane et al. 2009). In one study the cellular uptake of DNA polyplexes was reported to depend on nucleolin and flotillin which co-localized in lipid rafts at the surface of cells, suggesting that nucleolin could be a cell-surface receptor for polyplexes (Chen et al. 2011). In another study DNA polyplexes were internalized into cells by two distinct pathways – flotillin-1-dependent endocytosis and phagocytosis-like mechanism – but only the former mechanism led to significant gene expression (Vercauteren et al. 2011).

In addition to above-mentioned, ARF6- and Rho-dependent endocytosis have been suggested to act as distinct cellular uptake routes. ARF6 mediates the constitutive uptake and recycling of class I major histocompatibility complex molecules (Blagoveshchenskaya et al. 2002). ARF6-enriched endocytic vesicles are typically recycled back to the plasma membrane after fusion with sorting endosomes (Naslavsky et al. 2003). RhoA-dependent endocytosis is dynamin-dependent, sensitive to cholesterol depletion and is regulated by Rho GTPase (Subtil et al. 1994, Subtil et al. 1997). RhoA is involved in the cellular uptake of IL2-R in lymphocytes (Subtil et al. 1994, Subtil et al. 1997). Interestingly, RhoA regulated endocytosis of amyloid β -peptide is essential for the neurotoxicity of the peptide which probably causes Alzheimer disease, and therefore could be of interest as a therapeutic target (Yu et al. 2010). Nevertheless, RhoA-dependent endocytosis has remained the least examined endocytic pathway due to the low number of cargos utilizing the route.

Unfortunately, these clathrin- and caveolin- independent mechanisms of endocytosis are rarely examined as possible cell entry portals for drug delivery vectors.

1.4.2. Direct translocation

Some CPPs, for example, MPG (Simeoni et al. 2003, Deshayes et al. 2004), Pep peptides (Deshayes et al. 2004) and CADY (Crombez et al. 2009, Rydström et al. 2011) deliver nucleic acids into cells in an endocytosis-independent manner. Simeoni *et al.* demonstrated that MPG/luc-pDNA induced high luciferase expression in human fibroblasts (HS-68), and the luc-pDNA activity was not decreased in the presence of endocytosis inhibitors. In addition, incubation of MPG/luc-pDNA at 4°C had only marginal effect on the luciferase activity (Simeoni et al. 2003). MPG peptide acquires β -sheet conformation after the formation of MPG/cargo complexes and the association with the plasma membrane of cells. Thereafter, the complexes internalize into cells by formation of transient pore-like structure. After internalization, some cargo is released from the peptide due to the high affinity of the carrier to plasma membrane phospholipids (Deshayes et al. 2004). Similar cellular uptake mechanism was proposed

for Pep-1/cargo nanocomplexes, but instead of β -sheet structure, Pep-1 acquires helical conformation upon interactions with the cell surface (Deshayes et al. 2004). The conformational differences between the two peptides might determine the type of cargo that can be delivered into cells. MPG is more efficient for the delivery of nucleic acids whereas Pep-1 more suitable for the delivery of proteins and large peptides (Deshayes et al. 2004).

CADY peptide mediated siRNA delivery into cells also occurs independently of endosomal inhibitors (Crombez et al. 2009, Rydström et al. 2011). Since endocytic inhibitors are not 100% specific for one pathway, additional experiments were conducted by incubating CADY/siRNA complexes in the presence of different endosomal markers in HeLa cells. CADY/siRNA complexes did not co-localize with endocytic markers transferrin, Rab5 or caveolin. Instead, the complexes localized mainly in cytoplasm, as confirmed by electron microscopy analysis (Rydström et al. 2011). In addition, CADY/ siRNA complexes were incubated in HeLa cells in the presence of sodium azide which inhibits mitochondrial oxidative phosphorylation. The activity of siRNA remained the same in cells treated with sodium azide and in untreated cells, confirming that the uptake of siRNA/CADY complexes occurs via an ATP-energy independent mechanism (Rydström et al. 2011).

1.4.3. Intracellular trafficking

Despite diverse and complex cell-entry pathways, all internalized endocytic vesicles fuse with early endosomes (EE) after pinching off from the plasma membrane (Fig. 1). Early endosomes are tubulo-vesicular structures located at the periphery of cells, and function as major sorting compartments of cell (reviewed in Jovic et al. 2010). Within minutes after fusing with EEs, molecules are sorted to either recycling or degradation. Molecules which are destined for recycling accumulate to the tubular extensions of EEs, and cargo which is to be degraded stays in the lumen of endosome (Dunn et al. 1989, Mayor et al. 1993). By default, all molecules are destined to recycling, and only those which contain a specific targeting signal remain in the vesicles lumen (Haglund et al. 2003, Mosesson et al. 2003). The lumen of EEs is slightly acidic (pH~6.0), enabling the dissociation of a receptor from its ligand, and thus, the receptors and their ligands can be directed to different destinations. While most (but not all) cell-surface receptors are recycled back to the plasma membrane for reutilization, most ligands end up with degradation in lysosomes (reviewed in Jovic et al. 2010).

Early endosomes are not static structures, instead, shortly after homotypic fusion and fusion with transport vesicles, EEs start moving along microtubules to perinuclear region of cell, and mature into more acidic late endosomes (Fig. 1a). The maturation of endosomes is regulated by small GTPases of Rab family of proteins (Rink et al. 2005). EEs are enriched with active (GTP-bound) Rab5, which recruits effector proteins to the EE which function in their trafficking,

fusion and sorting (reviewed in Grosshans et al. 2006). During transition from EE to LE, Rab5 is switched with Rab7, and at the same time, endosomes become more acidic (pH~5). LEs are more spherical compared to EEs and contain numerous intraluminal vesicles (Murk et al. 2003). In addition, LEs have different membrane composition, being enriched with triglycerides, cholesterol esters and certain phospholipids (Kobayashi et al. 1998, Hao et al. 2004). LEs fuse with transport vesicles which carry lysosomal hydrolases derived from Golgi apparatus (reviewed in Braulke and Bonifacino 2009), and mature into lysosomes with heterogeneous size and content, and a pH below 5. Lysosomes contain about 50 different degradative enzymes which hydrolyse all types of biological polymers (Journet et al. 2002, Sleat et al. 2005, Czupalla et al. 2006). All lysosomal enzymes are acid hydrolases which are only active in acidic environment of lysosomes, but not in pH-neutral cytoplasm. The acidic environment of lysosomes is maintained by the proton pump activity in lysosomal membrane, which consistently pumps protons into lysosomes from cytosol (Ohkuma et al. 1982). Several growth factor receptors which are not recycled back to the plasma membrane for reutilization, are degraded in lysosomes which terminates their biological response (receptor down-regulation) (Beguinot et al. 1984, Moore et al. 1999).

Although it is clear that endocytosis is the predominant cellular uptake route for most CPPs and their complexes with nucleic acid, the following intracellular trafficking is far less examined. We have previously used TEM to examine the intracellular trafficking of TP10 based CPP/oligonucleotide nanocomplexes (Oskolkov et al. 2011). We found that the CPP/oligonucleotide complexes avidly associated with the plasma membrane of HeLa cells and inside cells resided in endosomes.

1.4.4. Endosomal release of CPP/nucleic acid nanocomplexes

One of the biggest obstacles of developing CPP-based systems for the delivery of biomolecules is the entrapment of the peptide and its cargo inside endosomes. In order to trigger the biological activity of therapeutic nucleic acids, their release from endosomes is essential. Various approaches have been employed to enable the release of bioactive cargo from endosomes such as the use of endosomotropic agents, fusogenic lipids or peptide modifications (reviewed in Hou et al. 2015).

The most well-known endosomotropic agent is chloroquine, a weak base which accumulates into endosomes and lysosomes due to protonation (Wibo and Poole 1974). The accumulation of chloroquine increases the concentration of ions inside endosomes, leading to the influx of water. The water influx, in turn, causes swelling of endosomes and their rupture. Indeed, chloroquine can increase the bioactivity of delivered nucleic acids. For example, Ezzat *et al.* showed that PF14-mediated SSO activity significantly increased in the presence

of chloroquine, while the cellular uptake remained at the same level (Ezzat et al. 2011).

Conjugation of lipids to CPPs is another efficient approach to increase the endosomal release of nucleic acids (Futaki et al. 2001, Khalil et al. 2004, Tönges et al. 2006, Nakamura et al. 2007, Mäe et al. 2009, Lehto et al. 2010). Addition of fatty acid increases the hydrophobicity of CPP, making the peptide more lipophilic, which results in better membrane penetration (Mäe et al. 2009). In addition, fatty acid modification yields higher stability of the forming nano-complexes between CPP and nucleic acid, probably by promoting DNA/RNA condensation and shielding from degradative enzymes (Lehto et al. 2010). Most commonly, conjugation of stearyl-group to the N-terminus of CPP is used. Stearylation has been shown to increase the delivery of nucleic acids by various peptides such as Tat peptide (Futaki et al. 2001), oligoarginines (Futaki et al. 2001, Khalil et al. 2004, Tönges et al. 2006), TP10 (Mäe et al. 2009) and (RxR)₄ (Lehto et al. 2010). Mäe *et al.* demonstrated that st-TP10 led to about 30 times higher splice correction activity compared to unmodified peptide, whereas the uptake of st-TP10/SSO complexes increased only 2 times. Besides stearylation, other fatty acids with different chain lengths can be conjugated to CPP. Langel *et al.* examined the fatty acid length on CPP to the transfection efficacy of CPP/SCO complexes, and found that fatty acids with 16–24 carbons in their tails yielded highest bioactivities of delivered SCO (Langel et al. 2010).

In addition to stearyl-moiety conjugation, other peptide modifications have been introduced to enhance the release of CPP/nucleic acid nanocomplexes from endosomes. For example, st-TP10 based peptide PF6 is modified by the addition of trifluoromethylquinolane side chains. These protonatable chloroquine analogues increase the endosomal release probably due to proton sponge effect (El-Andaloussi et al. 2011). Another st-TP10 analogue is PF14, which contains ornithines instead of lysines in its primary structure to avoid degradation by extracellular peptidases. Despite being significantly more efficient compared to its parental st-TP10, majority of PF14/SSO nanocomplexes remained entrapped inside endosomes (Ezzat et al. 2011). To overcome this obstacle, four chloroquine analogues were attached to the side chain of PF14 via a succinylated lysine-tree similarly to PF6. The resulting peptide, PepFect 15 (PF15) led to significantly higher splice correction activity of SSOs compared to PF14. Importantly, the addition of chloroquine did not increase the activity of SSOs delivered by PF15, while it significantly enhanced the bioactivity of PF14-delivered SSOs (Lindberg et al. 2013).

The octa-arginine modified multifunctional envelope-type device (R8-MEND) which condenses nucleic acids by polycations and is covered with lipid bilayer is also an efficient delivery system enabling endosomal release of nucleic acids (Kogure et al. 2004, Nakamura et al. 2007). The endosomal release of nucleic acids delivered by MEND was even higher when pH-responsive fusogenic GALA peptide (cholesteryl-GALA) was incorporated to the delivery device instead of R8 (Kakudo et al. 2004).

The mechanisms of how the release of CPP/nucleic acid complexes from endosomes occurs are not known in detail. In order to visualize endosomal release of CPP/cargo complexes in living cells, one needs to be able to detect small amounts of released cargo in cytoplasm in the presence of intensely fluorescent endosomes. This, however, is complicated using conventional fluorescence based microscopy approaches. Recently, Wittrup *et al.* used an elegant spinning-disc microscope-based method which for the first time enabled to directly visualize the endosomal release of lipid-formulated siRNA (LNA, lipid nanoparticle) (Wittrup *et al.* 2015). The authors revealed that LNA-delivered siRNA was released from endosomes which were associated with Rab5 and Rab7 meaning that the release event occurred from maturing endosomes. Since the diffuse signal of fluorescently labelled siRNA spread all over cytoplasm within seconds after the release, they suggested that siRNA rather than intact LNAs were released from endosomes. Importantly, only one release event was detected from each individual endosome, indicating that the endosomal membrane was not damaged during the release. Interestingly, the release of siRNA from endosomes triggered the activation of autophagy, resulting the formation of autophagosomes which eventually fused with lysosomes.

2. AIMS OF THE STUDY

The aims of the current thesis were to characterize the size and morphology of CPP/nucleic acid nanocomplexes and to examine their cell-entry mechanisms and intracellular trafficking.

More specifically, the goals were:

- To examine the cell surface interactions and the intracellular trafficking of NickFect51 nanocomplexes with oligonucleotides (Paper I)
- To examine the cellular uptake mechanisms and intracellular trafficking of PepFect14, NickFect1 and NickFect51 nanocomplexes with plasmid DNA (Paper II, Paper III)
- To characterize the size and morphology of NickFect1, NickFect51, PepFect6 and PepFect14 nanocomplexes with nucleic acids (Paper IV)

3. METHODOLOGICAL CONSIDERATIONS

The detailed characterization of the methods is provided in the respective publications attached to the thesis, and only the most comprehensively used techniques in the study will be discussed in the following chapter.

3.1. Cell lines

We used various cell-lines in Paper I–III to examine 1) transfection efficacy and 2) cellular uptake mechanisms of CPP/nucleic acid nanocomplexes. We employed commonly used HeLa and CHO cell lines and hard-to-transfect MEF cells, T and B lymphocytes, RD4 skeletal muscle cells and mES cells in the study.

In order to examine the splicing redirection activity of SSOs in cells (Paper II), we used HeLa pLuc 705 cell-line, developed by Kang *et al.* (Kang et al. 1998). HeLa pLuc 705 cells are the most commonly used cell-model for examination of splicing switching activity of SSOs. These cells are stably transfected with luciferase encoding gene that contains a mutated β -globin intron 2, producing an aberrant pre-mRNA splicing site, which results in synthesis of non-functional luciferase. However, binding of complementary oligonucleotide to the aberrant splicing site restores the expression of luciferase. Since HeLa pLuc 705 cells are typically used for the evaluation of SSO activity in transfected cells, the results obtained from diverse studies can be compared to each other.

In the experiments unravelling cell-entry mechanisms and intracellular trafficking of CPP/nucleic acid nanocomplexes we used CHO (Paper I), HeLa (Paper III) or HeLa pLuc 705 (Paper II) cells. We chose HeLa and CHO cells for the cellular uptake studies because these are easy to transfect and commonly used cell-lines in the field. Thus, the obtained results could be more easily compared with the data from literature. We used HeLa pLuc 705 cells in Paper II because we employed the same cell-line in functional assays for the measurement of the activity of SSOs delivered by NF51.

3.2. CPPs

Transportan, a chimeric peptide derived from the N-terminal fragment of the neuropeptide galanin and a wasp venom peptide mastoparan is one of the most studied CPPs since its discovery in 1998 (Pooga et al. 1998). Transportan is able to carry nucleic acids inside cells, but it is not capable of inducing the biological activity of delivered cargo due to the endosomal entrapment. Since the discovery of transportan several chemical modifications have been introduced to its primary sequence to improve the cellular uptake and endosomal release of CPP/nucleic acid nanocomplexes (Mäe et al. 2009, El-Andaloussi et al. 2011, Ezzat et al. 2011, Oskolkov et al. 2011).

In Paper II we designed three novel transportan-based CPPs – NickFect 51 (NF51), NickFect 53 (NF53) and NickFect 61 (NF61) for the cellular delivery of different types of nucleic acids. In Paper I and Paper III we examined the transfection efficacy, cell-entry mechanism and intracellular trafficking of CPP/pDNA nanocomplexes using three transportan-based peptides – PepFect14 (PF14), NickFect1 (NF1) and NF51. In Paper IV, we used PepFect 6 (PF6), PF14, NF1 and NF51 to examine their size and morphology when complexed with nucleic acids.

Table 5. Peptide sequences used in the thesis.

3.3. CPPs and their complexes with nucleic acids

For coupling of CPPs to nucleic acids we used non-covalent (or co-incubation) strategy throughout the studies. The co-incubation of CPPs with nucleic acids results the formation of nanocomplexes due to electrostatic and hydrophobic interactions between positively charged peptide and negatively charged cargo.

We formed CPP/nucleic acid nanocomplexes in similar manner in all studies (Paper I–IV). We complexed CPPs with nucleic acids in water at ambient temperature for 30 min–1 h. In experiments with cells we added serum-containing or serum-free tissue culture medium immediately before incubation of complexes with cells. For complexation of CPPs with nucleic acids we varied the molar ratio (CPP: oligonucleotide) or charge ratio (CPP: pDNA) of the used peptides and nucleic acids. The charge ratio was calculated taking into account the positive charges of used peptides and negative charges of used pDNA.

3.4. Characterization of CPP/nucleic acid nanocomplexes

3.4.1. Dynamic light scattering (DLS)

Dynamic light scattering (DLS) is the most commonly used method to analyse the properties of colloidal particles ranging from 1 nm to several micrometres in diameter. DLS is a simple and fast method for the characterization of size, surface charge and polydispersity of colloids. DLS technique is based on the property of colloidal particles to randomly move in solution, Brownian motion. Larger particles move slower and smaller particles move faster in the suspension. When laser light is directed through cuvette containing a colloidal suspension, the fluctuating particles cause change in the wavelength intensity. The time-scale fluctuations of scattered light are directly related to the diffusion coefficient, which in turn, is related to the size of particles. Thus, by measuring the scattered light intensity in time by detector, the size of particles can be estimated. The outcome of DLS measurement is the hydrodynamic diameter of particles. This is the diameter of the hard sphere (solution) that moves at the same speed as the particle being measured (reviewed in Philo 2006, Hassan et al. 2015).

Charged particles associate a thin layer of strongly bound counter-charged ions on their surface, called the Stern layer. Outside the Stern layer, there is another layer of ions, called diffuse outer layer where ions are loosely associated with the particle. The diffuse outer layer of ions generates a boundary between the particle and ions that remain in the surrounding medium. The electrostatic potential of this boundary is the ζ -potential of a particle. To measure ζ -potential, an electrical field is applied across the sample and the movements (electrophoretic mobility) of particles are measured by the light scattering of the particles (reviewed in Doane et al. 2012).

We used Zetasizer Nano ZS apparatus (Malvern Instruments, United Kingdom) to measure size, ζ -potential and polydispersity in our studies. We used

different incubation mediums for CPP/nucleic acid NPs – water, serum-free and serum-containing medium, and in Paper I NaCl aqueous solution was also used.

3.4.2. Transmission electron microscopy (TEM)

DLS is highly suitable method for fast screening to obtain a general overview of the properties of particles under investigation. However, this method does not provide detailed information about the morphology of the nanoparticles. In addition, DLS is an indirect measurement that presumes the particles to be spherical. Moreover, the signal from small particles can be easily underestimated in the background of large particles (Troiber et al. 2013). Lastly, the outcome of DLS is the hydrodynamic diameter of particles, not their actual size (Huang et al. 2010, Troiber et al. 2013). Thus, additional techniques should be used in parallel to obtain complementary and more reliable results. Negative staining TEM enables to directly visualize individual nanoparticles, and thus, provides information about their morphology, size, size distribution, and aggregation.

We employed negative staining TEM analysis (Paper IV) for the detailed characterization of CPP/nucleic acid nanocomplexes. Negative staining TEM has been used for the morphological characterization of liposomes and lipoplexes in various studies (Hatziantoniou et al. 2007, Ruozi et al. 2011, Gilleron et al. 2013), but to our knowledge, this approach has not been used for the examination of CPP/nucleic acid nanocomplexes before.

An important prerequisite for successful negative staining is the correct preparation of TEM support grids. We covered copper grids with formvar film and thin (5–6 nm) carbon layer. Since freshly prepared carbon deposit is hydrophobic, and results in poor and uneven distribution of stain, the carbon coated grids need to be treated prior experiment to obtain hydrophilic surface. In order to produce hydrophilic carbon layer, we employed glow discharge treatment before each experiment.

For conducting negative staining TEM analysis we adsorbed preformed CPP/nucleic acid NPs to carbon coated TEM grids, exposed samples to 2% uranyl acetate for, removed excess of stain, allowed to air-dry, and imaged at 120 kV accelerating voltage on FEI Tecnai G2 Spirit electron microscope (FEI, The Netherlands). The principle of negative staining TEM is simple. The heavy metal salts predominantly stain the surface of grids while nanoparticles remain unstained, and the TEM image is generated by distinct electron scattering from nanoparticles and stained background due to the mass-thickness difference.

Various heavy metal salts can be used for negative staining TEM experiments. The most well-known negative stains are uranyl-acetate (pH 4.2–4.5), sodium phosphotungstate (pH 5–8), ammonium molybdate (pH 5–7) and methylamine tungstate (pH 6–7) (reviewed in Harris and De Carlo 2014). We used 2% aqueous uranyl acetate because this stain produces high contrast of images, and assures even distribution of stain on samples.

3.5. Cellular uptake and intracellular trafficking of CPP/nucleic acid nanocomplexes

3.5.1. Confocal laser scanning microscopy (CLSM)

Confocal laser scanning microscopy (CLSM) is a highly suitable approach for intracellular trafficking of CPP/nucleic acid complexes in living cells. In Paper III we transfected cells with double-labelled CPP/pDNA nanocomplexes where peptide and plasmid DNA were tagged with different fluorophores – fluorescein (green) and CX-Rhodamine (red), respectively, to track their uptake in real time using CLSM. To be able to detect the rearrangements of nanocomplexes in cells we optimized the concentration of labelled molecules to yield an equal signal of both fluorochromes, which displays nanocomplexes in a yellow colour in a combined image. We captured images of live cells after 30 min and 2 h with Olympus Flow View FV1000 confocal laser scanning microscope (Olympus, Japan). This technique allowed us to visualize the changes in the composition of nanocomplexes in time and in specific loci. The dissociation of peptide which was labelled with green emitting fluorescence shifted the colour of complexes toward orange or red, and the dissociation of pDNA which was labelled with red emitting fluorescence changed the colour of nanocomplexes to green. Care must be taken in the interpretation of the results using this technique because accumulation of nanocomplexes into late endosomal compartments with low pH (pH 5–6) decreases the green emission of fluorescein that was used for labelling of the peptide.

3.5.2. TEM

The most widely used approach to investigate the cellular uptake and intracellular trafficking of CPP/nucleic acid nanocomplexes is co-localization analysis with endosomal markers using fluorescence microscopy. This approach is highly suitable for the studies using live cells, however, there are several limitations. Most importantly, the resolution of fluorescence microscopy is limited to about 200 nm (super-resolution 10–20 nm), which could cause the false co-localization signal of labelled complexes and markers of cellular compartments located in close proximity. Secondly, fluorescence signal can be quenched in cells upon non-covalent interactions between fluorophore and its molecular milieu. In addition, the ratio of fluorescently labelled markers needs to be optimized to avoid one fluorescent probe to eclipse the fluorescence of the other probe. Thus, complementary techniques should be used in parallel to assure relevant interpretation of the results. Transmission electron microscopy (TEM) provides high resolution (about 2 nm in cells), and thus, enables to investigate the plasma membrane association and cellular localization of CPP/cargo complexes at ultrastructural level. For TEM analysis cells need to be fixed and therefore dynamic events cannot be directly visualized, however, by varying the incubation times of CPP/cargo complexes on cells, one can examine the intracellular localization of the nanocomplexes in time-dependent manner.

We used conventional TEM for the fixation and embedding of cells for preserving the morphology at ultrastructural level for analysis (reviewed in Margus et al. 2015). We fixed cells using 2.5% glutaraldehyde, postfixed with 1% OsO₄, dehydrated with ethanol series, and flat-embedded in epoxy resin. Flat-embedding was used because this method allows visualizing the largest area of individual cells.

For visualization of nucleic acids with electron dense tag we used in principle two different approaches. In Paper II we tagged SSO molecule covalently with a NanogoldTM (NG; d=1.4 nm) label. Thus, we were able to directly visualize single oligonucleotide molecules at the cell surface and inside cells. In Paper I and III we performed a TEM analysis using pDNA instead of oligonucleotides. For visualization we first biotinylated pDNA and then complexed the biotinylated pDNA with streptavidin-NanogoldTM (SA-NG) (Paper I) or neutravidin-gold (NA-gold) (d=10 nm) (Paper III). We labelled each pDNA molecule with about three SA-NG (Paper I) or two NA-gold clusters (Paper III).

We captured TEM images at 100 kV accelerating voltage on JEM-100S (JEOL, Japan) or FEI Tecnai G2 Spirit (FEI, The Netherlands) electron microscope.

4. RESULTS

4.1. Cell-entry mechanisms and intracellular trafficking of PepFect14/pDNA NPs (Paper I)

Recently, Ezzat *et.al.* designed a novel stearyl-TP10 (st-TP10) based peptide vector PepFect14 (PF14) for nucleic acid delivery (Ezzat et al. 2011). PF14 contains ornithines and leucines instead of lysines and isoleucines in its primary sequence. This design is based on previous reports stating that poly-L-ornithine-based transfection systems yield higher biological activity of delivered biomolecules compared to poly-L-lysine-based delivery vectors (Ramsay and Gumbleton 2002). Ornithine as a non-standard amino acid was suggested to grant the peptide higher resistance against serum peptidases. The measurement of luciferase mRNA levels after running RT-PCR revealed high transfection efficacy of PF14/SSO nanocomplexes in HeLa pLuc 705 cells, yielding >85% of splicing correction after 24 h of transfection. The EC_{50} of PF14/SSO nanocomplexes was low (about 100 nM) in both serum free and serum-containing tissue culture media. Importantly, significant splice correction activity was measured in mdx mouse myotubes, a functional cell culture model for Duchenne muscular dystrophy, even in the presence of serum proteins (Ezzat et al. 2011) (Table 5).

In paper I we analysed whether PF14 is suitable for the delivery of pDNA. In addition we examined the formation of PF14/pDNA nanocomplexes, their cellular uptake mechanism, and intracellular trafficking.

4.1.1. PF14 forms stable NPs with pDNA

In order to examine whether PF14 forms NPs with pDNA we conducted a gel retardation assay using different CRs of PF14 and pDNA. We used CRs 0.5: 1–4:1 (CPP: pDNA) for the formation of nanocomplexes, and found that the charge of pDNA was completely masked (and probably incorporated into nanoparticles) at CR2 since at this and higher ratios pDNA did not migrate into the gel (Paper I, Fig. 1a). In addition, we employed ethidium bromide (EtBr) quenching assay and demonstrated that the fluorescence quenching reached a plateau at CR2, indicating the absence of free pDNA at higher CRs (Paper I, Fig. 1b). We obtained similar results when used PF14 which lacks N-terminal stearyl motif (ns-PF14) for the formation of nanocomplexes with pDNA (Paper I, Fig. 1b).

The stability of nanoparticles developed for drug delivery is an important parameter. On one hand, the CPP/nucleic acid complexes need to be stable in blood circulation in order to resist degradation by serum proteases and/or nucleases. On the other hand, inside cells, the dissociation of the carrier peptide from nucleic acid molecule needs to be ensured to yield biological function of the cargo in its action site in cytoplasm or nucleus. We used heparin displacement

to analyse the particle-dissociation properties of PF14/pDNA by gel electrophoresis. Incubation of PF14/pDNA with varying amounts of negatively charged heparin increased the concentration of free pDNA (Paper I, Fig. 1d). By using spectrofluorometer we revealed that about 50% of the pDNA was released from the NPs at heparin sodium concentration of 10 mg/ml. Interestingly, nano-complexes formed with ns-PF14 dissociated at lower heparin concentrations, suggesting that these complexes are less stable (Paper I, Fig. 1d). As discussed in the next chapter, ns-PF14 did not induce the transgene expression in transfected cells in contrast to PF14/pDNA which yielded high luciferase activity of delivered plasmid. Similar observations have also been made earlier when st-TP10 was shown to yield higher activity of delivered pDNA compared to ns-TP10/pDNA nanocomplexes which lacked biological functionality (Lehto et al. 2011). Taken together, our results indicate that the hydrophobic motif in the CPPs sequence is important for the formation of stable nanocomplexes, and the stability of CPP/nucleic acid NPs is crucial for inducing biological activity of bioactive molecules.

We analysed the size of PF14/pDNA NPs by DLS, and found that PF14/pDNA NPs had a size of 130–170 nm (CR 1–3) when formed in water (Paper I, Table 1). The addition of OptiMEM or OptiMEM and FBS increased the size of the NPs about 2-fold. The ζ -potential of the PF14/pDNA NPs (at CR 2) formed in water was about -40 mV. The addition of OptiMEM or OptiMEM and FBS shifted the ζ -potential to near neutral, but the overall charge of the nanocomplexes remained negative.

4.1.2. PF14/pDNA NPs internalize to cells via caveolin-mediated endocytosis and macropinocytosis

Next, we assessed whether PF14-mediated cellular delivery of plasmid DNA induces biological response in cells. We incubated CHO cells with preformed nanocomplexes of PF14 and luciferase encoding pGL3 plasmid. After 24 h of incubation, the luciferase activity had increased 4 orders of magnitude (Paper I, Fig. 2a). As mentioned above, complexes formed with ns-PF14 did not yield luciferase expression (Paper I, Fig. 2a). By using fluorescence-activated cell sorter (FACS) analysis we found that PF14/pDNA NPs were internalized by cells in dose-dependent manner in both serum free (Paper I, Fig. 2b) and serum containing (Paper I, Fig. 2c) tissue culture media. PF14 induced 20–30-fold higher luciferase activity compared to its predecessor PF3 (st-TP10) (Paper I, Fig. 2d).

In order to analyse the plasma membrane association, cellular uptake mechanism, and intracellular trafficking of PF14/pDNA nanocomplexes we performed a TEM analysis. To visualize pDNA in TEM we associated biotinylated pDNA with about 3 streptavidin-NanogoldTM (SA-NG) molecules, and complexed with PF14. PF14/pDNA associated with the cell-surface as small clusters which typically contained 2–10 SA-NG labels, indicating the incorporation of about 1–2

pDNA molecules in a nanocomplex (Paper I, Fig. 3a,b). Mostly, these complexes associated with the surface of cells as single NPs, but occasionally interacted to each other forming chain-like structures. Frequently, we detected the nanocomplexes in membrane invaginations of 50–100 nm in diameter (Paper I, Fig. 3b). Judged by their size and morphology, these invaginations were of caveolar origin. Occasionally, we detected nanocomplexes in rosette-like structures resembling so called caveosomes (paper I, Fig 3a, inset). After 1 h of incubation the vast majority of PF14/pDNA nanocomplexes resided in endosomes containing numerous small vesicles in the vesicles lumen – multivesicular bodies (MVBs)/late endosomes (Paper I, Fig. 3c,d). Occasionally, the endosomal membranes had lost their intactness, paving the way for the nanoparticles to escape to cytosol (Paper I, Fig. 3d). Still, we rarely detected SA-NG labels in cytoplasm without being surrounded by endosomal membrane after 1 h of incubation.

In the TEM experiments the amount of labelled SSOs detected at the plasma membrane and inside cells was much smaller than we expected. Possibly, the PF14 packed nanogold-labelled pDNA into very compact nanoparticles, making the nanogold label inaccessible for enhancement by silver ions. Therefore, we later repeated the experiments using biotinylated pDNA labelled with neutravidin-colloidal gold ($d = 10$ nm) (homemade) (NA-gold) which does not require silver enhancement due to sufficient size for detection in TEM. We labelled biotinylated pDNA with about 3 NA-gold molecules, and complexed with PF14. The PF14/pDNA complexes associated with the plasma membrane of CHO cells as in Paper I, typically containing 1–10 NG-gold particles, indicating the presence of 1–3 plasmid molecules in a nanoparticle (Fig. 2a–c). At the surface of cells, we detected PF14/pDNA nanocomplexes frequently in small membrane invaginations which resembled caveolae (Fig. 2b) or in lamellipodes which resembled macropinocytosis (Fig. 2c, arrows). A fraction of nanocomplexes localized in small transport vesicles near the plasma membrane (Fig. 2a,d). After 2 h of incubation most PF14/pDNA complexes that had internalized to cells were entrapped inside MVBs (Fig. 2e, arrows), but occasionally, SSOs were detected in cytosol (Fig. 2e, arrowhead). After 4 h of incubation, the nanocomplexes were still mostly entrapped inside MVBs (Fig. 2f, arrows), however, we rarely detected the complexes also in lysosomes (Fig. 2g, arrows). We did not see any PF14/pDNA nanocomplexes inside the nucleus of cells during 4 h of incubation.

Our results are in good correlation with earlier observations that incubation of PF14/SSO nanocomplexes at 4°C which inhibits energy-dependent cellular uptake mechanisms significantly decrease the activity of delivered SSO. In addition, chloroquine has been shown to increase the functional activity of PF14-mediated SSO, confirming that endosomal entrapment is the limiting factor of peptide mediated delivery of nucleic acids (Ezzat et al. 2011).

Recently, we employed pharmacological inhibitors of endocytosis to examine the cellular uptake mechanism of PF14/SSO nanocomplexes, and found that the bioactivity of SSO in HeLa pLuc 705 cells was significantly reduced in the

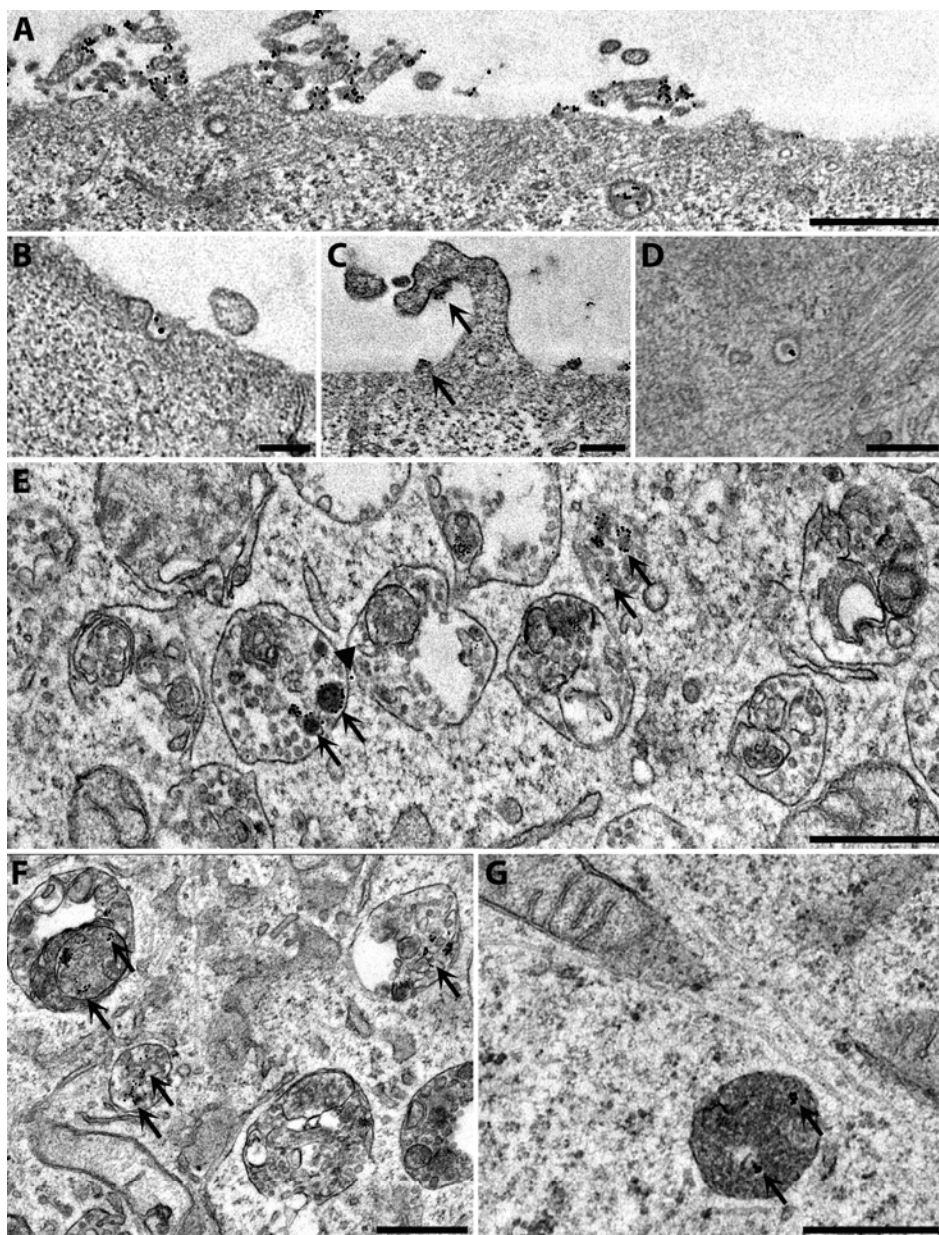


Figure 2. Cell-entry and intracellular trafficking of PF14/pDNA nanocomplexes. Cell-surface interactions (A–C) and intracellular localization (D–G) of PF14-pDNA complexes labelled with neutravidin-gold ($d=10$ nm) in CHO cells after 1 h (A–D), 2 h (E) or 4 h (F,G) of incubation in serum-containing tissue culture medium. Arrows show PF14/pDNA nanocomplexes at the plasma membrane (C), in multivesicular bodies (E, F) and in lysosome (G). Arrowhead in E shows pDNA in cytosol. Scale bars: 500 nm (A, E–G), 100 nm (B–D).

presence of amiloride and nystatin which impede macropinocytosis and caveolin-mediated endocytosis, respectively (Juks et al. 2015). Interestingly, although the nanocomplexes-containing endosomes translocated to perinuclear region of cells, these did not co-localize with Lysotracker, which specifically marks acidic compartments of cells, even after 4 h of incubation. By this time, approximately 8% of nanocomplexes had been released from endosomes. In addition, we demonstrated that PF14/SSO nanocomplexes are not directed to endoplasmic reticulum or Golgi complex as earlier been suggested for cargo internalized by caveolin-mediated endocytosis (Pelkmans et al. 2001, Le and Nabi 2003).

Together, these results show that PF14/nucleic acid nanocomplexes internalize cells via endocytic pathways, and macropinocytosis and caveolin-mediated endocytosis are important for yielding bioactivity of delivered cargo. Although PF14/nucleic acid nanocomplexes yield high bioactivity of cargo, most of the internalized PF14/cargo nanocomplexes still remain entrapped inside endosomes after 4 h of incubation.

4.1.3. Scavenger receptors are involved in the cellular uptake of PF14/pDNA nanocomplexes

Scavenger receptors are a large family of cell surface glycoproteins which can bind polyanionic ligands (Platt and Gordon 1998, Peiser and Gordon 2001). For example, class-A scavenger receptors (SCARAs) have been shown to be involved in the uptake of diverse nucleic acids (Pearson et al. 1993, Limmon et al. 2008, DeWitte-Orr et al. 2010) and oligonucleotide-functionalized gold nanoparticles (Patel et al. 2010). Recently, Ezzat *et al.* revealed that SCARA3 and SCARA5 are involved in the uptake of PF14/SSO nanocomplexes (Ezzat et al. 2012). To evaluate whether SCARAs are also involved in the uptake of PF14/pDNA NPs we pretreated CHO cells with SCARA inhibitory ligands polyinosinic acid (poly I), dextran sulfate and fucoidan and measured the luciferase activity after 24 h of incubation (Paper I, Fig. 4). Inhibition of SCARAs almost entirely abolished the luciferase activity indicating that these receptors are essential for the cellular uptake of PF14/pDNA nanocomplexes. As a negative control, we pretreated cells with polycytidylic acid (poly C), chondroitin sulfate and galactose (structurally similar to the used inhibitory ligands, but lack affinity to SCARAs), and these did not affect the bioactivity of PF14/pDNA nanocomplexes.

Collectively, in Paper I we showed that PF14 packed pDNA into stable nanoparticles which had a size of 130–170 nm in diameter when formed in water. The addition of tissue culture medium or physiological salt solution increased the size of particles 2-fold or 4-fold, respectively. The ζ -potential of the PF14/pDNA nanoparticles was slightly negative both when formed in water or in tissue culture media. PF14/pDNA nanocomplexes internalize to CHO cells by endocytosis, and specific mechanisms involve caveolin-mediated endocytosis and macropinocytosis. The limiting step of biofunctionality of the cargo is

the entrapment of complexes inside late endosomes as only a small fraction of plasmid molecules were detected free in cytosol.

4.2. NickFect 51 mediates the cellular uptake of SSO using endocytosis (Paper II)

In Paper II we designed three st-TP10 based CPPs in order to improve the effectiveness of the peptide to mediate the cellular uptake of nucleic acids. NickFect53 (NF53) was obtained by changing the Lys7 of st-TP10 with ornithine, NickFect61 (NF61) was obtained by using ϵ -NH₂ group of Lys7 for subsequent synthesis instead of α -NH₂ that is typically used, and NickFect51 (NF51) was obtained by replacing Lys7 with ornithine and continuing synthesis by coupling Gly6 to δ -NH₂ group of ornithine (Paper II, Fig. 1, Table 5).

We examined the transfection efficacy of these novel CPPs using different types of nucleic acids (pDNA, SSO, siRNA). In addition, we examined the cellular uptake and intracellular trafficking of CPP/SSO nanocomplexes, however, we only employed NF51 for these studies because this peptide led to significantly higher bioactivity of delivered nucleic acids compared to NF53 and NF61.

4.2.1. NFs form nanoparticles with nucleic acids

We evaluated the size of NF51, NF53 and NF61 nanoparticles with nucleic acid by DLS. We found that NFs packed pDNA, SSO or siRNA into particles which had a size of 60–75 nm, 86–135 nm and 70–159 nm respectively, when formed in water (Paper II, Table 1). The addition of serum proteins had a varying effect on the size of the NPs, either retaining, increasing, or decreasing the measured diameter depending on the used CPP and nucleic acid. In the presence of serum proteins NF/nucleic acid NPs had slightly negative ζ -potential in case of all studied peptides.

4.2.2. NF51 efficiently delivers different types of nucleic acids into cells

To analyse the effectiveness of NFs to deliver nucleic acids (SSO, siRNA, pDNA) into cells we incubated cells with preformed CPP/nucleic acid nanocomplexes and measured the biological activity of respective nucleic acid after 24 h of incubation.

We complexed luciferase encoding pGL3 plasmid with NF51, NF53 or NF61, incubated in CHO cells, and measured the luciferase expression level 24 h later. NF53 and NF61 led to 10–100-fold, and NF51 led to about 1000-fold increase in luciferase expression in serum-free cell growth medium compared to st-TP10 (Paper II, Fig. 2a). NF51/pDNA NPs induced target gene expression in

various cell-lines including hard-to-transfect mouse embryonic fibroblasts (MEFs), T and B lymphocytes, Jurkat and A20 cells (Paper II, Fig. 2b–d, Paper II, Fig. S1a–d). While NF53 and NF61 induced lower or same level of SSO activity, NF51/SSO NPs yielded 4–5-fold higher SSO activity compared to st-TP10 in HeLa pLuc 705 cells (Paper II, Fig. 4a). The splice correction activity induced by SSO delivered by NF51 was higher than that of LF2000, both in serum-containing and serum-free tissue culture media (Paper II, Fig. 4a,b). Although NF53 and NF61 effectively induced EGFP downregulation using siEGFP in CHO cells stably expressing EGFP in serum-free medium, the siRNA activity remained low in the presence of serum proteins (Paper II, Fig. 5a). In contrast, NF51/siEGFP induced strong EGFP downregulation in the absence and in the presence of serum proteins (Paper II, Fig. 5a,b).

Taken together, out of three novel TP10-based CPPs NF51 is the most promising vector for nucleic acid delivery. NF51 yields high bioactivity of pDNA, SSO and siRNA in various cell-lines including hard-to-transfect cells, and the activity is not decreased in the presence of serum proteins.

4.2.3. NF51/SSO NPs are released from endosomes

Subsequently, we used TEM analysis to examine the cellular uptake mechanisms and intracellular trafficking of NF51/SSO nanocomplexes. We used SSO molecules covalently tagged with NanogoldTM for the visualization of SSO in cells by TEM. We detected NF51/SSO-NG at the surface of cells as particles of varying size ranging from 80–170 nm (Paper II, Fig. 6a,b). The low electron density suggested that these NPs were loosely packed. Inside cells, we detected NF51/SSO NPs mostly in large (400–500) nm vesicles (Paper II, Fig. 6c). Frequently, the nanocomplexes were in close proximity to the endosomal membrane, and occasionally, the membrane had lost its intactness at the sites of association after 4 h of incubation (Paper II, Fig. 6d). Importantly, we detected some NG particles in the cytoplasm without being surrounded by the limiting endosomal membrane (Paper II, Fig. 6c–f). After 4 h of incubation, we rarely detected some SSO-NGs in nuclei of cells (Paper II, Fig. 6e).

Taken together, in Paper II we designed novel TP10-based CPPs – NF51, NF53 and NF61 – for the delivery of nucleic acids into cells. The CPPs condensed nucleic acids into nanoparticles which had a size range of 60–160 nm depending on the used peptide and nucleic acid, when formed in water. NF51 was the most effective of the three novel peptides for the delivery of pDNA, SSO and siRNA, inducing high biological activity of cargos both in the presence or absence of serum proteins in various cell-lines. Inside cells NF51/SSO nanoparticles localized mainly in large (400–500 nm in diameter) vesicles indicating their uptake via endocytosis. After 4 h of incubation we occasionally detected the NF51/SSO nanocomplexes in cytosol, however, similarly to PF14/pDNA nanocomplexes (Paper I), most of the complexes

remained entrapped in endosomes. Importantly, we detected SSOs in the nuclei of cells after 4 h of incubation, however, this was a rare event.

4.3. NickFects deliver nucleic acids into cells using different endocytic mechanisms (Paper III)

We recently developed a series of st-TP10 based CPPs, termed NickFects, for the delivery of nucleic acids such as SSO, siRNA and pDNA (Oskolkov et al. 2011, Paper II). These peptides yielded high transfection levels of nucleic acids in various cell-lines. In this paper, we examined the cell-entry mechanisms and intracellular trafficking of NF1/pDNA and NF51/pDNA nanocomplexes. NF1 contains a phosphorylated tyrosine in the third position and Ile11 is replaced with threonine as compared to st-TP10 (Table 5). NF51 has Lys7 replaced with ornithine and the δ -amino group of ornithine is used for the following synthesis instead of typically used α -NH₂ group in order to gain a kinked peptide (Table 5). Although different in their primary structures, these CPPs yielded equally high transfection levels of nucleic acids in transfected cells.

4.3.1. Characterization of NF/pDNA NPs

We measured the size of NF/pDNA NPs by DLS and found that both peptides formed NPs with pDNA at CR 2 and CR 3 which had a diameter of about 60 nm when complexed in water (Paper III, Table S1). The ζ -potential of NF51/pDNA nanocomplexes was positive (31–38 mV), and NF1/pDNA NPs had a negative (-18– -13) mV ζ -potential at both used CRs. The addition of serum-containing medium increased the size of NPs from 60 nm to 160 nm and yielded negative ζ -potential for both, NF1/pDNA and NF51/pDNA NPs. The incubation of NPs with serum-containing tissue culture media for 1 h increased the size up to 400–500 nm.

Next, we analysed the stability of nanoparticles by incubating preformed NF/pDNA NPs with varying concentrations of competitor molecule heparin, and analysed the dissociation of nanocomplexes using agarose gel electrophoresis (Paper III, Fig. 1). We found that NF51/pDNA NPs were more resistant to sodium heparin displacement compared to NF1/pDNA NPs. We confirmed these results by using spectrofluorometer, and demonstrated that while NF1/pDNA NPs required 2.5 mg/ml of heparin to replace 50% of pDNA in the NPs, NF51/pDNA needed 7 mg/ml to achieve the same level of heparin replacement in the respective NPs. This data indicates that NF51 forms more stable nanoparticles with plasmid DNA compared to NF1. The higher stability could grant NF51/pDNA nanocomplexes higher resistance against degradation by extracellular proteases and/or nucleases. Still, once inside cells, the release of pDNA from the carrier peptide need to occur in order to trigger the bioactivity of the cargo.

4.3.2. Cell-entry mechanisms of NF/pDNA NPs

Incubation of NF1/pDNA and NF51/pDNA NPs at low (4°C) temperature significantly decreased their cellular uptake, suggesting that their internalization occurs through energy-dependent mechanism (Paper III, Fig. S4). To further confirm that endocytosis is involved in the cellular uptake of NF/pDNA NPs we added chloroquine to the cells incubated with respective NPs. Interestingly, chloroquine did not increase the bioactivity of NF51/pDNA, while it elevated the gene expression level of NF1-mediated pDNA more than 3-fold (Paper III, Fig. 4a).

Subsequently, we used pharmacological inhibitors of endocytosis to impede the activity of common endocytic pathways. We pretreated cells with chlorpromazine, nystatin or cytochalasin D to suppress clathrin-mediated-, caveolin-mediated endocytosis or macropinocytosis, respectively, before transfection. Cytochalasin D reduced the bioactivity of NF51/pDNA NPs for 75% (Paper III, Fig. 4b). Other inhibitors did not affect the activity of NF51/pDNA, indicating that macropinocytosis is the major cell-entry pathway for NF51/pDNA NPs. In contrast, the activity of NF1/pDNA NPs was impeded by 50% in the presence of chlorpromazine or cytochalasin D, and by 20% with nystatin, suggesting that these NPs employ several endocytic pathways to gain entry into cells (Paper III, Fig. 4c). Still, it is important to keep in mind that pharmacological inhibitors of endocytosis are not very specific, and one inhibitor can affect the endocytosis by several mechanisms. Therefore, to gain additional information about the cell-entry mechanisms of NF/pDNA NPs we conducted an ultrastructural analysis using TEM. For visualization, we associated biotinylated pDNA with about 2 gold clusters using labelled neutravidin molecules, and complexed with respective peptides.

NF1/pDNA NPs associated with the cell-surface as small clusters that contained 1–10 NA-gold labels, suggesting the entrapment of 1–5 pDNA molecules in a nanocomplex (Paper III, Fig. 6a,b). The NF1/pDNA NPs were frequently associated with membrane ruffles at the cell surface. Occasionally, the membrane ruffles had fold back to the plasma membrane, encapsulating NF1/pDNA NPs in the resulting macropinosome (Paper III, Fig. 6b). In addition, NF1/pDNA NPs were detected in small (50–100 nm) membrane pits that resembled caveolar invaginations as judged by their size and morphology (Paper III, Fig. 6a). NF51/pDNA NPs associated with the cell-surface in a similar manner with NF1/pDNA NPs – the nanocomplexes contained 1–10 NA-gold clusters (Paper III, Fig. 6c,d). In line with NF1/pDNA NPs, these complexes were often associated with membrane ruffles or localized in their close proximity (Paper III, Fig. 6c,d).

Our TEM data suggested together with experiments using pharmaceutical inhibitors that macropinocytosis is involved in both NF51- and NF1- mediated pDNA delivery. NF1, however, employs also receptor-mediated endocytosis (CME, caveolin-mediated endocytosis) for the intracellular delivery of pDNA.

4.3.3. Intracellular trafficking of NF/pDNA NPs

Because of different response of NF1/pDNA and NF51/pDNA to chloroquine treatment we speculated whether NF1 and NF51 might have distinct intracellular trafficking paths. We examined the integrity of the NF/pDNA NPs during the cellular uptake and subsequent trafficking using double-labelled NF/pDNA nanocomplexes, where CPP and plasmid were labelled with different fluorophores. This approach allowed us to track their uptake in real time using confocal laser scanning microscopy. In order to be able to track the rearrangements in the nanoparticles, we optimized their composition to yield equal signal of both fluorophores, displaying complexes in a yellow colour in a combined image.

We incubated HeLa cells with double-labelled NF/pDNA nanocomplexes where CPP was labelled with green light emitting fluorescein and plasmid was labelled with red light emitting rhodamine. After 2 h of incubation, NF51 was still associated with pDNA in cells (yellowish signal of complexes) (Paper III, fig. 3d). However, NF1/pDNA NPs turned red (Paper III, Fig. 3b). The shift of NF1/pDNA NPs to red colour was probably caused by the maturation of early endosomes into late endosome, where the drop of pH to 5–6 drastically decreased the green signal. The loss of green signal could have been caused by the partial dissociation of NF1 from pDNA. These observations indicated that NF51/pDNA complexes might exploit endosomal pathways in which vesicles are kept near-neutral (Räägel et al. 2009), or the complexes interfere with the acidification of endosomes.

Interestingly, in case of both peptides we detected a fraction of peptide bound to the plasma membrane of cells that did not co-localize with plasmid (Paper III, Fig. 3, arrows). The free peptide was distributed all over the membrane and did not localize close to NF/pDNA nanocomplexes.

Next, we performed an ultrastructural analysis by TEM to further examine the intracellular localization of NF/pDNA NPs. After 4 h of incubation both NF1/pDNA- and NF51/pDNA-containing endosomes localized in the central region of the cell (Paper III, Fig. 6e,f). Almost all NF1/pDNA NPs stayed entrapped in multivesicular bodies, and we rarely detected NA-gold in cytoplasm (Paper III, Fig. 6e). In contrast, we detected about 1/10th of total intracellular NF51/pDNA particles in cytoplasm after 4 h of incubation (Paper III, Fig. 6f). NF51/pDNA NPs were able to disrupt the limiting endosomal membrane and pave their way to the cytoplasm easier/faster compared to NF1/pDNA NPs.

Although we detected NA-gold labels in cytoplasm in case of both, NF1/pDNA and NF51/pDNA NPs, we could not detect these in the nuclei of cells. This indicates that the translocation into nucleus is either a rare process, or 4 h of incubation is not sufficient to reach to the nucleus in amounts that are easily detectable by TEM.

4.3.4. Scavenger receptors are involved in the uptake of NF/pDNA NPs

In our previous publication (Paper I) we demonstrated that SCARAs are involved in the uptake of PF14/pDNA NPs. Since both NF/pDNA NPs obtain negative ζ -potential in the presence of serum proteins we speculated whether SCARAs can also be involved in the uptake of NF/pDNA NPs. By pretreating cells with inhibitory ligands of SCARAs (poly I, fucoidan, dextran sulfate) the transfection activity of NF-mediated pDNA decreased significantly, while pretreatment with poly C, galactose, and chondroitin sulphate did not have any respective effect (Paper III, Fig. 2a,b, Paper III, Fig. S2). This data suggests that scavenger receptors are involved in the cellular uptake of NF/pDNA NPs.

We found earlier (Paper I) that particularly scavenger receptors from class A, SCARA3 and SCARA5 are essential for the cellular uptake of CPP/nucleic acid NPs. Therefore, we examined whether SCARA3 and/or SCARA 5 are also important for the cellular uptake of NF/pDNA NPs. Indeed, pretreatment of HeLa cells with respective siRNAs yielded $\geq 85\%$ inhibition of transfection with both peptides, while scrambled siRNA did not affect the transfection efficacy (Paper III, Fig. 2c,d).

Taken together, in Paper III we showed that NF1 and NF51 condense pDNA into nanoparticles which have a size of about 60 nm in diameter when formed in water. Similarly to PF14/pDNA (Paper II), the addition of tissue culture media increased the size of the nanoparticles about 2–3-fold, and the particles obtained a slightly negative ζ -potential. The association of NF1/pDNA and NF51/pDNA nanocomplexes to scavenger receptors SCARA3 and SCARA5 at the plasma membrane is essential for the cell-entry. Both studied NickFects are internalised by cells via endocytosis, however, specific mechanisms vary. NF51/pDNA NPs are taken up by cells mainly via macropinocytosis, whereas NF1/pDNA NPs utilize several endocytic mechanisms in parallel, including macropinocytosis and clathrin- and caveolin-mediated endocytosis.

4.4. Characteristics of Cell-Penetrating Peptide/Nucleic Acid Nanoparticles (Paper IV)

In paper IV we systematically examined the size and morphology of CPP/nucleic acid nanoparticles using negative staining TEM and dynamic light scattering. We included four most promising and efficient st-TP10 based CPPs to the study – PF6, PF14, NF1 and NF51, and analysed the size and morphology of resulting nanoparticles using three types of nucleic acids (SSO, siRNA, pDNA) which differ in their size, chemical composition and biological activity. In addition we examined the effect of fluorescent or (nano)gold label on nucleic acids to the physical properties of the nanoparticles.

4.4.1. CPPs pack pDNA to nanoparticles which have similar size and morphology

In order to examine the size and morphology of CPP/nucleic acid NPs we conducted a negative staining TEM analysis. We used CPP: pDNA charge ratio 3 for the formation of nanoparticles because this ratio has previously yielded high transfection rates in functional cell-based assays (Paper I, Paper III). We found that all studied CPPs complexed with pDNA formed NPs which had homogeneous shape (Paper IV, Fig. 1). However, the morphology of the NPs depended on the primary sequence of the used peptide. PF6/pDNA NPs were spherical (AR 1.1 ± 0.1), most NF1/pDNA and NF51/pDNA NPs were also spherical but a small fraction of the NPs had irregular or elongated shape (AR ≤ 1.2). In contrast, PF14/pDNA nanoparticles had varying shapes which ranged from spherical and elliptic to branched and ones with irregular shape (AR 1.4 ± 0.5) (Paper IV, Fig. 1; Paper IV, Table 2).

To analyse the size of CPP/pDNA nanoparticles we measured the 2D projections of 600 individual NPs from three different experiments using Fiji image processing software package and calculated their circle equivalent diameter. We found that although different in their chemical composition, the studied CPP/pDNA NPs had similar mean size ranging from 50–60 nm depending on the used peptide (Paper IV, Figure 2a,b).

We have previously reported that the transfection efficiency of CPP-transduced pDNA depends on the CR of used CPP and nucleic acid. Specifically, we showed that PF14/pDNA NPs yield the highest biological activity at CR 3 and in some cell-lines NPs formed at CR 1 and CR 2 lead to only slight expression of transgene (Paper I). Thus, we examined the size and morphology of CPP/PF14 nanocomplexes formed at different CRs (CR 1, CR 3, CR 5). Interestingly, only a few PF14/pDNA NPs were formed at CR 1 and most of these were agglomerated. However, using CR 3 or CR 5 led to the formation of NPs which did not agglomerate and had uniform size and morphology (Paper IV, Fig. S4).

In addition, we examined whether NFs and PFs could form NPs on their own. However, we did not detect any NPs in the respective samples.

4.4.2. CPPs form smaller nanoparticles with SSO and siRNA compared to pDNA

In order to analyze the size and morphology of CPP/oligonucleotide NPs we included two different types of oligonucleotides to the study – SSO (2'OMe phosphorothioate ON; 18 nucleotides) and siRNA (42 nucleotides). We used MR 10 (CPP: peptide) for the formation of complexes because we previously showed that this molar ratio leads to the highest bioactivity of SSOs in functional cell-based assays (Paper II, Fig. 4b). The CPP/oligonucleotide complexes had similar shapes as in case of CPP/pDNA NPs (Paper IV, Fig. 3). While PF6 and NF51 formed spherical NPs, PF14 NPs had varying shapes ranging from

spherical to non-spherical elongated structures. Frequently, the smaller NPs had associated into larger particles. Unexpectedly, we only detected a few NF1/siRNA NPs by TEM. We speculated whether the negative charge of the phosphoryl group in the primary sequence of NF1 could reduce the complexation efficacy of these NPs, and thus, tested if NF1 could form NPs with siRNA at higher peptide concentrations. Indeed, NF1 efficiently formed NPs with siRNA at MR 20 and MR 30, and these had similar size and shape to PF6/siRNA and NF51/siRNA (Paper IV, Fig. 3).

The CPP/SSO and CPP/siRNA NPs had significantly ($p < 0.001$) smaller size compared to CPP/pDNA NPs ranging from 27–38 nm and 32–34 nm in diameter, respectively (Paper IV, Fig. 2a,c,d). The bigger size of CPP/pDNA NPs compared to CPP/oligonucleotide NPs could be explained by the different size of used nucleic acids. Since pGL3 plasmid ($M_w = 3.1 \times 10^6$ g/mol) is a much larger molecule compared to SSO ($M_w = 5900$ g/mol) or siRNA ($M_w = 14300$ g/mol) the dimensions of the pDNA could determine the size of the forming NPs.

In line with CPP/pDNA NPs, the transfection efficiency of CPP/SSO NPs has been shown to be dependent on the concentration ratio of CPP and SSO. For example, PF14/SSO NPs showed the highest splice correction efficiency at MR 5, and the activity was about three times lower at MR 20 (Ezzat et al. 2011). Therefore, we analyzed the size and morphology of PF14/SSO nanocomplexes formed at different MRs (MR 5, MR 10, MR 20). We found that PF14 efficiently formed NPs with SSO at all tested MRs and their size and shape were not dependent on the used peptide concentration (Paper IV, Fig. S3).

4.4.3. Dynamic light scattering overestimates the size of CPP/nucleic acid NPs

Dynamic light scattering (DLS) is the most commonly used method to measure the size of nanoparticles. We performed DLS analysis of PF14 and PF6 NPs with nucleic acids. DLS estimated that PF14/pDNA and PF14/SSO NPs had an average diameter of 94 nm and 142 nm, respectively. The diameter of PF6/pDNA and PF6/SSO NPs was 70 nm and 64 nm, respectively (Paper IV, Fig. 4). We noticed that in case of both peptides, the NPs formed with SSO had two distinct populations of particles. The fraction of smaller PF14/SSO and PF6/SSO NPs had a diameter of 25 nm and 23 nm, and the fraction of larger NPs had a size of 64 nm and 142 nm, respectively. The larger size of NPs measured by DLS compared to negative staining TEM could be explained by the higher sensitivity of DLS to detect larger particles as these dominate the scattering of light that is detected (Troiber et al. 2013). In addition, DLS measures the hydrodynamic size of the NPs rather than the actual diameter, which increases the estimated size of NPs (Huang et al. 2010, Troiber et al. 2013)

4.4.4. The fluorescent or (nano)-gold label on nucleic acid does not affect the gross-characteristics of CPP/nucleic acid nanoparticles

Recently, we used fluorescence and transmission electron microscopy using fluorescent or (nano)gold label on nucleic acid molecules to examine the cellular uptake and intracellular trafficking of CPP/nucleic acid nanocomplexes (Oskolkov et al. 2011, Paper I, Paper II, Paper III). We analyzed whether the addition of Cy5 or gold label affects the size and morphology of CPP/nucleic acid nanocomplexes. We used Cy5-SSO, SSO-NanogoldTM (SSO-NG), siRNA-NanogoldTM (siRNA-NG) and biotinylated pDNA complexed with neutravidin-gold (pDNA-b-NA-gold) for the formation of nanocomplexes with CPPs.

We found that PF6 and PF14 NPs formed by using siRNA-NG had similar size and shape with NPs formed with unlabelled siRNA (Paper IV, Fig. S2). Surprisingly, we detected only a few NPs with both NickFects using siRNA-NG, and these were frequently agglomerated. All studied peptides formed NPs with SSO-NG but these were slightly smaller compared to NPs formed with unlabelled SSO. Since SSO is two times smaller than siRNA, it is probable that the NanogoldTM label affects more the formation of CPP/SSO NPs compared to CPP/siRNA NPs. In addition, since the used SSO has modified backbone, this could together with NanogoldTM label influence the morphology of resulting CPP/SSO NPs more than in case of CPP/siRNA NPs.

The addition of Cy-5 label did not affect the properties of PF6/SSO or PF14/SSO NPs and these had similar size and morphology as unlabelled NPs. Both NickFects, however, formed NPs with Cy5-SSO less efficiently compared to unlabelled SSO, and the former were more often agglomerated (Paper IV, Fig. S2).

In order to analyse whether the addition of gold label to pDNA influences the morphology of CPP/pDNA NPs we labelled biotinylated pDNA with neutravidin gold, and formed nanocomplexes with NF51 and conducted negative staining TEM analysis. We found that the association of NA-gold label to pDNA did not change the morphology of NF51/pDNA NPs compared to unlabelled NF51/pDNA NPs. To analyse the degree of labelling we counted the number of gold labelled NPs, and found that out of 480 NPs 298 (62%) had associated one or more gold labels. The majority of NPs (73%) had associated 1–3 gold tags, and only 10% had associated more than 7 gold labels. 81% of gold particles had attached to the NPs, showing a high labelling efficacy (Paper IV, Fig. S5).

Taken together, our data shows that using labelled nucleic acids does not influence the gross-characteristics of CPP/nucleic acid nanocomplexes.

Collectively, in Paper IV, we examined the size and morphology of CPP/nucleic acid complexes. We found that PFs and NFs condense nucleic acids into NPs of homogeneous size ranging from 30–60 nm in diameter depending on the type of used nucleic acid and peptide. Importantly, the NPs did not aggregate when formed in water. The shape of CPP/nucleic acid complexes depended on the

sequence of used peptide. The major determinant of the NP size was the molecular weight of condensed nucleic acid. The fluorescence or (nano)gold label on nucleic acid did not affect the gross-characteristics of CPP/nucleic acid nano-complexes.

5. DISCUSSION

The development of nucleic acid-based therapeutics is an emerging field of molecular medicine due to the ability of nucleic acids to specifically regulate the function of genes. Since naked nucleic acids do not effectively enter cells and can be quickly degraded upon administration, there is a strong need for the development of delivery vehicles to facilitate the cellular delivery of nucleic acids. An ideal delivery vector should effectively internalize nucleic acids into cells without being toxic, and importantly, promote the endosomal release of cargo in order to reach their target sites in the cytoplasm or nucleus of cells. Nanoparticle-based delivery vectors such as polyplexes or lipoplexes which pack nucleic acids into particles generally <100 nm in diameter have shown high potential in the cellular delivery of nucleic acids, and many such systems are currently under clinical evaluation for the treatment of various diseases (reviewed in Yin et al. 2014). The advantages of nanoparticle-based drug delivery systems are their improved stability, biocompatibility and extended drug-release kinetics compared to non-nanoparticulate systems. Some recently designed cell-penetrating peptides (CPPs) also condense nucleic acids into particles upon co-incubation of CPP and cargo. During the last 20 years, various studies have shown that CPP/nucleic acid complexes effectively internalize to cells and trigger high bioactivity of cargo both *in vitro* and *in vivo* (reviewed in Margus et al. 2012). Regardless of promising experimental data, the CPP/nucleic acid non-covalent delivery systems have not yet reached clinical trials. One reason behind this is the insufficient information of the physical-chemical characteristics of the forming CPP/nucleic acid nanocomplexes such as their size, shape, charge and stability. Yet, in order to be considered for implementation in biomedicine the properties of a drug-delivery system need to be characterized in detail. In addition, very little is known about the cell-entry mechanisms and intracellular trafficking of CPP/nucleic acid complexes. However, the understanding of the underlying mechanisms of cell-entry and intracellular trafficking are important to avoid undesired side effects and to refine their properties to trigger higher bioactivities of cargo.

The physical-chemical characteristics of nanoparticles are of utmost importance in order to be used *in vivo* in experimental models and medical settings. One of the most important characteristics of nanoparticles is their size as it determines whether the particles are engulfed by cells, and which mechanisms are harnessed for their cellular uptake. In the current study we used PepFect and NickFect type CPPs and analysed the size of their nanocomplexes with nucleic acids using dynamic light scattering (DLS) and negative staining transmission electron microscopy (TEM) analysis. TEM analysis revealed that the studied CPPs condensed nucleic acids into homogeneous nanoparticles which did not aggregate and had a size in range of 50-60 nm (CPP/pDNA) and 30-40 nm (CPP/oligonucleotides) in diameter. According to DLS the size of CPP/pDNA nanoparticles varied from 60-70 nm (94 nm in case of PepFect14/pDNA) and

CPP/SSO complexes had a diameter of 60–80 nm (140 nm in case of PepFect14) depending on the used peptide. The higher diameter of nanoparticles measured by DLS compared to TEM have been earlier shown in various studies (Huang et al. 2010), and this can result from several methodological aspects. Firstly, the DLS analysis measures the hydrodynamic radius of nanoparticles rather than the actual size which could increase the diameter of NPs (Huang et al. 2010, Troiber et al. 2013). Secondly, in DLS analysis the signal from small particles can be underestimated in the background of larger particles (Troiber et al. 2013). Nevertheless, according to both DLS and TEM results, PepFects and NickFects condense nucleic acids into nanoparticles of small size (below 100 nm) and rather narrow size distribution. Importantly, the nanoparticles did not aggregate when formed in water. According to literature, the optimal diameter for the cellular uptake of nanoparticles is about 50–60 nm (Zhang et al. 2004, Chithrani et al. 2006, Chithrani and Chan 2007), and the upper limit for receptor-mediated endocytosis is about 200 nm. Larger nanoparticles can be internalized to cells via macropinocytosis. Our results clearly indicated that the studied CPPs condense nucleic acids into particles which have a suitable size range for the uptake via receptor-mediated endocytosis.

Interestingly, we found that all studied CPPs formed larger nanoparticles with pDNA than with oligonucleotides. The larger diameter of CPP/pDNA NPs compared to CPP/oligonucleotide NPs could be explained by the different size of used nucleic acids. Since pGL3 plasmid (MW= 3.1 MDa) is a much bigger molecule compared to SSO (Mw= 5.9 kDa) or siRNA (Mw= 14.3 kDa) the dimensions of plasmid DNA should determine the size of the forming NPs if one pDNA molecule is present in a nanoparticle. To our knowledge this is the first study showing that the size of CPP/nucleic acid nanoparticles depends on the type and molecular weight of nucleic acid. Interestingly, the label on the nucleic acid did not influence the size and morphology of forming nanoparticles. Even the colloidal gold label with 10 nm diameter did not interfere with the formation of CPP/pDNA nanoparticles or modify their properties. This suggests that both the fluorescent and gold-clusters can be coupled to nucleic acids for assessing their delivery by CPPs to cells and tissues.

Importantly, the formation of NickFect and PepFect nanocomplexes with nucleic acids for in vivo delivery studies has been performed in identical manner with our TEM experiments, e.g. the complexes were formed in water for 30–60 minutes. By that time, stable nanoparticles are formed, and the size and morphology of these do not change in time (even after 3 days of incubation in water at room temperature) as we have confirmed by TEM and DLS (our unpublished data). The only difference between the complexes used in our experiments compared to the complexes used for the in vivo studies is that we did not add glucose to the complexes prior the analysis. However, the addition of glucose which is routinely used for in vivo administration of CPP/nucleic acid formulations did not change the size or morphology of the particles (K. Freimann, unpublished data).

Very limited data has been previously published about the size of CPP/nucleic acid nanocomplexes. Recently, van Asbeck *et. al* analysed the size of CPP/siRNA complexes by dynamic light scattering using variety of CPPs (van Asbeck et al. 2013). They found that R9, r9, hLF and PepFect14 formed complexes with siRNA which had a size of 150–200 nm. Importantly, the size of the complexes did not depend on the used molar ratio of CPP and siRNA. In Paper IV we also examined whether the molar ratio of CPP and SSO could affect the size and morphology of the PepFect14/SSO complexes, and found by negative staining TEM analysis that their size and shape were not influenced by the amount (we used molar ratios 5–20 for examination) of CPP used for the formation of nanocomplexes. Interestingly, van Asbeck *et. al* found that in case of some peptides (TP10, Tat, hLF, PepFect6) the size of CPP/siRNA complexes depended on the used molar ratio. For example, TP10 did not form nanoparticles below molar ratio 20, but aggregated siRNA at high (≥ 30) molar ratios. PepFect6, in contrast, formed largest particles (around 200 nm) at molar ratio 15 and at lower (5) or higher (30–40) molar ratios smaller particles (around 100 nm) were formed. Although we analysed the size and morphology of PepFect6/nucleic acid nanoparticles in Paper IV, we did not vary the amount of peptide for the formation of particles. Nevertheless, negative staining TEM helps to distinguish whether the size differences of CPP/siRNA complexes at different molar ratios measured by DLS were caused by aggregation or increase of the size of particles. Our negative staining TEM images revealed that PepFects and NickFects pack nucleic acids into nanoparticles of homogeneous size and morphology. In case of all studied peptides except PepFect14 the particles were spherical or near-spherical. In terms of size, size distribution and morphology, the CPP/nucleic acid nanocomplexes resembled lipoplexes or polyplexes. For example, Gilleron *et. al* showed that lipid nanoparticles loaded with siRNA were spherical and had a mean diameter of about 60 nm and more than 80% of particles had a size range of 40–120 nm (Gilleron et al. 2013).

Negative staining TEM enabled us to directly visualize the CPP/nucleic nanocomplexes, and provided essential information about their size and shape. However, in order to gain more detailed information about the morphology of the NickFect and PepFect nanoparticles with nucleic acids scanning electron microscopy or atomic force microscopy should be used. Recently, Deshayes *et. al* showed by scanning electron microscopy and atomic force microscopy that CADY peptide condenses siRNA into globular particles of 70–80 nm in diameter, and the individual particles are composed of smaller spheres, forming “raspberry”-like structures (Deshayes et al. 2012). The resolution of negative staining TEM did not reveal whether PFs and/or NFs also pack oligonucleotides into similar structures. However, in case of PF14/nucleic acid NPs we frequently detected that smaller complexes had associated with each other forming larger elongated assemblies. PF6/nucleic acid complexes, in contrary, were almost ideal spheres with both small oligonucleotides and larger plasmid DNA, and we consider it highly unlikely that these were formed by association of several smaller sub-particles.

DLS analysis revealed that the size of NickFect and PepFect nanocomplexes with nucleic acids increased 2–3-fold (up to 160–200 nm in diameter) when incubated in tissue culture media which contained serum proteins. This was probably caused by the accumulation of serum proteins onto CPP/nucleic acid nanocomplexes, forming a “protein corona”. All types of nanoparticles absorb some amount of plasma proteins on their surface in biological milieu, and the composition of the protein coat depends on various characteristics of NPs, e.g. surface chemistry, size and charge (Walkey et al. 2014). Interestingly, we found that the size of PepFect14/pDNA nanoparticles increased 2-fold and 3-fold also in tissue culture media without serum proteins and in physiological salt solution, respectively, compared to nanoparticles formed in water. The reasons behind this are not clear but we can consider surreal possibilities for such behaviour of nanoparticles. The change in ionic concentrations in tissue culture media or physiological solution might have caused the reorganization of the nanocomplexes and result more loosely packed nanocomplexes. On the other hand, in these conditions nanoparticles could also associate to form bigger assemblies. Similarly to our results, Asbeck *et. al* also found by DLS that in physiological solution CPP/siRNA nanocomplexes form larger particles (van Asbeck et al. 2013). The authors of study suggested that salt ions form bridges between CPPs, which results bigger and more loosely packed particles.

The vast majority of studies devoted to examining the specific endocytic mechanisms involved in the cellular uptake of delivery vectors and their cargos have employed pharmacological inhibitors to suppress individual endocytic pathways in cells. Yet, it has become evident that pharmacological inhibitors might lack specificity and could yield misleading results (Ivanov 2008). In addition, the inhibition of one endocytic pathway is usually compensated by upregulation of the cellular uptake of nanocomplexes through other routes, which could hamper the interpretation of obtained data. Thus, in addition to inhibiting specific endocytic pathways we employed TEM analysis to examine the cellular uptake routes of PepFect and NickFect nanocomplexes with nucleic acids. We found that the studied CPPs (PepFect14, NickFect51, NickFect1) mediated the cellular uptake of nucleic acids via endocytosis, and the involved specific endocytic routes depended mostly on the used CPP. In Paper I we demonstrated that PepFect14/pDNA nanocomplexes utilize caveolin-mediated endocytosis and macropinocytosis for the internalization to cells. In Paper III we used TEM analysis and pharmacological inhibition of the main endocytic routes, and found that NickFect51/pDNA nanocomplexes induce mainly macropinocytosis, whereas NickFect1/pDNA complexes trigger various endocytic events simultaneously including macropinocytosis, caveolin-mediated endocytosis and clathrin-mediated endocytosis to gain access to the interior of cells.

Only a few reports are published about cell-entry mechanisms of CPP/nucleic acid non-covalent complexes. Hassane *et. al* found that PepFect6 complexes with SSO internalize to cells via endocytosis since the cellular uptake of the complexes was significantly reduced when incubation was performed at 4°C, which abolishes the energy-dependent cellular uptake (Hassane

et al. 2011). In addition, they demonstrated that the complexes are internalized by clathrin-mediated endocytosis because chlorpromazine and potassium depletion severely reduced the activity of splicing switching activity of PepFect6/SSO complexes in HeLa pLuc 705 reporter cells. Yet, inhibition of caveolin-dependent endocytosis or macropinocytosis did not affect the bioactivity of the complexes. In contrast, we very recently examined the cell-entry mechanisms of PepFect14/SSO complexes, and found that the bioactivity of SSO in HeLa pLuc 705 cells was significantly reduced in the presence of amiloride and nystatin which impede macropinocytosis and caveolin-mediated endocytosis, respectively (Juks et al. 2015). Similarly to our results, spherical nucleic acids translocate into cells via lipid raft/caveolin-mediated endocytosis (Choi et al. 2013).

The effectiveness of endocytic pathways which yield highest bioactivity of CPP/nucleic acid nanocomplexes is not very clear. Rehman *et. al* recently analysed the cellular uptake and bioactivity of lipoplexes and polyplexes, and found that lipoplexes internalized to cells via clathrin-mediated endocytosis and polyplexes utilized both clathrin- and caveolin-mediated endocytosis (ur Rehman et al. 2013). In case of liposomes, the cellular uptake via clathrin-mediated endocytosis led to the high level expression of luciferase from delivered pDNA. However, in case of polyplexes, only the uptake via caveolin-mediated endocytosis ensured the high activity of delivered cargo. Therefore, the effective endocytic pathway (or pathways) leading to high biological response is perhaps mostly determined by the nature of delivery vector. Macropinosomes are suggested to be more leakier compared to other endocytic vesicles, which could be beneficial for the release of drug-delivery vectors and their cargo from endosomal vesicles, and thus, yield higher bioactivity of delivered molecules (Meier et al. 2002). This pathway could be harnessed for the delivery of drugs into cancer cells or macrophages in which macropinocytosis is highly active. However, since clathrin-mediated endocytosis is the major endocytic pathway (about 90% of endocytosed material is internalized by clathrin-mediated endocytosis in cultured cells) (Bitsikas et al. 2014) this pathway could contribute most significantly to yielding bioactivity of delivered cargo in vivo. On the other hand, high expression of caveolin-1 and caveolin-2 in some cell types (e.g smooth muscle cells and adipocytes) could favour the delivery of cargo through caveolin-mediated endocytosis. Importantly, the transcytosis of cargo across the endothelial barrier occurs through caveolin-mediated endocytosis (reviewed in Simionescu et al. 2009). For example, 50–70% of lung endothelial cell plasma membranes are occupied by caveolae, and therefore, caveolin-mediated endocytosis could be exploited to deliver therapeutics into lungs (reviewed in Chrasztina et al. 2011).

Inside cells the studied CPP/nucleic acid nanocomplexes localized mainly inside endosomes. By 4 h of incubation the early endosomes had matured into late endosomes as revealed by their multivesicular content. Importantly, we rarely detected nanocomplexes in lysosomes after 4 h of incubation. We recently analysed the intracellular trafficking of PF14/SSO nanocomplexes also

by confocal laser scanning microscopy. Although the nanocomplexes-containing endosomes translocated to the perinuclear region of cells, these did not co-localize with LysoTracker, which specifically marks acidic compartments, mostly lysosomes, even after 4 h of incubation (Juks et al. 2015).

In case of all peptide/nucleic acid complexes we occasionally detected that the endosomal membranes of multivesicular bodies had lost their intactness, paving the way for the nanoparticles to escape to cytosol. We have previously shown by TEM that NickFect1/SSO and NickFect2/SSO nanocomplexes rupture the endosomal membranes resulting in their release from entrapping vesicles (Oskolkov et al. 2011). In addition we have conducted a TEM analysis to examine the intracellular trafficking of cationic polymer/SSO nanocomplexes, and found that similarly to NickFects and PepFects, a fraction of these complexes were released during 4 h of incubation from endosomes with multivesicular bodies' morphology (T. Lehto, unpublished data). Still, in case of all studied peptides in Papers I–III the vast majority of the CPP/nucleic acid complexes remained entrapped inside endosomes. Similarly, Gilleron *et al.* found that in case of lipid nanoparticle encapsulated siRNAs only a small fraction (1–2%) of cargo is released from endosomes and the cytosolic release occurred only at a defined stage of endosomal progression (Gilleron et al. 2013). We recently revealed by quantitative TEM that about 8% of PepFect14/SSO complexes localized in cytosol after 4 h of incubation (Juks et al. 2015). Thus, the endosomal escape probably remains the limiting step in efficient delivery of nucleic acids via nanoparticulate systems.

Recently, Wittrup *et al.* demonstrated that lipid-encapsulated siRNAs were released from endosomes which had associated Rab5 and Rab7 meaning that the release event occurred from maturing endosomes (Wittrup et al. 2015). Since the diffuse signal of fluorescently labelled siRNA spread all over cytoplasm within seconds after the release, they suggested that siRNA rather than intact lipid-encapsulated siRNAs were released from endosomes. Importantly, only one release event was detected from each individual endosome, indicating that the endosomal membrane was only temporarily damaged during the release. In parallel with the release of siRNA from endosomes the activation of autophagy was triggered, resulting the formation of autophagosomes which eventually fused with lysosomes. Similar studies should be conducted for CPP/nucleic acid nanocomplexes to clarify how CPP/nucleic acid complexes or nucleic acids themselves are released from endosomes.

The endosomal release could occur through “proton sponge” mechanism caused by endosomal acidification. Namely, during maturation of early endosomes to late endosomes, the pH of vesicles is lowered by H-ATPase, which results in the protonation of amine groups of peptide and influx of counter-ions into the lumen of endosomes. This, in turn, triggers the intake of water into the endosomes, leading to osmotic swelling, which could rupture their membranes, resulting in the release of nanoparticles. This mechanism is involved in the endosomal release of polyplexes (Boussif et al. 1995). Whether this mechanism

is involved also in the release of CPP/nucleic acid nanocomplexes, should be addressed in future studies.

In order to function in gene regulation pDNA or SSOs need to translocate into the nucleus of transfected cells. Indeed, in case of NickFect51/SSO nanocomplexes a small fraction of SSOs had translocated into the nucleus of HeLa pLuc 705 cells after 4 h of incubation, and these were detected in TEM as sole gold particles, suggesting that SSOs rather than CPP/SSO complexes had translocated into the nucleus. We recently showed that SSOs delivered into cells by NickFect1 or NickFect2 also localize in the nucleus after 4 h of incubation in HeLa pLuc 705 cells (Oskolkov et al. 2011). In addition, we examined the intracellular trafficking of PepFect6 and PepFect5 complexes with SSOs, and found that similarly to NickFects, a fraction of oligonucleotides translocated into the nucleus during 4 h of incubation (our unpublished data). Interestingly, we detected SSOs delivered by PepFect5 in the nucleus as single gold particles, however, in case of PepFect6, the nuclear SSOs typically localized as clusters of 2–3 gold particles. Nevertheless, we detected the nanocomplexes of PepFects and NickFects with SSOs in the nucleus very rarely during 4 h of incubation. One reason behind this could be that the 4 h of incubation time is not sufficient for the SSOs to reach nuclei of cells in amounts that are easily detected by TEM. We did not use longer incubation times because the small ($d=1.4$ nm) nanogold tag would be dissociated in the reducing environment of cytoplasm causing the loss of signal. In contrast to oligonucleotides, we did not detect labelled pDNA in the nuclei of cells during 4 h of incubation. Probably, the translocation of pDNA into nucleus is even slower process than the translocation of oligonucleotides. This is supported by earlier finding that the PEI-mediated cytosolic delivery of pDNA occurs in a similar manner with oligonucleotide delivery, but in contrast to oligonucleotides which were highly mobile in cytosol and accumulated into nucleus, pDNA remained immobile in cytosol (ur Rehman et al. 2013). However, our functional assays revealed that NickFect51, NickFect1 and PepFect14 complexes with pDNA yielded high gene expression in various cell types during 24 h of transfection. Perhaps, the nuclear accumulation at levels detectable in TEM occurs after 4 h of incubation of CPP/pDNA complexes in cells. In addition to Nano-gold labelled pDNA we used colloidal gold (10 nm) labelled pDNA to visualize the CPP/pDNA complexes in cells. The large colloidal gold particles remain stable in the reducing environment of the cytosol of cells for longer period of time compared to small nanogold label, and thus, longer incubation times could in principle be used to analyse the presence of pDNA in the nucleus. However, the pores in nuclear envelope of cells are generally permeable only for molecules with molecular mass below 40 kDa (about 10 nm in diameter) (reviewed in Wentz and Rout 2010). siRNA and SSOs have a suitable size, whereas pDNA is too large, even when condensed by CPPs, for the passive diffusion into the nuclei of cells. Therefore, while SSOs could passively diffuse through the nuclear membrane, other mechanisms should be involved in the nuclear uptake of CPP/plasmid complexes or pDNA. One hypothesis is that pDNA translocates

into the nucleus of cells during cell division. However, other mechanisms could also be used. One might speculate, that the nanocomplexes of CPP/pDNA or pDNA itself are reorganized for the translocation to nucleus despite of large size. For example, the mRNP particles of about 50 nm have been shown to rearrange into rod like structures, decreasing their diameter to around 25 nm after associating with the nuclear pore complex (Mehlin et al. 1992). Also, the fusion of CPP/pDNA complexes with the nuclear membrane can cause the nuclear translocation. Previously, it has been shown that lipoplexes can fuse with nuclear membrane, releasing the pDNA to the nucleus (Kamiya et al. 2002). Nevertheless, the understanding of mechanisms of how nucleic acids are delivered into the nuclei of cells is an intriguing topic and need to be studied in more detail.

SUMMARY

Cell-penetrating peptides are efficient delivery vectors for various types of nucleic acids. CPPs can be coupled to nucleic acids either by covalent conjugation or by co-incubation of the peptide and cargo. Co-incubation of CPPs and nucleic acids leads to the formation of nanocomplexes due to electrostatic and hydrophobic interactions. However, the knowledge about the physical-chemical properties and morphology of the forming nanocomplexes is still fragmentary and hinders their application in biomedicine. The cell-entry mechanisms and intracellular trafficking of CPP/nucleic acid nanocomplexes are poorly understood, which impedes the further refinement of carrier peptides to achieve higher transfection efficacies.

Therefore, the focus of the current thesis was the characterization of the size, shape and charge of CPP/nucleic acid nanocomplexes using dynamic light scattering and transmission electron microscopy. Furthermore, the cell-entry mechanisms and intracellular trafficking of CPP/nucleic acid nanocomplexes were analysed using pharmacological inhibitors of endocytosis, siRNA technology, fluorescence and transmission electron microscopy.

The main results of the current thesis are as follows:

1. TP10-based CPPs from PepFect (PF6, PF14) and NickFect families (NF1, NF51) condense nucleic acids into nanoparticles (NPs) which have uniform size and morphology (Paper IV).
2. The size of CPP/nucleic acid NPs depends on the type and molecular mass of nucleic acid. CPP/oligonucleotide nanocomplexes are smaller ($d \approx 30$ nm) than CPP/plasmid DNA nanocomplexes ($d = 50\text{--}60$ nm) (Paper IV).
3. DLS overestimates the size of CPP/nucleic acid NPs (Paper IV).
4. The shape of CPP/nucleic acid nanocomplexes depends on the peptide rather than the type of nucleic acid (Paper IV).
5. NickFect and PepFect nanocomplexes with nucleic acid have a negative zeta potential in serum-containing tissue culture media (Paper I–III).
6. Fluorescent or (nano-)gold label on nucleic acid molecule does not affect the gross-characteristics of CPP/nucleic acid nanocomplexes (Paper IV).
7. NickFects and PepFects mediate the internalization of nucleic acids into mammalian cells by endocytosis, and the cellular uptake pathway(s) depend(s) on the used peptide (Paper I–III):
 - PF14/pDNA nanocomplexes utilize mainly caveolin-mediated endocytosis and macropinocytosis to gain access to the interior of cells;
 - NF51/pDNA nanocomplexes are internalized by cells mainly via macropinocytosis;
 - NF1/pDNA nanocomplexes utilize various endocytic pathways for the cellular uptake including caveolin- and clathrin- mediated endocytosis and macropinocytosis.

8. Scavenger receptor class A proteins SCARA3 and SCARA5 are involved in the cellular uptake of PepFect and NickFect nanocomplexes with plasmid DNA (Paper I and Paper III).
9. Most of the PepFect and NickFect nanocomplexes with nucleic acids localize inside MVBs/late endosomes after 4 h of incubation. Only a small fraction of the nanocomplexes are released from endosomes by this time (Paper I–III).

SUMMARY IN ESTONIAN

Rakku sisenevate peptiidi/nukleiinhappe komplekside kirjeldamine ja nende rakku sisenemise mehhanismid

Nukleiinhapete abil on võimalik moduleerida rakkude geeniekspressiooni. Kõrge spetsiifilisuse ja madala kõrvalmõjude tekkeriski tõttu on nukleiinhapped kõrgelt hinnatud ravipotentsiaaliga molekulid. Bioloogilise funktsionaalsuse saavutamiseks on vajalik nukleiinhapete sisenemine rakkudesse ning jõudmine sihtkohta – rakutuuma või tsütoplasmasse. Suure molekulmassi ja negatiivse laengu tõttu ei ole aga nukleiinhapped võimelised vabalt läbima raku plasmamembraani. Seetõttu on arendatud mitmesuguseid meetodeid, mille abil nukleiinhappeid rakkudesse transportida, ning üheks neist on rakku sisenevate peptiidide (RSP; i.k. *cell-penetrating peptide*, CPP) kasutamine. RSPd on lühikesed, enamasti katioonsed ja/või amfipaatsed aminohappelised järjestused, mis on võimelised läbima rakkude plasmamembraani ning transportima rakkudesse bioaktiivseid molekule, sh nukleiinhappeid.

RSPsid on nukleiinhapetega võimalik siduda kahel erineval viisil kasutades kas kovalentset või mittekovalentset strateegiat. Kovalentse strateegia puhul moodustatakse peptiidi ja lastmolekuli vahele kovalentne side. Mittekovalentse strateegia puhul aga toimub nukleiinhapete seondumine RSPdega peamiselt elektrostaatiliste ja hüdrofoobsete intraktsioonide vahendusel. Mittekovalentse strateegia rakendamine on võrreldes kovalentse meetodiga lihtsam, kiirem ja odavam. Samuti piisab selle lähenemise puhul bioloogilise vastuse saamiseks väiksematest peptiidi ja nukleiinhappe kogustest, mis vähendab kõrvalmõjude tekkeriski. Samas on mittekovalentsel sidumisstrateegial ka puudusi. Kui kovalentse sidumise puhul saadakse täpselt defineeritavad RSP-nukleiinhappe konjugaadid, siis mittekovalentse sidumisstrateegia puhul tekivad nanokompleksid, mille koostise täpne kirjeldamine on oluliselt komplitseeritum, eriti heterogeensete nanopartiklite moodustumise korral. RSP/nukleiinhappe komplekside omaduste (nt suurus, kuju, laeng) detailne kirjeldamine on aga vajalikud nende kasutuselevõtuks biomeditsiinis. Teine probleem, mis takistab mittekovalentse strateegia rakendamist, on vähene arusaam nanokomplekside rakku sisenemise mehhanismidest ja rakusisest suunamisest. Rakku sisenemise mehhanismide ja rakusisese suunamise mõistmine on aga vajalikud vältimaks soovimatuid kõrvalmõjusid ning parendamaks peptiidide omadusi ja saavutamaks lastmolekulide võimalikult kõrget aktiivsust. Käesoleva doktoritöö eesmärgid olid RSP/nukleiinhappe komplekside omaduste iseloomustamine ning nende rakkudesse sisenemise mehhanismide ja rakusisese suunamise selgitamine. Kõik kasutatud peptiidid on transportaan-10 (TP10) analoogid, mis on disainitud spetsiaalselt nukleiinhapete transpordiks imetajarakkudesse.

RSP/nukleiinhappe nanokomplekside kirjeldamiseks kasutasime dünaamilise valguse hajumise meetodit (DLS; i.k. *dynamic light scattering*) ning transmissioon elektronmikroskoopiat (TEM; i.k. *transmission electron microscopy*). TEMi abil leidsime et TP10 järjestusest lähtuvalt disainitud transportpeptiidid PepFectid

(PF) ja NickFectid (NF) kondenseerivad nukleiinhappe molekulid suhteliselt homogeenseteks nanopartikliteks (NP). Uuritud RSPd moodustasid plasmiidse DNAGA (pDNA) 50–60 nm diameetriga ning oligonukleotiididega oluliselt väiksemaid, 25–35 nm läbimõõduga partikleid, kui kompleksid moodustati vees. Tekkivate partiklite läbimõõdu erinevus tuleneb tõenäoliselt kondenseeritavate lastmolekulide suuruse erinevustest. pDNA ($M_w = 3,1$ MDa) on väga suur molekul võrreldes spleissingut muutva oligonukleotiidi (*splicing switching oligonucleotide*, SCO) ($M_w = 5,9$ kDa) või lühikese interferents RNAGA (*short interfering RNA*, siRNA) ($M_w = 14,3$ kDa) ning määrab ilmselt moodustuvate partiklite suuruse. Lisaks sellele leidsime, et RSP/nukleiinhappe nanopartiklite kuju sõltub mõnevõrra ka uuritava peptiidi järjestusest/omadustest. PF6, NF1 ja NF51 moodustasid kõigi kasutatud nukleiinhappe molekulidega sfäärilisi (PF6) või enamjaolt sfäärilisi (NF1, NF51) nanopartikleid. Seevastu PF14 moodustas kõigi uuritud nukleiinhapetega partikleid, mis olid kas sfäärilised, ellipsikujulised või loperguse kujuga. Sageli olid PF14 sisaldavad partiklid omavahel assotsieerunud, moodustades ahelataolisi struktuure. Mitte ükski uuritud peptiid ei moodustanud stabiilseid nanopartikleid ilma nukleiinhappe juuresolekuta. DLSiga näitasime, et RSP/nukleiinhappe komplekside suurus ja pinnalaeng (ζ -potentsiaal) sõltuvad ka neid ümbritseva lahuse omadustest. Nii seerumvabas kui seerumiga rakukultuuri söötmes ja NaCl füsioloogilises lahuses moodustusid umbes kaks korda suuremad nanopartiklid kui vees. Lisaks sellele leidsime, et RSP/nukleiinhappe kompleksid omandavad söötmes või soolalahuses kergelt negatiivse pinnalaengu.

Positiivse laengu tõttu seonduvad RSP-d plasmamembraaniga interakteerudes rakupinna negatiivse laenguga proteoglykaanidega. Hiljuti läbiviidud uuringud (Ezzat et al. 2012, van Asbeck et al. 2013) ning meie tulemused näitasid aga, et PepFectide ja NickFectide kompleksid nukleiinhappe molekulidega on raku söötmes negatiivse laenguga, mistõttu ei saa nende esmast seondumist rakkudega selgitada pelgalt elektrostaatiliste interaktsioonidega rakupinna negatiivse laenguga molekulidega. Ezzat jt. näitasid, et PF14/SSO nanokompleksid seonduvad rakkude plasmamembraanil koristusretseptoritega SCARA3 (*Class A Scavenger Receptor 3*) ja SCARA5 (*Class A Scavenger Receptor 5*) (Ezzat et al. 2012). Ka meie töö tulemused kinnitasid, et RSP/nukleiinhappe komplekside rakkudesse sisenemine toimub läbi SCARA3 ja SCARA5 retseptoritega seondumise. Rakkude eeltötlus SCARA inhibiitorite polüinosiinhappe, dekstraansulfaadi või fukoidaaniga blokeeris peaaegu täielikult PF14/pDNA, NF1/pDNA ja NF51/pDNA rakkudesse sisenemise, samas kui identse laengu ja sarnase struktuuriga, ent SCARAdega mitteseonduvad polütsütidüülhappe, kondroitiinsulfaat ja galaktoos nanokomplekside bioaktiivsust ei mõjutanud. Kontrollimaks konkreetsete retseptorite osalust nukleiinhapete rakku transpordis NF-dega pärsisime SCARA3 ja SCARA5 valkude sünteesi, kasutades vastavaid siRNAsid, mis põhjustas enam kui 85% transfektsiooni efektiivsuse languse mõlema peptiidi puhul.

RSP/nukleiinhappe komplekside plasmamembraaniga seondumise ja raku sisese suunamise uurimiseks kasutasime TEM analüüsi. Nanopartiklite visua-

liseerimiseks märgistasime oligonukleotiidid kovalentselt nanokullaga (NanogoldTM, 1,4 nm) ning biotinüleeritud plasmidi mittekovalentselt streptavidiin-nanokullaga või neutravidiin-kolloidkullaga. NF51/SSO nanopartiklid seondusid HeLa pLuc 705 rakkude plasmamembraaniga partiklitenä, mille läbimõõt oli 80–170 nm. Juba 30 minutit pärast nanokomplekside inkubatsiooni detekteerisime rakkude sees märkimisväärselt rohkem nanopartikleid kui plasmamembraanil. Rakkudes paiknesid nanopartiklid enamasti suurtes (400–500 nm) vesiikulites, endosoomides, aga juba ühe tunni möödudes tuvastasime üksikuid SSOsid tsütosoolis ilma ümbritseva vesiikuli membraanita. 4 h pärast inkubatsiooni algust paiknesid mõned SSOd ka rakutuumas. PF14, NF1 ja NF51 nanokompleksid pDNAga assotsieerusid rakupinnaga väikeste klastritena, mis sisaldasid 1–10 neutravidiin-kulla või streptavidiin-nanokulla märgist, viidates sellele, et ühes RSP/pDNA nanokompleksis oli 1–2 plasmidse DNA molekuli. Rakupinnal paiknesid PF14/pDNA nanokompleksid sageli väikeses, 50–100 nm diameetriga membraani-invaginatsioonides, mis oma suuruse ja morfoloogia poolest sarnanesid kaveoolidele. NF51/pDNA nanokompleksid lokaliseerusid plasmamembraanil sageli membraanijätkete/filopoodide pinnal (i.k. *ruffles*), mis on omased makropinotsütoosile. NF1/pDNA nanopartiklid paiknesid kas membraanijätketel või väikeses (d= 50–100 nm) membraani-invaginatsioonides. 30 min–1 h pärast inkubatsiooni algust detekteerisime RSP/pDNA nanopartikleid enamasti varajastes endosoomides või hilistes endosoomides ehk multivesikulaarsetes kehades. 4 h pärast inkubatsiooni algust lokaliseerus enamus partikleid multivesikulaarsetes kehades, kuid üksikuid lastmolekule detekteerisime ka vabalt tsütosoolis. Tähelepanuväärselt ei lokaliseerunud nanokompleksid lüsoosoomides, mis viitab, et PF-id ja NF-id takistavad hiliste endosoomide küpsemist lüsoosoomideks. Me ei detekteerinud plasmidset DNA-d tuumas 4 tunni inkubatsiooni järel.

Lisaks TEM analüüsile kasutasime NF51/pDNA ja NF1/pDNA nanopartiklite rakkudesse sisenemise mehhanismi uurimiseks peamiste endotsütoosiradade farmakoloogilist inhibeerimist. Me eeltöötlesime rakke kloorpromasiini, nüstatiiini või tsütohalasiini D-ga, et takistada vastavalt klatriin-vahendatud endotsütoosi, kaveoliin-vahendatud endotsütoosi või makropinotsütoosi. Tsütohalasiin D vähendas NF51/pDNA transfektsiooni efektiivsust umbes 75%. Teised kasutatud inhibiitorid NF51/pDNA transfektsiooni efektiivsust oluliselt ei mõjutanud, mis sarnaselt TEMi tulemustele viitavad, et NF51/pDNA nanokompleksid sisenevad rakkudesse peamiselt makropinotsütoosi teel. NF1/pDNA transfektsiooniefektiivsus vähenes rakkude eeltöötlemisel tsütohalasiini D-ga või kloorpromasiiniga mõlemal juhul 50% ning nüstatiiiniga 20%, viidates, et NF1/pDNA nanopartiklid kasutavad rakkudesse sisenemiseks mitut endotsütoosirada.

Meie tulemused korreleeruvad hästi varasemate uurimuste tulemustega antud valdkonnas. Ezzat jt. on näidanud, et PF14/SCO nanopartiklite sisenemine väheneb drastiliselt komplekside inkubeerimisel 4°C juures, mis inhibeerib raku energiast sõltuvad raku sisenemise mehhanismid. Lisaks sellele suurendas rakkude töötlemine endosomotroopilise molekuli klorokviiniga PF14/SSO nano-

komplekside bioaktiivsust, viidates nende paiknemisele endosoomides (Ezzat et al. 2012).

Käesolevas doktoritöös näitasime, et TP10 analoogid PepFectid ja NickFectid moodustavad nukleiinhapetega ühtlase suurusega nanopartikleid, mis sõltuvalt nukleiinhappest on 30–60 nm diameetriga. Rakusöötmes ja füsioloogilises lahuses on partiklid umbes 2 korda suuremad ning omandavad negatiivse laengu. Uuritud RSP/nukleiinhappe kompleksid seonduvad rakupinnal koristuse retseptorite SCARA3 ja SCARA5ga. Rakkudesse sisenevad uuritud peptiidide/nukleiinhappe kompleksid endotsütoosi teel ning kasutatavad endotsütoosirajad määrab eelkõige kompleksi moodustamiseks kasutatud peptiid. Enamus RSP/nukleiinhappe komplekse paikneb 4 h pärast inkubatsiooni algust hilistes endosoomides, viidates, et endosoomidesse kinnijäämine on peamine bioaktiivsust limiteeriv faktor.

REFERENCES

- Abes, S., J. J. Turner, G. D. Ivanova, D. Owen, D. Williams, A. Arzumanov, P. Clair, M. J. Gait and B. Lebleu (2007). "Efficient splicing correction by PNA conjugation to an R6-Penetratin delivery peptide." *Nucleic Acids Res* 35(13): 4495–4502.
- Agrawal, P., S. Bhalla, S. S. Usmani, S. Singh, K. Chaudhary, G. P. Raghava and A. Gautam (2016). "CPPsite 2.0: a repository of experimentally validated cell-penetrating peptides." *Nucleic Acids Res* 44(D1): D1098–1103.
- Ait-Slimane, T., R. Galmes, G. Trugnan and M. Maurice (2009). "Basolateral internalization of GPI-anchored proteins occurs via a clathrin-independent flotillin-dependent pathway in polarized hepatic cells." *Mol Biol Cell* 20(17): 3792–3800.
- Alexis, F., E. Pridgen, L. K. Molnar and O. C. Farokhzad (2008). "Factors affecting the clearance and biodistribution of polymeric nanoparticles." *Mol Pharm* 5(4): 505–515.
- Amyere, M., B. Payrastre, U. Krause, P. Van Der Smissen, A. Veithen and P. J. Courtoy (2000). "Constitutive macropinocytosis in oncogene-transformed fibroblasts depends on sequential permanent activation of phosphoinositide 3-kinase and phospholipase C." *Mol Biol Cell* 11(10): 3453–3467.
- Anderson, H. A., Y. Chen and L. C. Norkin (1996). "Bound simian virus 40 translocates to caveolin-enriched membrane domains, and its entry is inhibited by drugs that selectively disrupt caveolae." *Mol Biol Cell* 7(11): 1825–1834.
- Anton, I. M., S. P. Saville, M. J. Byrne, C. Curcio, N. Ramesh, J. H. Hartwig and R. S. Geha (2003). "WIP participates in actin reorganization and ruffle formation induced by PDGF." *J Cell Sci* 116(Pt 12): 2443–2451.
- Bar-Sagi, D. and J. R. Feramisco (1986). "Induction of membrane ruffling and fluid-phase pinocytosis in quiescent fibroblasts by ras proteins." *Science* 233(4768): 1061–1068.
- Bar-Sagi, D., F. McCormick, R. J. Milley and J. R. Feramisco (1987). "Inhibition of cell surface ruffling and fluid-phase pinocytosis by microinjection of anti-ras antibodies into living cells." *J Cell Physiol Suppl* 5: 69–73.
- Barany-Wallje, E., J. Gaur, P. Lundberg, U. Langel and A. Graslund (2007). "Differential membrane perturbation caused by the cell penetrating peptide Tp10 depending on attached cargo." *FEBS Lett* 581(13): 2389–2393.
- Beguinet, L., R. M. Lyall, M. C. Willingham and I. Pastan (1984). "Down-regulation of the epidermal growth factor receptor in KB cells is due to receptor internalization and subsequent degradation in lysosomes." *Proc Natl Acad Sci U S A* 81(8): 2384–2388.
- Bennett, C. F. and E. E. Swayze (2010). "RNA targeting therapeutics: molecular mechanisms of antisense oligonucleotides as a therapeutic platform." *Annu Rev Pharmacol Toxicol* 50: 259–293.
- Betts, C., A. F. Saleh, A. A. Arzumanov, S. M. Hammond, C. Godfrey, T. Coursindel, M. J. Gait and M. J. Wood (2012). "Pip6-PMO, A New Generation of Peptide-oligonucleotide Conjugates With Improved Cardiac Exon Skipping Activity for DMD Treatment." *Mol Ther Nucleic Acids* 1: e38.
- Betts, C. A., A. F. Saleh, C. A. Carr, S. M. Hammond, A. M. Coenen-Stass, C. Godfrey, G. McClorey, M. A. Varela, T. C. Roberts, K. Clarke, et al. (2015). "Prevention of exercised induced cardiomyopathy following Pip-PMO treatment in dystrophic mdx mice." *Sci Rep* 5: 8986.

- Bevilacqua, P. C. and T. R. Cech (1996). "Minor-groove recognition of double-stranded RNA by the double-stranded RNA-binding domain from the RNA-activated protein kinase PKR." *Biochemistry* 35(31): 9983–9994.
- Bitsikas, V., I. R. Correa, Jr. and B. J. Nichols (2014). "Clathrin-independent pathways do not contribute significantly to endocytic flux." *Elife* 3: e03970.
- Blagoveshchenskaya, A. D., L. Thomas, S. F. Felicangeli, C. H. Hung and G. Thomas (2002). "HIV-1 Nef downregulates MHC-I by a PACS-1- and PI3K-regulated ARF6 endocytic pathway." *Cell* 111(6): 853–866.
- Blanchard, E., S. Belouzard, L. Goueslain, T. Wakita, J. Dubuisson, C. Wychowski and Y. Rouille (2006). "Hepatitis C virus entry depends on clathrin-mediated endocytosis." *J Virol* 80(14): 6964–6972.
- Bohdanowicz, M., D. Schlam, M. Hermansson, D. Rizzuti, G. D. Fairn, T. Ueyama, P. Somerharju, G. Du and S. Grinstein (2013). "Phosphatidic acid is required for the constitutive ruffling and macropinocytosis of phagocytes." *Mol Biol Cell* 24(11): 1700–1712, S1701–1707.
- Bos, J. L. (1989). "ras oncogenes in human cancer: a review." *Cancer Res* 49(17): 4682–4689.
- Boussif, O., F. Lezoualc'h, M. A. Zanta, M. D. Mergny, D. Scherman, B. Demeneix and J. P. Behr (1995). "A versatile vector for gene and oligonucleotide transfer into cells in culture and in vivo: polyethylenimine." *Proc Natl Acad Sci U S A* 92(16): 7297–7301.
- Braulke, T. and J. S. Bonifacio (2009). "Sorting of lysosomal proteins." *Biochim Biophys Acta* 1793(4): 605–614.
- Brekken, R. A. and P. E. Thorpe (2001). "Vascular endothelial growth factor and vascular targeting of solid tumors." *Anticancer Res* 21(6B): 4221–4229.
- Chen, X., S. Shank, P. B. Davis and A. G. Ziady (2011). "Nucleolin-mediated cellular trafficking of DNA nanoparticle is lipid raft and microtubule dependent and can be modulated by glucocorticoid." *Mol Ther* 19(1): 93–102.
- Chithrani, B. D. and W. C. Chan (2007). "Elucidating the mechanism of cellular uptake and removal of protein-coated gold nanoparticles of different sizes and shapes." *Nano Lett* 7(6): 1542–1550.
- Chithrani, B. D., A. A. Ghazani and W. C. Chan (2006). "Determining the size and shape dependence of gold nanoparticle uptake into mammalian cells." *Nano Lett* 6(4): 662–668.
- Choi, C. H., L. Hao, S. P. Narayan, E. Auyeung and C. A. Mirkin (2013). "Mechanism for the endocytosis of spherical nucleic acid nanoparticle conjugates." *Proc Natl Acad Sci U S A* 110(19): 7625–7630.
- Chrastina, A., K. A. Massey and J. E. Schnitzer (2011). "Overcoming in vivo barriers to targeted nanodelivery." *Wiley Interdiscip Rev Nanomed Nanobiotechnol* 3(4): 421–437.
- Collins, B. M., A. J. McCoy, H. M. Kent, P. R. Evans and D. J. Owen (2002). "Molecular architecture and functional model of the endocytic AP2 complex." *Cell* 109(4): 523–535.
- Commisso, C., S. M. Davidson, R. G. Soydaner-Azeloglu, S. J. Parker, J. J. Kamphorst, S. Hackett, E. Grabocka, M. Nofal, J. A. Drebin, C. B. Thompson, et al. (2013). "Macropinocytosis of protein is an amino acid supply route in Ras-transformed cells." *Nature* 497(7451): 633–637.
- Crombez, L., G. Aldrian-Herrada, K. Konate, Q. N. Nguyen, G. K. McMaster, R. Brasseur, F. Heitz and G. Divita (2009). "A new potent secondary amphipathic cell-

- penetrating peptide for siRNA delivery into mammalian cells.” *Mol Ther* 17(1): 95–103.
- Crombez, L., M. C. Morris, S. Dufort, G. Aldrian-Herrada, Q. Nguyen, G. Mc Master, J. L. Coll, F. Heitz and G. Divita (2009). “Targeting cyclin B1 through peptide-based delivery of siRNA prevents tumour growth.” *Nucleic Acids Res* 37(14): 4559–4569.
- Czupalla, C., H. Mansukoski, T. Riedl, D. Thiel, E. Krause and B. Hoflack (2006). “Proteomic analysis of lysosomal acid hydrolases secreted by osteoclasts: implications for lytic enzyme transport and bone metabolism.” *Mol Cell Proteomics* 5(1): 134–143.
- Dathe, M., M. Schumann, T. Wieprecht, A. Winkler, M. Beyermann, E. Krause, K. Matsuzaki, O. Murase and M. Bienert (1996). “Peptide helicity and membrane surface charge modulate the balance of electrostatic and hydrophobic interactions with lipid bilayers and biological membranes.” *Biochemistry* 35(38): 12612–12622.
- de Gassart, A., C. Geminard, B. Fevrier, G. Raposo and M. Vidal (2003). “Lipid raft-associated protein sorting in exosomes.” *Blood* 102(13): 4336–4344.
- De Jong, W. H., W. I. Hagens, P. Krystek, M. C. Burger, A. J. Sips and R. E. Geertsma (2008). “Particle size-dependent organ distribution of gold nanoparticles after intravenous administration.” *Biomaterials* 29(12): 1912–1919.
- Derossi, D., A. H. Joliot, G. Chassaing and A. Prochiantz (1994). “The third helix of the Antennapedia homeodomain translocates through biological membranes.” *J. Biol. Chem.* 269(14): 10444–10450.
- Deshayes, S., S. Gerbal-Chaloin, M. C. Morris, G. Aldrian-Herrada, P. Charnet, G. Divita and F. Heitz (2004). “On the mechanism of non-endosomal peptide-mediated cellular delivery of nucleic acids.” *Biochim Biophys Acta* 1667(2): 141–147.
- Deshayes, S., A. Heitz, M. C. Morris, P. Charnet, G. Divita and F. Heitz (2004). “Insight into the mechanism of internalization of the cell-penetrating carrier peptide Pep-1 through conformational analysis.” *Biochemistry* 43(6): 1449–1457.
- Deshayes, S., K. Konate, A. Rydstrom, L. Crombez, C. Godefroy, P. E. Milhiet, A. Thomas, R. Brasseur, G. Aldrian, F. Heitz, et al. (2012). “Self-assembling peptide-based nanoparticles for siRNA delivery in primary cell lines.” *Small* 8(14): 2184–2188.
- Deshayes, S., T. Plenat, G. Aldrian-Herrada, G. Divita, C. Le Grimellec and F. Heitz (2004). “Primary amphipathic cell-penetrating peptides: structural requirements and interactions with model membranes.” *Biochemistry* 43(24): 7698–7706.
- Devadas, D., T. Koithan, R. Diestel, U. Prank, B. Sodeik and K. Dohner (2014). “Herpes simplex virus internalization into epithelial cells requires Na⁺/H⁺ exchangers and p21-activated kinases but neither clathrin- nor caveolin-mediated endocytosis.” *J Virol* 88(22): 13378–13395.
- DeWitte-Orr, S. J., S. E. Collins, C. M. Bauer, D. M. Bowdish and K. L. Mossman (2010). “An accessory to the 'Trinity': SR-As are essential pathogen sensors of extracellular dsRNA, mediating entry and leading to subsequent type I IFN responses.” *PLoS Pathog* 6(3): e1000829.
- Dharmawardhane, S., D. Brownson, M. Lennartz and G. M. Bokoch (1999). “Localization of p21-activated kinase 1 (PAK1) to pseudopodia, membrane ruffles, and phagocytic cups in activated human neutrophils.” *J Leukoc Biol* 66(3): 521–527.
- Dharmawardhane, S., A. Schurmann, M. A. Sells, J. Chernoff, S. L. Schmid and G. M. Bokoch (2000). “Regulation of macropinocytosis by p21-activated kinase-1.” *Mol Biol Cell* 11(10): 3341–3352.

- Doane, T. L., C. H. Chuang, R. J. Hill and C. Burda (2012). "Nanoparticle zeta – potentials." *Acc Chem Res* 45(3): 317–326.
- Doherty, G. J. and H. T. McMahon (2009). "Mechanisms of endocytosis." *Annu Rev Biochem* 78: 857–902.
- Dowrick, P., P. Kenworthy, B. McCann and R. Warn (1993). "Circular ruffle formation and closure lead to macropinocytosis in hepatocyte growth factor/scatter factor-treated cells." *Eur J Cell Biol* 61(1): 44–53.
- Dunn, K. W., T. E. McGraw and F. R. Maxfield (1989). "Iterative fractionation of recycling receptors from lysosomally destined ligands in an early sorting endosome." *J Cell Biol* 109(6 Pt 2): 3303–3314.
- Edeling, M. A., S. K. Mishra, P. A. Keyel, A. L. Steinhauser, B. M. Collins, R. Roth, J. E. Heuser, D. J. Owen and L. M. Traub (2006). "Molecular switches involving the AP-2 beta2 appendage regulate endocytic cargo selection and clathrin coat assembly." *Dev Cell* 10(3): 329–342.
- Eguchi, A., B. R. Meade, Y. C. Chang, C. T. Fredrickson, K. Willert, N. Puri and S. F. Dowdy (2009). "Efficient siRNA delivery into primary cells by a peptide transduction domain-dsRNA binding domain fusion protein." *Nat Biotechnol* 27(6): 567–571.
- El-Andaloussi, S., T. Lehto, I. Mager, K. Rosenthal-Aizman, Oprea, II, O. E. Simonson, H. Sork, K. Ezzat, D. M. Copolovici, K. Kurrikoff, et al. (2011). "Design of a peptide-based vector, PepFect6, for efficient delivery of siRNA in cell culture and systemically in vivo." *Nucleic Acids Res* 39(9): 3972–3987.
- El Andaloussi, S., F. Said Hassane, P. Boisguerin, R. Sillard, U. Langel and B. Lebleu (2011). "Cell-penetrating peptides-based strategies for the delivery of splice redirecting antisense oligonucleotides." *Methods Mol Biol* 764: 75–89.
- Ezzat, K., S. E. Andaloussi, E. M. Zaghoul, T. Lehto, S. Lindberg, P. M. Moreno, J. R. Viola, T. Magdy, R. Abdo, P. Guterstam, et al. (2011). "PepFect 14, a novel cell-penetrating peptide for oligonucleotide delivery in solution and as solid formulation." *Nucleic Acids Res* 39(12): 5284–5298.
- Ezzat, K., H. Helmfors, O. Tudoran, C. Juks, S. Lindberg, K. Padari, S. El-Andaloussi, M. Pooga and Ü. Langel (2012). "Scavenger receptor-mediated uptake of cell-penetrating peptide nanocomplexes with oligonucleotides." *FASEB J* 26(3): 1172–1180.
- Even-Faitelson, L., M. Rosenberg and S. Ravid (2005). "PAK1 regulates myosin II-B phosphorylation, filament assembly, localization and cell chemotaxis." *Cell Signal* 17(9): 1137–1148.
- Frankel, A. D. and C. O. Pabo (1988). "Cellular uptake of the tat protein from human immunodeficiency virus." *Cell* 55(6): 1189–1193.
- Frick, M., N. A. Bright, K. Riento, A. Bray, C. Merrified and B. J. Nichols (2007). "Coassembly of flotillins induces formation of membrane microdomains, membrane curvature, and vesicle budding." *Curr Biol* 17(13): 1151–1156.
- Futaki, S., W. Ohashi, T. Suzuki, M. Niwa, S. Tanaka, K. Ueda, H. Harashima and Y. Sugiura (2001). "Stearylarginine-rich peptides: a new class of transfection systems." *Bioconj Chem* 12(6): 1005–1011.
- Galisteo, M. L., J. Chernoff, Y. C. Su, E. Y. Skolnik and J. Schlessinger (1996). "The adaptor protein Nck links receptor tyrosine kinases with the serine-threonine kinase Pak1." *J Biol Chem* 271(35): 20997–21000.
- Gauthier, N. C., P. Monzo, V. Kaddai, A. Doye, V. Ricci and P. Boquet (2005). "Helicobacter pylori VacA cytotoxin: a probe for a clathrin-independent and Cdc42-

- dependent pinocytic pathway routed to late endosomes.” *Mol Biol Cell* 16(10): 4852–4866.
- Ge, S., L. Song, D. R. Serwanski, W. A. Kuziel and J. S. Pachter (2008). “Transcellular transport of CCL2 across brain microvascular endothelial cells.” *J Neurochem* 104(5): 1219–1232.
- Geng, Y., P. Dalhaimer, S. Cai, R. Tsai, M. Tewari, T. Minko and D. E. Discher (2007). “Shape effects of filaments versus spherical particles in flow and drug delivery.” *Nat Nanotechnol* 2(4): 249–255.
- Gerbal-Chaloin, S., C. Gondeau, G. Aldrian-Herrada, F. Heitz, C. Gauthier-Rouviere and G. Divita (2007). “First step of the cell-penetrating peptide mechanism involves Rac1 GTPase-dependent actin-network remodelling.” *Biol Cell* 99(4): 223–238.
- Ghitescu, L., A. Fixman, M. Simionescu and N. Simionescu (1986). “Specific binding sites for albumin restricted to plasmalemmal vesicles of continuous capillary endothelium: receptor-mediated transcytosis.” *J Cell Biol* 102(4): 1304–1311.
- Gilleron, J., W. Querbes, A. Zeigerer, A. Borodovsky, G. Marsico, U. Schubert, K. Manygoats, S. Seifert, C. Andree, M. Stoter, et al. (2013). “Image-based analysis of lipid nanoparticle-mediated siRNA delivery, intracellular trafficking and endosomal escape.” *Nat Biotechnol* 31(7): 638–646.
- Glebov, O. O., N. A. Bright and B. J. Nichols (2006). “Flotillin-1 defines a clathrin-independent endocytic pathway in mammalian cells.” *Nat Cell Biol* 8(1): 46–54.
- Grassart, A., A. Dujeancourt, P. B. Lazarow, A. Dautry-Varsat and N. Sauvonnet (2008). “Clathrin-independent endocytosis used by the IL-2 receptor is regulated by Rac1, Pak1 and Pak2.” *EMBO Rep* 9(4): 356–362.
- Grosshans, B. L., D. Ortiz and P. Novick (2006). “Rabs and their effectors: achieving specificity in membrane traffic.” *Proc Natl Acad Sci U S A* 103(32): 11821–11827.
- Gump, J. M., R. K. June and S. F. Dowdy (2010). “Revised role of glycosaminoglycans in TAT protein transduction domain-mediated cellular transduction.” *J Biol Chem* 285(2): 1500–1507.
- Haglund, K., S. Sigismund, S. Polo, I. Szymkiewicz, P. P. Di Fiore and I. Dikic (2003). “Multiple monoubiquitination of RTKs is sufficient for their endocytosis and degradation.” *Nat Cell Biol* 5(5): 461–466.
- Haigler, H. T., J. A. McKanna and S. Cohen (1979). “Rapid stimulation of pinocytosis in human carcinoma cells A-431 by epidermal growth factor.” *J Cell Biol* 83(1): 82–90.
- Hao, M., S. Mukherjee, Y. Sun and F. R. Maxfield (2004). “Effects of cholesterol depletion and increased lipid unsaturation on the properties of endocytic membranes.” *J Biol Chem* 279(14): 14171–14178.
- Harris, J. R. and S. De Carlo (2014). “Negative staining and cryo-negative staining: applications in biology and medicine.” *Methods Mol Biol* 1117: 215–258.
- Hassan, P. A., S. Rana and G. Verma (2015). “Making sense of Brownian motion: colloid characterization by dynamic light scattering.” *Langmuir* 31(1): 3–12.
- Hassane, F. S., R. Abes, S. El Andaloussi, T. Lehto, R. Sillard, U. Langel and B. Lebleu (2011). “Insights into the cellular trafficking of splice redirecting oligonucleotides complexed with chemically modified cell-penetrating peptides.” *J Control Release* 153(2): 163–172.
- Hatziantoniou, S., I. P. Nezis, L. H. Margaritis and C. Demetzos (2007). “Visualisation of liposomes prepared from skin and stratum corneum lipids by transmission electron microscopy.” *Micron* 38(8): 777–781.

- Hayer, A., M. Stoeber, D. Ritz, S. Engel, H. H. Meyer and A. Helenius (2010). "Caveolin-1 is ubiquitinated and targeted to intraluminal vesicles in endolysosomes for degradation." *J Cell Biol* 191(3): 615–629.
- Henne, W. M., E. Boucrot, M. Meinecke, E. Evergren, Y. Vallis, R. Mittal and H. T. McMahon (2010). "FCHo proteins are nucleators of clathrin-mediated endocytosis." *Science* 328(5983): 1281–1284.
- Herskovits, J. S., H. S. Shpetner, C. C. Burgess and R. B. Vallee (1993). "Microtubules and Src homology 3 domains stimulate the dynamin GTPase via its C-terminal domain." *Proc Natl Acad Sci U S A* 90(24): 11468–11472.
- Hewlett, L. J., A. R. Prescott and C. Watts (1994). "The coated pit and macropinocytic pathways serve distinct endosome populations." *J Cell Biol* 124(5): 689–703.
- Holash, J., S. J. Wiegand and G. D. Yancopoulos (1999). "New model of tumor angiogenesis: dynamic balance between vessel regression and growth mediated by angiopoietins and VEGF." *Oncogene* 18(38): 5356–5362.
- Hou, K. K., H. Pan, P. H. Schlesinger and S. A. Wickline (2015). "A role for peptides in overcoming endosomal entrapment in siRNA delivery – A focus on melittin." *Biotechnol Adv* 33(6 Pt 1): 931–940.
- Huang, J., L. Bu, J. Xie, K. Chen, Z. Cheng, X. Li and X. Chen (2010). "Effects of nanoparticle size on cellular uptake and liver MRI with polyvinylpyrrolidone-coated iron oxide nanoparticles." *ACS Nano* 4(12): 7151–7160.
- Huang, R. Q., Y. Y. Pei and C. Jiang (2007). "Enhanced gene transfer into brain capillary endothelial cells using Antp-modified DNA-loaded nanoparticles." *J Biomed Sci* 14(5): 595–605.
- Ignatovich, I. A., E. B. Dizhe, A. V. Pavlotskaya, B. N. Akifiev, S. V. Burov, S. V. Orlov and A. P. Perevozchikov (2003). "Complexes of plasmid DNA with basic domain 47–57 of the HIV-1 Tat protein are transferred to mammalian cells by endocytosis-mediated pathways." *J Biol Chem* 278(43): 42625–42636.
- Ivanov, A. I. (2008). "Pharmacological inhibition of endocytic pathways: is it specific enough to be useful?" *Methods Mol Biol* 440: 15–33.
- Jiao, C. Y., D. Delaroche, F. Burlina, I. D. Alves, G. Chassaing and S. Sagan (2009). "Translocation and endocytosis for cell-penetrating peptide internalization." *J Biol Chem* 284(49): 33957–33965.
- Joliot, A., C. Pernelle, H. Deagostini-Bazin and A. Prochiantz (1991). "Antennapedia homeobox peptide regulates neural morphogenesis." *Proc Natl Acad Sci U S A* 88(5): 1864–1868.
- Joseph, K. C., A. Stieber and N. K. Gonatas (1979). "Endocytosis of cholera toxin in GERL-like structures of murine neuroblastoma cells pretreated with GM1 ganglioside. Cholera toxin internalization into Neuroblastoma GERL." *J Cell Biol* 81(3): 543–554.
- Journet, A., A. Chapel, S. Kieffer, F. Roux and J. Garin (2002). "Proteomic analysis of human lysosomes: application to monocytic and breast cancer cells." *Proteomics* 2(8): 1026–1040.
- Jovic, M., M. Sharma, J. Rahajeng and S. Caplan (2010). "The early endosome: a busy sorting station for proteins at the crossroads." *Histol Histopathol* 25(1): 99–112.
- Juks, C., K. Padari, H. Margus, A. Kriiska, I. Etverk, P. Arukuusk, K. Koppel, K. Ezzat, U. Langel and M. Pooga (2015). "The role of endocytosis in the uptake and intracellular trafficking of PepFect14-nucleic acid nanocomplexes via class A scavenger receptors." *Biochim Biophys Acta* 1848(12): 3205–3216.

- Kakudo, T., S. Chaki, S. Futaki, I. Nakase, K. Akaji, T. Kawakami, K. Maruyama, H. Kamiya and H. Harashima (2004). "Transferrin-modified liposomes equipped with a pH-sensitive fusogenic peptide: an artificial viral-like delivery system." *Biochemistry* 43(19): 5618–5628.
- Kamiya, H., Y. Fujimura, I. Matsuoka and H. Harashima (2002). "Visualization of intracellular trafficking of exogenous DNA delivered by cationic liposomes." *Biochem Biophys Res Commun* 298(4): 591–597.
- Kang, S. H., M. J. Cho and R. Kole (1998). "Up-regulation of luciferase gene expression with antisense oligonucleotides: implications and applications in functional assay development." *Biochemistry* 37(18): 6235–6239.
- Kaplan, I. M., J. S. Wadia and S. F. Dowdy (2005). "Cationic TAT peptide transduction domain enters cells by macropinocytosis." *J Control Release* 102(1): 247–253.
- Kartenbeck, J., H. Stukenbrok and A. Helenius (1989). "Endocytosis of simian virus 40 into the endoplasmic reticulum." *J Cell Biol* 109(6 Pt 1): 2721–2729.
- Kasahara, K., Y. Nakayama, I. Sato, K. Ikeda, M. Hoshino, T. Endo and N. Yamaguchi (2007). "Role of Src-family kinases in formation and trafficking of macropinosomes." *J Cell Physiol* 211(1): 220–232.
- Kelly, B. T., A. J. McCoy, K. Spate, S. E. Miller, P. R. Evans, S. Honing and D. J. Owen (2008). "A structural explanation for the binding of endocytic dileucine motifs by the AP2 complex." *Nature* 456(7224): 976–979.
- Khalil, I. A., S. Futaki, M. Niwa, Y. Baba, N. Kaji, H. Kamiya and H. Harashima (2004). "Mechanism of improved gene transfer by the N-terminal stearylization of octaarginine: enhanced cellular association by hydrophobic core formation." *Gene Ther* 11(7): 636–644.
- Khalil, I. A., K. Kogure, S. Futaki, S. Hama, H. Akita, M. Ueno, H. Kishida, M. Kudoh, Y. Mishina, K. Kataoka, et al. (2007). "Octaarginine-modified multifunctional envelope-type nanoparticles for gene delivery." *Gene Ther* 14(8): 682–689.
- Kim, W. J., L. V. Christensen, S. Jo, J. W. Yockman, J. H. Jeong, Y. H. Kim and S. W. Kim (2006). "Cholesteryl oligoarginine delivering vascular endothelial growth factor siRNA effectively inhibits tumor growth in colon adenocarcinoma." *Mol Ther* 14(3): 343–350.
- Kirchhausen, T. (2000). "Clathrin." *Annu Rev Biochem* 69: 699–727.
- Kirkham, M., A. Fujita, R. Chadda, S. J. Nixon, T. V. Kurzchalia, D. K. Sharma, R. E. Pagano, J. F. Hancock, S. Mayor and R. G. Parton (2005). "Ultrastructural identification of uncoated caveolin-independent early endocytic vehicles." *J Cell Biol* 168(3): 465–476.
- Kleemann, E., M. Neu, N. Jekel, L. Fink, T. Schmehl, T. Gessler, W. Seeger and T. Kissel (2005). "Nano-carriers for DNA delivery to the lung based upon a TAT-derived peptide covalently coupled to PEG-PEI." *J Control Release* 109(1–3): 299–316.
- Kobayashi, T., E. Stang, K. S. Fang, P. de Moerloose, R. G. Parton and J. Gruenberg (1998). "A lipid associated with the antiphospholipid syndrome regulates endosome structure and function." *Nature* 392(6672): 193–197.
- Kogure, K., R. Moriguchi, K. Sasaki, M. Ueno, S. Futaki and H. Harashima (2004). "Development of a non-viral multifunctional envelope-type nano device by a novel lipid film hydration method." *J Control Release* 98(2): 317–323.
- Koivusalo, M., C. Welch, H. Hayashi, C. C. Scott, M. Kim, T. Alexander, N. Touret, K. M. Hahn and S. Grinstein (2010). "Amiloride inhibits macropinocytosis by lowering

- submembranous pH and preventing Rac1 and Cdc42 signaling.” *J Cell Biol* 188(4): 547–563.
- Kokubo, H., J. B. Helms, Y. Ohno-Iwashita, Y. Shimada, Y. Horikoshi and H. Yamaguchi (2003). “Ultrastructural localization of flotillin-1 to cholesterol-rich membrane microdomains, rafts, in rat brain tissue.” *Brain Res* 965(1–2): 83–90.
- Kumar, P., H. Wu, J. L. McBride, K. E. Jung, M. H. Kim, B. L. Davidson, S. K. Lee, P. Shankar and N. Manjunath (2007). “Transvascular delivery of small interfering RNA to the central nervous system.” *Nature* 448(7149): 39–43.
- Lamaze, C., A. Dujancourt, T. Baba, C. G. Lo, A. Benmerah and A. Dautry-Varsat (2001). “Interleukin 2 receptors and detergent-resistant membrane domains define a clathrin-independent endocytic pathway.” *Mol Cell* 7(3): 661–671.
- Lamaziere, A., F. Burlina, C. Wolf, G. Chassaing, G. Trugnan and J. Ayala-Sanmartin (2007). “Non-metabolic membrane tubulation and permeability induced by bioactive peptides.” *PLoS ONE* 2(2): e201.
- Langel, K., S. Lindberg, D. M. Copolovici, P. Arukuusk, R. Sillard and Ü. Langel (2010). “Novel Fatty Acid Modifications of Transportan 10.” *Int. J. Pept. Res. Ther* 16(4): 247–255.
- Langel, Ü. (2011). *Cell-Penetrating Peptides: Methods and Protocols*, 2nd edition. New York, NY, USA, Humana Press, Springer.
- Larkin, J. M., M. S. Brown, J. L. Goldstein and R. G. Anderson (1983). “Depletion of intracellular potassium arrests coated pit formation and receptor-mediated endocytosis in fibroblasts.” *Cell* 33(1): 273–285.
- Le, P. U. and I. R. Nabi (2003). “Distinct caveolae-mediated endocytic pathways target the Golgi apparatus and the endoplasmic reticulum.” *J Cell Sci* 116(Pt 6): 1059–1071.
- Lecot, S., S. Belouzard, J. Dubuisson and Y. Rouille (2005). “Bovine viral diarrhea virus entry is dependent on clathrin-mediated endocytosis.” *J Virol* 79(16): 10826–10829.
- Lehto, T., R. Abes, N. Oskolkov, J. Suhorutsenko, D. M. Copolovici, I. Mager, J. R. Viola, O. E. Simonson, K. Ezzat, P. Guterstam, et al. (2010). “Delivery of nucleic acids with a stearylated (RxR)₄ peptide using a non-covalent co-incubation strategy.” *J Control Release* 141(1): 42–51.
- Lehto, T., A. Castillo Alvarez, S. Gauck, M. J. Gait, T. Coursindel, M. J. Wood, B. Lebleu and P. Boissier (2014). “Cellular trafficking determines the exon skipping activity of Pip6a-PMO in mdx skeletal and cardiac muscle cells.” *Nucleic Acids Res* 42(5): 3207–3217.
- Lehto, T., O. E. Simonson, I. Mager, K. Ezzat, H. Sork, D. M. Copolovici, J. R. Viola, E. M. Zaghloul, P. Lundin, P. M. Moreno, et al. (2011). “A Peptide-based Vector for Efficient Gene Transfer In Vitro and In Vivo.” *Mol Ther* 19(8): 1457–1467.
- Leung, D. W., G. Cachianes, W. J. Kuang, D. V. Goeddel and N. Ferrara (1989). “Vascular endothelial growth factor is a secreted angiogenic mitogen.” *Science* 246(4935): 1306–1309.
- Lewis, W. (1931). “Pinocytosis.” *Bull. Johns Hopkins Hosp.* 49: 17–23.
- Liberali, P., P. Ramo and L. Pelkmans (2008). “Protein kinases: starting a molecular systems view of endocytosis.” *Annu Rev Cell Dev Biol* 24: 501–523.
- Limmon, G. V., M. Arredouani, K. L. McCann, R. A. Corn Minor, L. Kobzik and F. Imani (2008). “Scavenger receptor class-A is a novel cell surface receptor for double-stranded RNA.” *FASEB J* 22(1): 159–167.

- Lindberg, S., A. Munoz-Alarcon, H. Helmfors, D. Mosqueira, D. Gyllborg, O. Tudoran and U. Langel (2013). "PepFect15, a novel endosomolytic cell-penetrating peptide for oligonucleotide delivery via scavenger receptors." *Int J Pharm* 441(1–2): 242–247.
- Lundberg, P., S. El-Andaloussi, T. Sutlu, H. Johansson and U. Langel (2007). "Delivery of short interfering RNA using endosomolytic cell-penetrating peptides." *FASEB J* 21(11): 2664–2671.
- Lundmark, R., G. J. Doherty, M. T. Howes, K. Cortese, Y. Vallis, R. G. Parton and H. T. McMahon (2008). "The GTPase-activating protein GRAF1 regulates the CLIC/GEEC endocytic pathway." *Curr Biol* 18(22): 1802–1808.
- Magzoub, M., K. Kilk, L. E. Eriksson, U. Langel and A. Graslund (2001). "Interaction and structure induction of cell-penetrating peptides in the presence of phospholipid vesicles." *Biochim Biophys Acta* 1512(1): 77–89.
- Marechal, V., M. C. Prevost, C. Petit, E. Perret, J. M. Heard and O. Schwartz (2001). "Human immunodeficiency virus type 1 entry into macrophages mediated by macropinocytosis." *J Virol* 75(22): 11166–11177.
- Margus, H., C. Juks and M. Pooga (2015). "Unraveling the Mechanisms of Peptide-Mediated Delivery of Nucleic Acids Using Electron Microscopy." *Methods Mol Biol* 1324: 149–162.
- Margus, H., K. Padari and M. Pooga (2012). "Cell-penetrating peptides as versatile vehicles for oligonucleotide delivery." *Mol Ther* 20(3): 525–533.
- Mayor, S., J. F. Presley and F. R. Maxfield (1993). "Sorting of membrane components from endosomes and subsequent recycling to the cell surface occurs by a bulk flow process." *J Cell Biol* 121(6): 1257–1269.
- McMahon, H. T. and E. Boucrot (2011). "Molecular mechanism and physiological functions of clathrin-mediated endocytosis." *Nat Rev Mol Cell Biol* 12(8): 517–533.
- Mehlin, H., B. Daneholt and U. Skoglund (1992). "Translocation of a specific premessenger ribonucleoprotein particle through the nuclear pore studied with electron microscope tomography." *Cell* 69(4): 605–613.
- Meier, O., K. Boucke, S. V. Hammer, S. Keller, R. P. Stidwill, S. Hemmi and U. F. Greber (2002). "Adenovirus triggers macropinocytosis and endosomal leakage together with its clathrin-mediated uptake." *J Cell Biol* 158(6): 1119–1131.
- Mercer, J. and A. Helenius (2008). "Vaccinia virus uses macropinocytosis and apoptotic mimicry to enter host cells." *Science* 320(5875): 531–535.
- Mercer, J. and A. Helenius (2009). "Virus entry by macropinocytosis." *Nat Cell Biol* 11(5): 510–520.
- Mitchell, D. J., D. T. Kim, L. Steinman, C. G. Fathman and J. B. Rothbard (2000). "Polyarginine enters cells more efficiently than other polycationic homopolymers." *J. Pept. Res.* 56(5): 318–325.
- Miyata, Y., E. Nishida, S. Koyasu, I. Yahara and H. Sakai (1989). "Protein kinase C-dependent and -independent pathways in the growth factor-induced cytoskeletal reorganization." *J Biol Chem* 264(26): 15565–15568.
- Moore, R. H., A. Tuffaha, E. E. Millman, W. Dai, H. S. Hall, B. F. Dickey and B. J. Knoll (1999). "Agonist-induced sorting of human beta2-adrenergic receptors to lysosomes during downregulation." *J Cell Sci* 112 (Pt 3): 329–338.
- Morris, M. C., L. Chaloin, M. Choob, J. Archdeacon, F. Heitz and G. Divita (2004). "Combination of a new generation of PNAs with a peptide-based carrier enables efficient targeting of cell cycle progression." *Gene Ther* 11(9): 757–764.

- Morris, M. C., L. Chaloin, J. Mery, F. Heitz and G. Divita (1999). "A novel potent strategy for gene delivery using a single peptide vector as a carrier." *Nucleic Acids Res* 27(17): 3510–3517.
- Morris, M. C., J. Depollier, J. Mery, F. Heitz and G. Divita (2001). "A peptide carrier for the delivery of biologically active proteins into mammalian cells." *Nat Biotechnol* 19(12): 1173–1176.
- Morris, M. C., E. Gros, G. Aldrian-Herrada, M. Choob, J. Archdeacon, F. Heitz and G. Divita (2007). "A non-covalent peptide-based carrier for in vivo delivery of DNA mimics." *Nucleic Acids Res* 35(7): e49.
- Morris, M. C., P. Vidal, L. Chaloin, F. Heitz and G. Divita (1997). "A new peptide vector for efficient delivery of oligonucleotides into mammalian cells." *Nucleic Acids Res* 25(14): 2730–2736.
- Mosesson, Y., K. Shtiegman, M. Katz, Y. Zwang, G. Vereb, J. Szollosi and Y. Yarden (2003). "Endocytosis of receptor tyrosine kinases is driven by monoubiquitylation, not polyubiquitylation." *J Biol Chem* 278(24): 21323–21326.
- Muratovska, A. and M. R. Eccles (2004). "Conjugate for efficient delivery of short interfering RNA (siRNA) into mammalian cells." *FEBS Lett* 558(1–3): 63–68.
- Murk, J. L., G. Posthuma, A. J. Koster, H. J. Geuze, A. J. Verkleij, M. J. Kleijmeer and B. M. Humbel (2003). "Influence of aldehyde fixation on the morphology of endosomes and lysosomes: quantitative analysis and electron tomography." *J Microsc* 212(Pt 1): 81–90.
- Mäe, M., S. El Andaloussi, P. Lundin, N. Oskolkov, H. J. Johansson, P. Guterstam and Ü. Langel (2009). "A stearylated CPP for delivery of splice correcting oligonucleotides using a non-covalent co-incubation strategy." *J Control Release* 134(3): 221–227.
- Nakamura, Y., K. Kogure, S. Futaki and H. Harashima (2007). "Octaarginine-modified multifunctional envelope-type nano device for siRNA." *J Control Release* 119(3): 360–367.
- Nakase, I., N. B. Kobayashi, T. Takatani-Nakase and T. Yoshida (2015). "Active macropinocytosis induction by stimulation of epidermal growth factor receptor and oncogenic Ras expression potentiates cellular uptake efficacy of exosomes." *Sci Rep* 5: 10300.
- Nakase, I., M. Niwa, T. Takeuchi, K. Sonomura, N. Kawabata, Y. Koike, M. Takehashi, S. Tanaka, K. Ueda, J. C. Simpson, et al. (2004). "Cellular uptake of arginine-rich peptides: roles for macropinocytosis and actin rearrangement." *Mol Ther* 10(6): 1011–1022.
- Nakase, I., A. Tadokoro, N. Kawabata, T. Takeuchi, H. Katoh, K. Hiramoto, M. Negishi, M. Nomizu, Y. Sugiura and S. Futaki (2007). "Interaction of arginine-rich peptides with membrane-associated proteoglycans is crucial for induction of actin organization and macropinocytosis." *Biochemistry* 46(2): 492–501.
- Naslavsky, N., R. Weigert and J. G. Donaldson (2003). "Convergence of non-clathrin- and clathrin-derived endosomes involves Arf6 inactivation and changes in phosphoinositides." *Mol Biol Cell* 14(2): 417–431.
- Nassar, Z. D. and M. O. Parat (2015). "Cavin Family: New Players in the Biology of Caveolae." *Int Rev Cell Mol Biol* 320: 235–305.
- Nel, A. E., L. Madler, D. Velegol, T. Xia, E. M. Hoek, P. Somasundaran, F. Klaessig, V. Castranova and M. Thompson (2009). "Understanding biophysicochemical interactions at the nano-bio interface." *Nat Mater* 8(7): 543–557.

- Norbury, C. C., B. J. Chambers, A. R. Prescott, H. G. Ljunggren and C. Watts (1997). "Constitutive macropinocytosis allows TAP-dependent major histocompatibility complex class I presentation of exogenous soluble antigen by bone marrow-derived dendritic cells." *Eur J Immunol* 27(1): 280–288.
- Norbury, C. C., L. J. Hewlett, A. R. Prescott, N. Shastri and C. Watts (1995). "Class I MHC presentation of exogenous soluble antigen via macropinocytosis in bone marrow macrophages." *Immunity* 3(6): 783–791.
- Oehlke, J., E. Krause, B. Wiesner, M. Beyermann and M. Bienert (1997). "Extensive cellular uptake into endothelial cells of an amphipathic beta- sheet forming peptide." *FEBS Lett* 415(2): 196–199.
- Oehlke, J., A. Scheller, B. Wiesner, E. Krause, M. Beyermann, E. Klauschenz, M. Melzig and M. Bienert (1998). "Cellular uptake of an alpha-helical amphipathic model peptide with the potential to deliver polar compounds into the cell interior non- endocytically." *Biochim Biophys Acta* 1414(1–2): 127–139.
- Ohkuma, S., Y. Moriyama and T. Takano (1982). "Identification and characterization of a proton pump on lysosomes by fluorescein-isothiocyanate-dextran fluorescence." *Proc Natl Acad Sci U S A* 79(9): 2758–2762.
- Ortegren, U., M. Karlsson, N. Blazic, M. Blomqvist, F. H. Nystrom, J. Gustavsson, P. Fredman and P. Stralfors (2004). "Lipids and glycosphingolipids in caveolae and surrounding plasma membrane of primary rat adipocytes." *Eur J Biochem* 271(10): 2028–2036.
- Oskolkov, N., P. Arukuusk, D. M. Copolovici, S. Lindberg, H. Margus, K. Padari, M. Pooga and Ü. Langel (2011). "NickFects, Phosphorylated Derivatives of Transportan 10 for Cellular Delivery of Oligonucleotides." *Int J Pept Res Ther* 17: 147–157.
- Owens, D. E., 3rd and N. A. Peppas (2006). "Opsonization, biodistribution, and pharmacokinetics of polymeric nanoparticles." *Int J Pharm* 307(1): 93–102.
- Padari, K., K. Koppel, A. Lorents, M. Hällbrink, M. Mano, M. C. Pedroso de Lima and M. Pooga (2010). "S4(13)-PV cell-penetrating peptide forms nanoparticle-like structures to gain entry into cells." *Bioconjug Chem* 21(4): 774–783.
- Palade, G. E. (1953). "An electron microscope study of the mitochondrial structure." *J Histochem Cytochem* 1(4): 188–211.
- Palade, G. E. and R. R. Bruns (1968). "Structural modulations of plasmalemmal vesicles." *J Cell Biol* 37(3): 633–649.
- Pan, Q., O. Shai, L. J. Lee, B. J. Frey and B. J. Blencowe (2008). "Deep surveying of alternative splicing complexity in the human transcriptome by high-throughput sequencing." *Nat Genet* 40(12): 1413–1415.
- Parrini, M. C., M. Matsuda and J. de Gunzburg (2005). "Spatiotemporal regulation of the Pak1 kinase." *Biochem Soc Trans* 33(Pt 4): 646–648.
- Parton, R. G. and M. T. Howes (2010). "Revisiting caveolin trafficking: the end of the caveosome." *J Cell Biol* 191(3): 439–441.
- Parton, R. G. and K. Simons (2007). "The multiple faces of caveolae." *Nature Reviews Molecular Cell Biology* 8(3): 185–194.
- Patel, P. C., D. A. Giljohann, W. L. Daniel, D. Zheng, A. E. Prigodich and C. A. Mirkin (2010). "Scavenger receptors mediate cellular uptake of polyvalent oligonucleotide-functionalized gold nanoparticles." *Bioconjug Chem* 21(12): 2250–2256.
- Payne, C. K., S. A. Jones, C. Chen and X. Zhuang (2007). "Internalization and trafficking of cell surface proteoglycans and proteoglycan-binding ligands." *Traffic* 8(4): 389–401.

- Pearson, A. M., A. Rich and M. Krieger (1993). "Polynucleotide binding to macrophage scavenger receptors depends on the formation of base-quartet-stabilized four-stranded helices." *J Biol Chem* 268(5): 3546–3554.
- Peiser, L. and S. Gordon (2001). "The function of scavenger receptors expressed by macrophages and their role in the regulation of inflammation." *Microbes Infect* 3(2): 149–159.
- Pelkmans, L., J. Kartenbeck and A. Helenius (2001). "Caveolar endocytosis of simian virus 40 reveals a new two-step vesicular-transport pathway to the ER." *Nat Cell Biol* 3(5): 473–483.
- Philo, J. S. (2006). "Is any measurement method optimal for all aggregate sizes and types?" *AAPS J* 8(3): E564–571.
- Platt, N. and S. Gordon (1998). "Scavenger receptors: diverse activities and promiscuous binding of polyanionic ligands." *Chem Biol* 5(8): R193–203.
- Pooga, M., M. Hällbrink, M. Zorko and Ü. Langel (1998). "Cell penetration by transportan." *FASEB J.* 12(1): 67–77.
- Prabha, S., W. Z. Zhou, J. Panyam and V. Labhasetwar (2002). "Size-dependency of nanoparticle-mediated gene transfection: studies with fractionated nanoparticles." *Int J Pharm* 244(1–2): 105–115.
- Prabhudas, M., D. Bowdish, K. Drickamer, M. Febbraio, J. Herz, L. Kobzik, M. Krieger, J. Loike, T. K. Means, S. K. Moestrup, et al. (2014). "Standardizing scavenger receptor nomenclature." *J Immunol* 192(5): 1997–2006.
- Racoosin, E. L. and J. A. Swanson (1993). "Macropinosome maturation and fusion with tubular lysosomes in macrophages." *J Cell Biol* 121(5): 1011–1020.
- Ramsay, E. and M. Gumbleton (2002). "Polylysine and polyornithine gene transfer complexes: a study of complex stability and cellular uptake as a basis for their differential in-vitro transfection efficiency." *J Drug Target* 10(1): 1–9.
- Ramsey, J. D. and N. H. Flynn (2015). "Cell-penetrating peptides transport therapeutics into cells." *Pharmacol Ther* 154: 78–86.
- Richard, J. P., K. Melikov, H. Brooks, P. Prevot, B. Lebleu and L. V. Chernomordik (2005). "Cellular uptake of unconjugated TAT peptide involves clathrin-dependent endocytosis and heparan sulfate receptors." *J Biol Chem* 280(15): 15300–15306.
- Richter, T., M. Floetenmeyer, C. Ferguson, J. Galea, J. Goh, M. R. Lindsay, G. P. Morgan, B. J. Marsh and R. G. Parton (2008). "High-resolution 3D quantitative analysis of caveolar ultrastructure and caveola-cytoskeleton interactions." *Traffic* 9(6): 893–909.
- Richterova, Z., D. Liebl, M. Horak, Z. Palkova, J. Stokrova, P. Hozak, J. Korb and J. Forstova (2001). "Caveolae are involved in the trafficking of mouse polyomavirus virions and artificial VP1 pseudocapsids toward cell nuclei." *J Virol* 75(22): 10880–10891.
- Riento, K., M. Frick, I. Schafer and B. J. Nichols (2009). "Endocytosis of flotillin-1 and flotillin-2 is regulated by Fyn kinase." *J Cell Sci* 122(Pt 7): 912–918.
- Rink, J., E. Ghigo, Y. Kalaidzidis and M. Zerial (2005). "Rab conversion as a mechanism of progression from early to late endosomes." *Cell* 122(5): 735–749.
- Rothberg, K. G., J. E. Heuser, W. C. Donzell, Y. S. Ying, J. R. Glenney and R. G. Anderson (1992). "Caveolin, a protein component of caveolae membrane coats." *Cell* 68(4): 673–682.
- Rothnie, A., A. R. Clarke, P. Kuzmic, A. Cameron and C. J. Smith (2011). "A sequential mechanism for clathrin cage disassembly by 70-kDa heat-shock cognate protein (Hsc70) and auxilin." *Proc Natl Acad Sci U S A* 108(17): 6927–6932.

- Rudolph, C., C. Plank, J. Lausier, U. Schillinger, R. H. Muller and J. Rosenecker (2003). "Oligomers of the arginine-rich motif of the HIV-1 TAT protein are capable of transferring plasmid DNA into cells." *J Biol Chem* 278(13): 11411–11418.
- Ruozzi, B., D. Belletti, A. Tombesi, G. Tosi, L. Bondioli, F. Forni and M. A. Vandelli (2011). "AFM, ESEM, TEM, and CLSM in liposomal characterization: a comparative study." *Int J Nanomedicine* 6: 557–563.
- Räägel, H., P. Saalik, M. Hansen, Ü. Langel and M. Pooga (2009). "CPP-protein constructs induce a population of non-acidic vesicles during trafficking through endo-lysosomal pathway." *J Control Release* 139(2): 108–117.
- Rydström, A., S. Deshayes, K. Konate, L. Crombez, K. Padari, H. Boukhaddaoui, G. Aldrian, M. Pooga and G. Divita (2011). "Direct Translocation as Major Cellular Uptake for CADY Self-Assembling Peptide-Based Nanoparticles." *PLoS One* 6(10): e25924.
- Ryter, J. M. and S. C. Schultz (1998). "Molecular basis of double-stranded RNA-protein interactions: structure of a dsRNA-binding domain complexed with dsRNA." *EMBO J* 17(24): 7505–7513.
- Sabharanjak, S., P. Sharma, R. G. Parton and S. Mayor (2002). "GPI-anchored proteins are delivered to recycling endosomes via a distinct cdc42-regulated, clathrin-independent pinocytic pathway." *Dev Cell* 2(4): 411–423.
- Safran, M., W. Y. Kim, A. L. Kung, J. W. Horner, R. A. DePinho and W. G. Kaelin, Jr. (2003). "Mouse reporter strain for noninvasive bioluminescent imaging of cells that have undergone Cre-mediated recombination." *Mol Imaging* 2(4): 297–302.
- Sallusto, F., M. Cella, C. Danieli and A. Lanzavecchia (1995). "Dendritic cells use macropinocytosis and the mannose receptor to concentrate macromolecules in the major histocompatibility complex class II compartment: downregulation by cytokines and bacterial products." *J Exp Med* 182(2): 389–400.
- Salzer, U. and R. Prohaska (2001). "Stomatin, flotillin-1, and flotillin-2 are major integral proteins of erythrocyte lipid rafts." *Blood* 97(4): 1141–1143.
- Sandgren, S., F. Cheng and M. Belting (2002). "Nuclear targeting of macromolecular polyanions by an HIV-Tat derived peptide. Role for cell-surface proteoglycans." *J Biol Chem* 277(41): 38877–38883.
- Santamaria, A., E. Castellanos, V. Gomez, P. Bénédict, J. Renau-Piqueras, J. Morote, J. Reventos, T. M. Thomson and R. Paciucci (2005). "PTOV1 enables the nuclear translocation and mitogenic activity of flotillin-1, a major protein of lipid rafts." *Mol Cell Biol* 25(5): 1900–1911.
- Scherer, P. E., R. Y. Lewis, D. Volonte, J. A. Engelman, F. Galbiati, J. Couet, D. S. Kohtz, E. van Donselaar, P. Peters and M. P. Lisanti (1997). "Cell-type and tissue-specific expression of caveolin-2. Caveolins 1 and 2 co-localize and form a stable hetero-oligomeric complex in vivo." *J Biol Chem* 272(46): 29337–29346.
- Scherer, P. E., T. Okamoto, M. Chun, I. Nishimoto, H. F. Lodish and M. P. Lisanti (1996). "Identification, sequence, and expression of caveolin-2 defines a caveolin gene family." *Proc Natl Acad Sci U S A* 93(1): 131–135.
- Schmid, E. M., M. G. Ford, A. Burtey, G. J. Praefcke, S. Y. Peak-Chew, I. G. Mills, A. Benmerah and H. T. McMahon (2006). "Role of the AP2 beta-appendage hub in recruiting partners for clathrin-coated vesicle assembly." *PLoS Biol* 4(9): e262.
- Simeoni, F., M. C. Morris, F. Heitz and G. Divita (2003). "Insight into the mechanism of the peptide-based gene delivery system MPG: implications for delivery of siRNA into mammalian cells." *Nucleic Acids Res* 31(11): 2717–2724.

- Simionescu, M., D. Popov and A. Sima (2009). "Endothelial transcytosis in health and disease." *Cell Tissue Res* 335(1): 27–40.
- Sleat, D. E., H. Lackland, Y. Wang, I. Sohar, G. Xiao, H. Li and P. Lobel (2005). "The human brain mannose 6-phosphate glycoproteome: a complex mixture composed of multiple isoforms of many soluble lysosomal proteins." *Proteomics* 5(6): 1520–1532.
- Sonavane, G., K. Tomoda and K. Makino (2008). "Biodistribution of colloidal gold nanoparticles after intravenous administration: effect of particle size." *Colloids Surf B Biointerfaces* 66(2): 274–280.
- Song, K. S., P. E. Scherer, Z. Tang, T. Okamoto, S. Li, M. Chafel, C. Chu, D. S. Kohtz and M. P. Lisanti (1996). "Expression of caveolin-3 in skeletal, cardiac, and smooth muscle cells. Caveolin-3 is a component of the sarcolemma and co-fractionates with dystrophin and dystrophin-associated glycoproteins." *J Biol Chem* 271(25): 15160–15165.
- Stang, E., J. Kartenbeck and R. G. Parton (1997). "Major histocompatibility complex class I molecules mediate association of SV40 with caveolae." *Mol Biol Cell* 8(1): 47–57.
- Stenson, P. D., M. Mort, E. V. Ball, K. Shaw, A. Phillips and D. N. Cooper (2014). "The Human Gene Mutation Database: building a comprehensive mutation repository for clinical and molecular genetics, diagnostic testing and personalized genomic medicine." *Hum Genet* 133(1): 1–9.
- Stimpson, H. E., C. P. Toret, A. T. Cheng, B. S. Pauly and D. G. Drubin (2009). "Early-arriving Syplp and Edelp function in endocytic site placement and formation in budding yeast." *Mol Biol Cell* 20(22): 4640–4651.
- Subtil, A., M. Delepiepierre and A. Dautry-Varsat (1997). "An alpha-helical signal in the cytosolic domain of the interleukin 2 receptor beta chain mediates sorting towards degradation after endocytosis." *J Cell Biol* 136(3): 583–595.
- Subtil, A., A. Hemar and A. Dautry-Varsat (1994). "Rapid endocytosis of interleukin 2 receptors when clathrin-coated pit endocytosis is inhibited." *J Cell Sci* 107 (Pt 12): 3461–3468.
- Swanson, J. A. (1989). "Phorbol esters stimulate macropinocytosis and solute flow through macrophages." *J Cell Sci* 94 (Pt 1): 135–142.
- Zauner, W., N. A. Farrow and A. M. Haines (2001). "In vitro uptake of polystyrene microspheres: effect of particle size, cell line and cell density." *J Control Release* 71(1): 39–51.
- Zhang, S., J. Li, G. Lykotrafitis, G. Bao and S. Suresh (2009). "Size-Dependent Endocytosis of Nanoparticles." *Adv Mater* 21: 419–424.
- Zhang, S., Y. Xu, B. Wang, W. Qiao, D. Liu and Z. Li (2004). "Cationic compounds used in lipoplexes and polyplexes for gene delivery." *J Control Release* 100(2): 165–180.
- Zhao, F., J. Zhang, Y. S. Liu, L. Li and Y. L. He (2011). "Research advances on flotilins." *Virol J* 8: 479.
- Ziegler, A. (2008). "Thermodynamic studies and binding mechanisms of cell-penetrating peptides with lipids and glycosaminoglycans." *Adv Drug Deliv Rev* 60(4–5): 580–597.
- Ziegler, A., X. L. Blatter, A. Seelig and J. Seelig (2003). "Protein transduction domains of HIV-1 and SIV TAT interact with charged lipid vesicles. Binding mechanism and thermodynamic analysis." *Biochemistry* 42(30): 9185–9194.

- Tang, Z., P. E. Scherer, T. Okamoto, K. Song, C. Chu, D. S. Kohtz, I. Nishimoto, H. F. Lodish and M. P. Lisanti (1996). "Molecular cloning of caveolin-3, a novel member of the caveolin gene family expressed predominantly in muscle." *J Biol Chem* 271(4): 2255–2261.
- Thomsen, P., K. Roepstorff, M. Stahlhut and B. van Deurs (2002). "Caveolae are highly immobile plasma membrane microdomains, which are not involved in constitutive endocytic trafficking." *Mol. Biol. Cell* 13(1): 238–250.
- Tian, B., P. C. Bevilacqua, A. Diegelman-Parente and M. B. Mathews (2004). "The double-stranded-RNA-binding motif: interference and much more." *Nat Rev Mol Cell Biol* 5(12): 1013–1023.
- Tiriveedhi, V. and P. Butko (2007). "A fluorescence spectroscopy study on the interactions of the TAT-PTD peptide with model lipid membranes." *Biochemistry* 46(12): 3888–3895.
- Trabulo, S., S. Resina, S. Simoes, B. Lebleu and M. C. Pedroso de Lima (2010). "A non-covalent strategy combining cationic lipids and CPPs to enhance the delivery of splice correcting oligonucleotides." *J Control Release* 145(2): 149–158.
- Troiber, C., J. C. Kasper, S. Milani, M. Scheible, I. Martin, F. Schaubhut, S. Kuchler, J. Radler, F. C. Simmel, W. Friess, et al. (2013). "Comparison of four different particle sizing methods for siRNA polyplex characterization." *Eur J Pharm Biopharm* 84(2): 255–264.
- Tung, C. H., S. Mueller and R. Weissleder (2002). "Novel branching membrane translocational peptide as gene delivery vector." *Bioorg Med Chem* 10(11): 3609–3614.
- Tönges, L., P. Lingor, R. Egle, G. P. Dietz, A. Fahr and M. Bahr (2006). "Stearylated octaarginine and artificial virus-like particles for transfection of siRNA into primary rat neurons." *RNA* 12(7): 1431–1438.
- Tyagi, M., M. Rusnati, M. Presta and M. Giacca (2001). "Internalization of HIV-1 tat requires cell surface heparan sulfate proteoglycans." *J Biol Chem* 276(5): 3254–3261. Epub 2000 Oct 3256.
- ur Rehman, Z., D. Hoekstra and I. S. Zuhorn (2013). "Mechanism of polyplex- and lipoplex-mediated delivery of nucleic acids: real-time visualization of transient membrane destabilization without endosomal lysis." *ACS Nano* 7(5): 3767–3777.
- Wadia, J. S., R. V. Stan and S. F. Dowdy (2004). "Transducible TAT-HA fusogenic peptide enhances escape of TAT-fusion proteins after lipid raft macropinocytosis." *Nat. Med.* 10(3): 310–315.
- Walkey, C. D., J. B. Olsen, F. Song, R. Liu, H. Guo, D. W. Olsen, Y. Cohen, A. Emili and W. C. Chan (2014). "Protein corona fingerprinting predicts the cellular interaction of gold and silver nanoparticles." *ACS Nano* 8(3): 2439–2455.
- van Asbeck, A. H., A. Beyerle, H. McNeill, P. H. Bovee-Geurts, S. Lindberg, W. P. Verdurmen, M. Hallbrink, U. Langel, O. Heidenreich and R. Brock (2013). "Molecular parameters of siRNA--cell penetrating peptide nanocomplexes for efficient cellular delivery." *ACS Nano* 7(5): 3797–3807.
- van der Blik, A. M., T. E. Redelmeier, H. Damke, E. J. Tisdale, E. M. Meyerowitz and S. L. Schmid (1993). "Mutations in human dynamin block an intermediate stage in coated vesicle formation." *J Cell Biol* 122(3): 553–563.
- van der Schaar, H. M., M. J. Rust, C. Chen, H. van der Ende-Metselaar, J. Wilschut, X. Zhuang and J. M. Smit (2008). "Dissecting the cell entry pathway of dengue virus by single-particle tracking in living cells." *PLoS Pathog* 4(12): e1000244.

- Wang, E. T., R. Sandberg, S. Luo, I. Khrebtkova, L. Zhang, C. Mayr, S. F. Kingsmore, G. P. Schroth and C. B. Burge (2008). "Alternative isoform regulation in human tissue transcriptomes." *Nature* 456(7221): 470–476.
- Way, M. and R. G. Parton (1995). "M-caveolin, a muscle-specific caveolin-related protein." *FEBS Lett* 376(1–2): 108–112.
- Veldhoen, S., S. D. Laufer, A. Trampe and T. Restle (2006). "Cellular delivery of small interfering RNA by a non-covalently attached cell-penetrating peptide: quantitative analysis of uptake and biological effect." *Nucleic Acids Res* 34(22): 6561–6573.
- Wente, S. R. and M. P. Rout (2010). "The nuclear pore complex and nuclear transport." *Cold Spring Harb Perspect Biol* 2(10): a000562.
- Vercauteren, D., M. Piest, L. J. van der Aa, M. Al Soraj, A. T. Jones, J. F. Engbersen, S. C. De Smedt and K. Braeckmans (2011). "Flotillin-dependent endocytosis and a phagocytosis-like mechanism for cellular internalization of disulfide-based poly(amido amine)/DNA polyplexes." *Biomaterials* 32(11): 3072–3084.
- West, M. A., A. R. Prescott, E. L. Eskelinen, A. J. Ridley and C. Watts (2000). "Rac is required for constitutive macropinocytosis by dendritic cells but does not control its downregulation." *Curr Biol* 10(14): 839–848.
- Wibo, M. and B. Poole (1974). "Protein degradation in cultured cells. II. The uptake of chloroquine by rat fibroblasts and the inhibition of cellular protein degradation and cathepsin B1." *J Cell Biol* 63(2 Pt 1): 430–440.
- Wimley, W. C. W., S.H. (1994). "Peptides in lipid bilayers: structural and thermodynamic basis for partitioning and folding." *Curr. Opin. Struc. Biol* 4: 79–86.
- Wittrup, A., A. Ai, X. Liu, P. Hamar, R. Trifonova, K. Charisse, M. Manoharan, T. Kirchhausen and J. Lieberman (2015). "Visualizing lipid-formulated siRNA release from endosomes and target gene knockdown." *Nat Biotechnol* 33(8): 870–876.
- Vives, E., P. Brodin and B. Lebleu (1997). "A truncated HIV-1 Tat protein basic domain rapidly translocates through the plasma membrane and accumulates in the cell nucleus." *J Biol Chem* 272(25): 16010–16017.
- Yamada, E. (1955). "The fine structure of the gall bladder epithelium of the mouse." *J Biophys Biochem Cytol* 1(5): 445–458.
- Yandek, L. E., A. Pokorný, A. Florén, K. Knoelke, Ü. Langel and P. F. Almeida (2007). "Mechanism of the cell-penetrating peptide transportan 10 permeation of lipid bilayers." *Biophys J* 92(7): 2434–2444.
- Yin, H., R. L. Kanasty, A. A. Eltoukhy, A. J. Vegas, J. R. Dorkin and D. G. Anderson (2014). "Non-viral vectors for gene-based therapy." *Nat Rev Genet* 15(8): 541–555.
- Yu, C., E. Nwabuisi-Heath, K. Laxton and M. J. Ladu (2010). "Endocytic pathways mediating oligomeric Abeta42 neurotoxicity." *Mol Neurodegener* 5: 19.

ACKNOWLEDGMENTS

First and foremost, I want to express my deepest gratitude to my supervisor, Prof. Margus Pooga for introducing me to the world of CPP research. It was only due to his support and guidance that I was able to reach to the completion of my Ph.D studies. I am also very thankful to my co-supervisor dr. Kärt Padari for sharing her knowledge of fascinating field of transmission electron microscopy.

I thank Janely, Carmen, Annely and Indrek for being good lab mates. Special thanks to Janely for the small and deep talks which were particularly necessary during writing my thesis, and to Indrek for endless supplies of candies and chocolate which saved my brain from shutting down in countless times. I also thank my colleagues from the department of developmental biology for the quality time spent either in the labs coffee-corner or on yearly canoeing trips.

I am grateful to dr. Tiina Tamm for proofreading my thesis. Her comments and suggestions significantly improved the overall quality of my thesis. I acknowledge my colleagues from the Institute of Technology, especially Prof. Ülo Langel and dr. Piret Arukuusk for prosperous collaborations.

I express my gratitude to the staff of EMCF at the EMBL for training me to become a better electron microscopy specialist. Especially, I would like to thank dr. Yannick Schwab for taking me in his facility, and Pedro for being the funniest, craziest and sweetest lab mate one could wish for.

I thank Grete K, Grete T, Kärt and Marilyn for all the time we have spent together during the past 10 years of our friendship. I am glad that despite walking entirely different roads in life we still stick together and support each other. PS: It's a pity that we did not play the "Guess who will get to the Ph.D first" game. Now we can only stick to "Who would have guessed that...".

I thank the members of Sulgpalliakadeemikud, especially Karro, Laura, Arthur, Sander, Sten and Sven for the passionate games on the court and in the pubs.

Thank you, Ivar-Endrik. I couldn't have done this without your endless support and faith in me.

*Tänan oma perekonda,
kes on minu valikutes alati toetanud.*

PUBLICATIONS

CURRICULUM VITAE

Name: Helerin Margus
Date of Birth: June 22, 1987
Nationality: Estonian
Contact: University of Tartu, Institute of Molecular and Cell Biology,
23 Riia Street, 51010, Tartu, Estonia
E-mail: helerin.margus@ut.ee

Education and professional employment:

2003–2006 Rakvere Gymnasium
2006–2009 University of Tartu, BSc in gene technology
2009–2011 University of Tartu, MSc in gene technology
2011–... University of Tartu, PhD student in Institute of Molecular and Cell Biology

Special courses:

2014 FEBS-EMBO conference, Paris, France
2013–2014 Visiting predoctoral fellow at the European Molecular Biology Laboratory (EMBL), Heidelberg, Germany, 5 months
2012 FEI practical course “Electron Tomography”, Eindhoven, Netherlands
2012 Leica instrument and application training course “Cryo-sectioning According to Tokuyasu Method”, Vienna, Austria
2012 EMBO practical course “Electron Microscopy and Stereology in Cell Biology”, České Budějovice, Czech Republic (oral presentation)
2011 University of Tartu conference “Peptide Vectors and Delivery of Pharmaceuticals”, Tallinn, Estonia

Scientific work:

The focus of my research is characterizing cell-penetrating peptide complexes with nucleic acids and examining their cell-entry pathways and intracellular trafficking.

List of publications:

Sork, H., Nordin J.C., Turunen, J.J., Wiklander, O.P.B., Bestas B., Zaghloul E.M., Margus, H., Padari K., Duru, A.D., Corso, G., Bost, J., Vader, P., Pooga, M., Smith, C.E., Wood, M.J.A, M Schiffelers, R.M., Hällbrink, M. and El Andaloussi, S. (2016) “Lipid-based transfection reagents exhibit cryo-induced increase in Transfection efficiency” *Molecular Pharmaceutics* 5, e290; doi:10.1038/mtna.2016.8

- Margus, H., Arukuusk, P., Langel, Ü., Pooga, M. (2016). "Characteristics of cell-penetrating peptide/nucleic acid nanocomplexes" *Molecular Pharmaceutics* 13(1):172–179
- Juks C, Padari K, Margus H, Kriiska A, Etverk I, Arukuusk P, Koppel K, Ezzat K, Langel Ü, Pooga M. (2015) "The role of endocytosis in the uptake and intracellular trafficking of PepFect14-nucleic acid nanocomplexes via class A scavenger receptors" *Biochimica. et Biophysica Acta* 1848(12):3205–3216.
- Margus, Helerin; Juks, Carmen; Pooga, Margus (2015) "Unraveling the mechanisms of peptide-mediated delivery of nucleic acids using electron microscopy" in *Cell-Penetrating Peptides. Methods and Protocols. Methods in Molecular Biology*, Ed. By Ülo Langel, pp 149–162
- Arukuusk, P., Pärnaste, L., Margus, H., Eriksson, NK., Vasconcelos, L., Padari, K., Pooga, M., Langel, Ü. (2013) "Differential endosomal pathways for radically modified peptide vectors" *Bioconjugate Chemistry* 24(10):1721–1732.
- Margus, H., Padari, K., Pooga, M. (2013) "Insights into cell entry and intracellular trafficking of peptide and protein drugs provided by electron microscopy. *Advanced Drug Delivery Reviews*. 65(8):1031–1038. Review
- Arukuusk, P. Pärnaste, L., Oskolkov, N., Copolovici, D-M., Margus, H., Padari, K. ö K Maslovskaja J, Tegova R, Kivi G, Langel, Ü. (2013) "New generation of efficient peptide-based vectors, NickFects, for the delivery of nucleic acids" *Biochimica et Biophysica Acta*. 1828(5):1365–1373.
- Veiman, K-L , Ezzat, K., Margus, H., Lehto, T., Langel, K., Kurrikoff, K., Arukuusk, P. h š k , J., Padari, K., Pooga, M., Lehto, T., Langel, Ü. (2013) "PepFect14 peptide vector for efficient gene delivery in cell cultures" *Molecular Pharmaceutics* 10(1):199- 210.
- Margus, H., Padari, K., Pooga, M. (2012) "Cell-penetrating peptides as versatile vehicles for oligonucleotide delivery" *Molecular Therapy* 20(3):525–33. Review
- Oskolkov, N., Arukuusk, P., Copolovici, D-M., Lindberg, S., Margus, H., Padari, K., Pooga, M., Langel Ü. (2011) "NickFects, phosphorylated derivatives of transportan 10 for cellular delivery of oligonucleotides". *International Journal of Peptide Research and Therapeutics* 17(2):147–157.

Social activities:

Member of the Tartu University Academic Sports Club (badminton), Member of the Estonian National Defence League

ELULOOKIRJELDUS

Nimi: Helerin Margus
Sünniaeg: 22. juuni 1987
Kodakondsus: Eesti
Kontaktandmed: Molekulaar- ja rakubioloogia instituut, Tartu Ülikool
Riia 23, 51010 Tartu, Eesti
E-mail: helerin.margus@ut.ee

Haridus ja erialane teenistuskäik:

2003–2006 Rakvere Gümnaasium
2006–2009 Tartu Ülikool, Molekulaar- ja rakubioloogia instituut, BSc
geenitehnoloogia erialal
2009–2011 Tartu Ülikool, Molekulaar ja rakubioloogia instituut, MSc
geenitehnoloogia erialal
2011–... Tartu Ülikool, Molekulaar- ja rakubioloogia instituut,
doktoriõpingud molekulaar- ja rakubioloogia erialal

Erialane enesetäiendus:

2014 FEBS-EMBO konverents bioteadustes, Pariis, Prantsusmaa
2013–2014 Külalisdoktorant Euroopa Molekulaarbioloogia Laboris,
Heidelberg, Saksamaa, 5 kuud
2012 FEI praktiline kursus “Elektrontomograafia”, Eindhoven,
Holland
2012 Leica kursus “Krüolõikamine Tokuyasu meetodil”, Viin,
Austria
2012 EMBO kursus “Elektronmikroskoopia ja stereoloogia raku-
bioloogias”, České Budějovice, Tšehhi (suuline ettekanne)
2011 Tartu Ülikooli konverents “Peptiidsed vektorid ja ravimite
transport”, Tallinn, Eesti

Teadustöö:

Minu uurimistöö põhisuund on rakku sisenevate peptiidide ja nukleiinhappe komplekside iseloomustamine ning nende rakku sisenemise mehhanismide ja rakusisese suunamise uurimine.

Teaduspublikatsioonid:

Sork, H., Nordin J.C., Turunen, J.J., Wiklander, O.P.B., Bestas B., Zaghloul E.M., Margus, H., Padari K., Duru, A.D., Corso, G., Bost, J., Vader, P., Pooga, M., Smith, C.E., Wood, M.J.A., M Schiffelers, R.M., Hällbrink, M. and El Andaloussi, S. (2016) “Lipid-based transfection reagents exhibit cryo-induced increase in Transfection efficiency” Molecular Pharmaceutics 5, e290; doi:10.1038/mtna.2016.8

- Margus, H., Arukuusk, P., Langel, Ü., Pooga, M. (2016). "Characteristics of cell-penetrating peptide/nucleic acid nanocomplexes" *Molecular Pharmaceutics* 13(1):172–179
- Juhs C, Padari K, Margus H, Kriiska A, Etverk I, Arukuusk P, Koppel K, Ezzat K, Langel Ü, Pooga M. (2015) "The role of endocytosis in the uptake and intracellular trafficking of PepFect14-nucleic acid nanocomplexes via class A scavenger receptors" *Biochimica. et Biophysica Acta* 1848(12):3205–3216.
- Margus, Helerin; Juhs, Carmen; Pooga, Margus (2015) "Unraveling the mechanisms of peptide-mediated delivery of nucleic acids using electron microscopy" in *Cell-Penetrating Peptides. Methods and Protocols. Methods in Molecular Biology*, Ed. By Ülo Langel, pp 149–162
- Arukuusk, P., Pärnaste, L., Margus, H., Eriksson, NK., Vasconcelos, L., Padari, K., Pooga, M., Langel, Ü. (2013) "Differential endosomal pathways for radically modified peptide vectors" *Bioconjugate Chemistry* 24(10):1721–1732.
- Margus, H., Padari, K., Pooga, M. (2013) "Insights into cell entry and intracellular trafficking of peptide and protein drugs provided by electron microscopy. *Advanced Drug Delivery Reviews*. 65(8):1031–1038. Review
- Arukuusk, P. Pärnaste, L., Oskolkov, N., Copolovici, D-M., Margus, H., Padari, K. ö K Maslovskaja J, Tegova R, Kivi G, Langel, Ü. (2013) "New generation of efficient peptide-based vectors, NickFects, for the delivery of nucleic acids" *Biochimica et Biophysica Acta*. 1828(5):1365–1373.
- Veiman, K-L , Ezzat, K., Margus, H., Lehto, T., Langel, K., Kurrikoff, K., Arukuusk, P. h š k , J., Padari, K., Pooga, M., Lehto, T., Langel, Ü. (2013) "PepFect14 peptide vector for efficient gene delivery in cell cultures" *Molecular Pharmaceutics* 10(1):199- 210.
- Margus, H., Padari, K., Pooga, M. (2012) "Cell-penetrating peptides as versatile vehicles for oligonucleotide delivery" *Molecular Therapy* 20(3):525–33. Review
- Oskolkov, N., Arukuusk, P., Copolovici, D-M., Lindberg, S., Margus, H., Padari, K., Pooga, M., Langel Ü. (2011) "NickFects, phosphorylated derivatives of transportan 10 for cellular delivery of oligonucleotides". *International Journal of Peptide Research and Therapeutics* 17(2):147–157.

Ühiskondlik tegevus:

Tartu Ülikooli Akadeemilise Spordiklubi liige (sulgpall), Kaitseliidu liige

DISSERTATIONES BIOLOGICAE UNIVERSITATIS TARTUENSIS

1. **Toivo Maimets.** Studies of human oncoprotein p53. Tartu, 1991, 96 p.
2. **Enn K. Seppet.** Thyroid state control over energy metabolism, ion transport and contractile functions in rat heart. Tartu, 1991, 135 p.
3. **Kristjan Zobel.** Epifüütsete makrosamblike väärtus õhu saastuse indikaatoritena Hamar-Dobani boreaalsetes mägimetsades. Tartu, 1992, 131 lk.
4. **Andres Mäe.** Conjugal mobilization of catabolic plasmids by transposable elements in helper plasmids. Tartu, 1992, 91 p.
5. **Maia Kivisaar.** Studies on phenol degradation genes of *Pseudomonas* sp. strain EST 1001. Tartu, 1992, 61 p.
6. **Allan Nurk.** Nucleotide sequences of phenol degradative genes from *Pseudomonas* sp. strain EST 1001 and their transcriptional activation in *Pseudomonas putida*. Tartu, 1992, 72 p.
7. **Ülo Tamm.** The genus *Populus* L. in Estonia: variation of the species biology and introduction. Tartu, 1993, 91 p.
8. **Jaanus Remme.** Studies on the peptidyltransferase centre of the *E.coli* ribosome. Tartu, 1993, 68 p.
9. **Ülo Langel.** Galanin and galanin antagonists. Tartu, 1993, 97 p.
10. **Arvo Käär.** The development of an automatic online dynamic fluorescence-based pH-dependent fiber optic penicillin flowthrough biosensor for the control of the benzylpenicillin hydrolysis. Tartu, 1993, 117 p.
11. **Lilian Järvekülg.** Antigenic analysis and development of sensitive immunoassay for potato viruses. Tartu, 1993, 147 p.
12. **Jaak Palumets.** Analysis of phytomass partition in Norway spruce. Tartu, 1993, 47 p.
13. **Arne Sellin.** Variation in hydraulic architecture of *Picea abies* (L.) Karst. trees grown under different environmental conditions. Tartu, 1994, 119 p.
13. **Mati Reeben.** Regulation of light neurofilament gene expression. Tartu, 1994, 108 p.
14. **Urmas Tartes.** Respiration rhythms in insects. Tartu, 1995, 109 p.
15. **Ülo Puurand.** The complete nucleotide sequence and infections *in vitro* transcripts from cloned cDNA of a potato A potyvirus. Tartu, 1995, 96 p.
16. **Peeter Hõrak.** Pathways of selection in avian reproduction: a functional framework and its application in the population study of the great tit (*Parus major*). Tartu, 1995, 118 p.
17. **Erkki Truve.** Studies on specific and broad spectrum virus resistance in transgenic plants. Tartu, 1996, 158 p.
18. **Illar Pata.** Cloning and characterization of human and mouse ribosomal protein S6-encoding genes. Tartu, 1996, 60 p.
19. **Ülo Niinemets.** Importance of structural features of leaves and canopy in determining species shade-tolerance in temperature deciduous woody taxa. Tartu, 1996, 150 p.

20. **Ants Kurg.** Bovine leukemia virus: molecular studies on the packaging region and DNA diagnostics in cattle. Tartu, 1996, 104 p.
21. **Ene Ustav.** E2 as the modulator of the BPV1 DNA replication. Tartu, 1996, 100 p.
22. **Aksel Soosaar.** Role of helix-loop-helix and nuclear hormone receptor transcription factors in neurogenesis. Tartu, 1996, 109 p.
23. **Maido Remm.** Human papillomavirus type 18: replication, transformation and gene expression. Tartu, 1997, 117 p.
24. **Tiiu Kull.** Population dynamics in *Cypripedium calceolus* L. Tartu, 1997, 124 p.
25. **Kalle Olli.** Evolutionary life-strategies of autotrophic planktonic micro-organisms in the Baltic Sea. Tartu, 1997, 180 p.
26. **Meelis Pärtel.** Species diversity and community dynamics in calcareous grassland communities in Western Estonia. Tartu, 1997, 124 p.
27. **Malle Leht.** The Genus *Potentilla* L. in Estonia, Latvia and Lithuania: distribution, morphology and taxonomy. Tartu, 1997, 186 p.
28. **Tanel Tenson.** Ribosomes, peptides and antibiotic resistance. Tartu, 1997, 80 p.
29. **Arvo Tuvikene.** Assessment of inland water pollution using biomarker responses in fish *in vivo* and *in vitro*. Tartu, 1997, 160 p.
30. **Urmas Saarma.** Tuning ribosomal elongation cycle by mutagenesis of 23S rRNA. Tartu, 1997, 134 p.
31. **Henn Ojaveer.** Composition and dynamics of fish stocks in the gulf of Riga ecosystem. Tartu, 1997, 138 p.
32. **Lembi Lõugas.** Post-glacial development of vertebrate fauna in Estonian water bodies. Tartu, 1997, 138 p.
33. **Margus Pooga.** Cell penetrating peptide, transportan, and its predecessors, galanin-based chimeric peptides. Tartu, 1998, 110 p.
34. **Andres Saag.** Evolutionary relationships in some cetrarioid genera (Lichenized Ascomycota). Tartu, 1998, 196 p.
35. **Aivar Liiv.** Ribosomal large subunit assembly *in vivo*. Tartu, 1998, 158 p.
36. **Tatjana Oja.** Isoenzyme diversity and phylogenetic affinities among the eurasian annual bromes (*Bromus* L., Poaceae). Tartu, 1998, 92 p.
37. **Mari Moora.** The influence of arbuscular mycorrhizal (AM) symbiosis on the competition and coexistence of calcareous grassland plant species. Tartu, 1998, 78 p.
38. **Olavi Kurina.** Fungus gnats in Estonia (*Diptera: Bolitophilidae, Kero-platidae, Macroceridae, Ditomyiidae, Diadocidiidae, Mycetophilidae*). Tartu, 1998, 200 p.
39. **Andrus Tasa.** Biological leaching of shales: black shale and oil shale. Tartu, 1998, 98 p.
40. **Arnold Kristjuhan.** Studies on transcriptional activator properties of tumor suppressor protein p53. Tartu, 1998, 86 p.
41. **Sulev Ingerpuu.** Characterization of some human myeloid cell surface and nuclear differentiation antigens. Tartu, 1998, 163 p.

42. **Veljo Kisand.** Responses of planktonic bacteria to the abiotic and biotic factors in the shallow lake Võrtsjärv. Tartu, 1998, 118 p.
43. **Kadri Põldmaa.** Studies in the systematics of hypomyces and allied genera (Hypocreales, Ascomycota). Tartu, 1998, 178 p.
44. **Markus Vetemaa.** Reproduction parameters of fish as indicators in environmental monitoring. Tartu, 1998, 117 p.
45. **Heli Talvik.** Prepatent periods and species composition of different *Oesophagostomum* spp. populations in Estonia and Denmark. Tartu, 1998, 104 p.
46. **Katrin Heinsoo.** Cuticular and stomatal antechamber conductance to water vapour diffusion in *Picea abies* (L.) karst. Tartu, 1999, 133 p.
47. **Tarmo Annilo.** Studies on mammalian ribosomal protein S7. Tartu, 1998, 77 p.
48. **Indrek Ots.** Health state indicies of reproducing great tits (*Parus major*): sources of variation and connections with life-history traits. Tartu, 1999, 117 p.
49. **Juan Jose Cantero.** Plant community diversity and habitat relationships in central Argentina grasslands. Tartu, 1999, 161 p.
50. **Rein Kalamees.** Seed bank, seed rain and community regeneration in Estonian calcareous grasslands. Tartu, 1999, 107 p.
51. **Sulev Kõks.** Cholecystokinin (CCK) — induced anxiety in rats: influence of environmental stimuli and involvement of endopioid mechanisms and serotonin. Tartu, 1999, 123 p.
52. **Ebe Sild.** Impact of increasing concentrations of O₃ and CO₂ on wheat, clover and pasture. Tartu, 1999, 123 p.
53. **Ljudmilla Timofejeva.** Electron microscopical analysis of the synaptosomal complex formation in cereals. Tartu, 1999, 99 p.
54. **Andres Valkna.** Interactions of galanin receptor with ligands and G-proteins: studies with synthetic peptides. Tartu, 1999, 103 p.
55. **Taavi Virro.** Life cycles of planktonic rotifers in lake Peipsi. Tartu, 1999, 101 p.
56. **Ana Rebane.** Mammalian ribosomal protein S3a genes and intron-encoded small nucleolar RNAs U73 and U82. Tartu, 1999, 85 p.
57. **Tiina Tamm.** Cocksfoot mottle virus: the genome organisation and translational strategies. Tartu, 2000, 101 p.
58. **Reet Kurg.** Structure-function relationship of the bovine papilloma virus E2 protein. Tartu, 2000, 89 p.
59. **Toomas Kivisild.** The origins of Southern and Western Eurasian populations: an mtDNA study. Tartu, 2000, 121 p.
60. **Niilo Kaldalu.** Studies of the TOL plasmid transcription factor XylS. Tartu 2000. 88 p.
61. **Dina Lepik.** Modulation of viral DNA replication by tumor suppressor protein p53. Tartu 2000. 106 p.

62. **Kai Vellak.** Influence of different factors on the diversity of the bryophyte vegetation in forest and wooded meadow communities. Tartu 2000. 122 p.
63. **Jonne Kotta.** Impact of eutrophication and biological invasions on the structure and functions of benthic macrofauna. Tartu 2000. 160 p.
64. **Georg Martin.** Phytobenthic communities of the Gulf of Riga and the inner sea the West-Estonian archipelago. Tartu, 2000. 139 p.
65. **Silvia Sepp.** Morphological and genetical variation of *Alchemilla L.* in Estonia. Tartu, 2000. 124 p.
66. **Jaan Liira.** On the determinants of structure and diversity in herbaceous plant communities. Tartu, 2000. 96 p.
67. **Priit Zingel.** The role of planktonic ciliates in lake ecosystems. Tartu 2001. 111 p.
68. **Tiit Teder.** Direct and indirect effects in Host-parasitoid interactions: ecological and evolutionary consequences. Tartu 2001. 122 p.
69. **Hannes Kollist.** Leaf apoplastic ascorbate as ozone scavenger and its transport across the plasma membrane. Tartu 2001. 80 p.
70. **Reet Marits.** Role of two-component regulator system PehR-PehS and extracellular protease PrtW in virulence of *Erwinia Carotovora* subsp. *Carotovora*. Tartu 2001. 112 p.
71. **Vallo Tilgar.** Effect of calcium supplementation on reproductive performance of the pied flycatcher *Ficedula hypoleuca* and the great tit *Parus major*, breeding in Northern temperate forests. Tartu, 2002. 126 p.
72. **Rita Hõrak.** Regulation of transposition of transposon Tn4652 in *Pseudomonas putida*. Tartu, 2002. 108 p.
73. **Liina Eek-Piirsoo.** The effect of fertilization, mowing and additional illumination on the structure of a species-rich grassland community. Tartu, 2002. 74 p.
74. **Krõõt Aasamaa.** Shoot hydraulic conductance and stomatal conductance of six temperate deciduous tree species. Tartu, 2002. 110 p.
75. **Nele Ingerpuu.** Bryophyte diversity and vascular plants. Tartu, 2002. 112 p.
76. **Neeme Tõnisson.** Mutation detection by primer extension on oligonucleotide microarrays. Tartu, 2002. 124 p.
77. **Margus Pensa.** Variation in needle retention of Scots pine in relation to leaf morphology, nitrogen conservation and tree age. Tartu, 2003. 110 p.
78. **Asko Lõhmus.** Habitat preferences and quality for birds of prey: from principles to applications. Tartu, 2003. 168 p.
79. **Viljar Jaks.** p53 — a switch in cellular circuit. Tartu, 2003. 160 p.
80. **Jaana Männik.** Characterization and genetic studies of four ATP-binding cassette (ABC) transporters. Tartu, 2003. 140 p.
81. **Marek Sammul.** Competition and coexistence of clonal plants in relation to productivity. Tartu, 2003. 159 p.
82. **Ivar Iives.** Virus-cell interactions in the replication cycle of bovine papillomavirus type 1. Tartu, 2003. 89 p.

83. **Andres Männik.** Design and characterization of a novel vector system based on the stable replicator of bovine papillomavirus type 1. Tartu, 2003. 109 p.
84. **Ivika Ostonen.** Fine root structure, dynamics and proportion in net primary production of Norway spruce forest ecosystem in relation to site conditions. Tartu, 2003. 158 p.
85. **Gudrun Veldre.** Somatic status of 12–15-year-old Tartu schoolchildren. Tartu, 2003. 199 p.
86. **Ülo Väli.** The greater spotted eagle *Aquila clanga* and the lesser spotted eagle *A. pomarina*: taxonomy, phylogeography and ecology. Tartu, 2004. 159 p.
87. **Aare Abroi.** The determinants for the native activities of the bovine papillomavirus type 1 E2 protein are separable. Tartu, 2004. 135 p.
88. **Tiina Kahre.** Cystic fibrosis in Estonia. Tartu, 2004. 116 p.
89. **Helen Orav-Kotta.** Habitat choice and feeding activity of benthic suspension feeders and mesograzers in the northern Baltic Sea. Tartu, 2004. 117 p.
90. **Maarja Öpik.** Diversity of arbuscular mycorrhizal fungi in the roots of perennial plants and their effect on plant performance. Tartu, 2004. 175 p.
91. **Kadri Tali.** Species structure of *Neotinea ustulata*. Tartu, 2004. 109 p.
92. **Kristiina Tambets.** Towards the understanding of post-glacial spread of human mitochondrial DNA haplogroups in Europe and beyond: a phylogeographic approach. Tartu, 2004. 163 p.
93. **Arvi Jõers.** Regulation of p53-dependent transcription. Tartu, 2004. 103 p.
94. **Lilian Kadaja.** Studies on modulation of the activity of tumor suppressor protein p53. Tartu, 2004. 103 p.
95. **Jaak Truu.** Oil shale industry wastewater: impact on river microbial community and possibilities for bioremediation. Tartu, 2004. 128 p.
96. **Maire Peters.** Natural horizontal transfer of the *pheBA* operon. Tartu, 2004. 105 p.
97. **Ülo Maiväli.** Studies on the structure-function relationship of the bacterial ribosome. Tartu, 2004. 130 p.
98. **Merit Otsus.** Plant community regeneration and species diversity in dry calcareous grasslands. Tartu, 2004. 103 p.
99. **Mikk Heidemaa.** Systematic studies on sawflies of the genera *Dolerus*, *Empria*, and *Caliroa* (Hymenoptera: Tenthredinidae). Tartu, 2004. 167 p.
100. **Ilmar Tõnno.** The impact of nitrogen and phosphorus concentration and N/P ratio on cyanobacterial dominance and N₂ fixation in some Estonian lakes. Tartu, 2004. 111 p.
101. **Lauri Saks.** Immune function, parasites, and carotenoid-based ornaments in greenfinches. Tartu, 2004. 144 p.
102. **Siiri Rootsi.** Human Y-chromosomal variation in European populations. Tartu, 2004. 142 p.

103. **Eve Vedler.** Structure of the 2,4-dichloro-phenoxyacetic acid-degradative plasmid pEST4011. Tartu, 2005. 106 p.
104. **Andres Tover.** Regulation of transcription of the phenol degradation *pheBA* operon in *Pseudomonas putida*. Tartu, 2005. 126 p.
105. **Helen Udras.** Hexose kinases and glucose transport in the yeast *Hansenula polymorpha*. Tartu, 2005. 100 p.
106. **Ave Suija.** Lichens and lichenicolous fungi in Estonia: diversity, distribution patterns, taxonomy. Tartu, 2005. 162 p.
107. **Piret Lõhmus.** Forest lichens and their substrata in Estonia. Tartu, 2005. 162 p.
108. **Inga Lips.** Abiotic factors controlling the cyanobacterial bloom occurrence in the Gulf of Finland. Tartu, 2005. 156 p.
109. **Kaasik, Krista.** Circadian clock genes in mammalian clockwork, metabolism and behaviour. Tartu, 2005. 121 p.
110. **Juhan Javoiš.** The effects of experience on host acceptance in ovipositing moths. Tartu, 2005. 112 p.
111. **Tiina Sedman.** Characterization of the yeast *Saccharomyces cerevisiae* mitochondrial DNA helicase Hmi1. Tartu, 2005. 103 p.
112. **Ruth Aguraiuja.** Hawaiian endemic fern lineage *Diellia* (Aspleniaceae): distribution, population structure and ecology. Tartu, 2005. 112 p.
113. **Riho Teras.** Regulation of transcription from the fusion promoters generated by transposition of Tn4652 into the upstream region of *pheBA* operon in *Pseudomonas putida*. Tartu, 2005. 106 p.
114. **Mait Metspalu.** Through the course of prehistory in india: tracing the mtDNA trail. Tartu, 2005. 138 p.
115. **Elin Lõhmussaar.** The comparative patterns of linkage disequilibrium in European populations and its implication for genetic association studies. Tartu, 2006. 124 p.
116. **Priit Kupper.** Hydraulic and environmental limitations to leaf water relations in trees with respect to canopy position. Tartu, 2006. 126 p.
117. **Heili Ilves.** Stress-induced transposition of Tn4652 in *Pseudomonas Putida*. Tartu, 2006. 120 p.
118. **Silja Kuusk.** Biochemical properties of Hmi1p, a DNA helicase from *Saccharomyces cerevisiae* mitochondria. Tartu, 2006. 126 p.
119. **Kersti Püssa.** Forest edges on medium resolution landsat thematic mapper satellite images. Tartu, 2006. 90 p.
120. **Lea Tummeleht.** Physiological condition and immune function in great tits (*Parus major* L.): Sources of variation and trade-offs in relation to growth. Tartu, 2006. 94 p.
121. **Toomas Esperk.** Larval instar as a key element of insect growth schedules. Tartu, 2006. 186 p.
122. **Harri Valdmann.** Lynx (*Lynx lynx*) and wolf (*Canis lupus*) in the Baltic region: Diets, helminth parasites and genetic variation. Tartu, 2006. 102 p.

123. **Priit Jõers.** Studies of the mitochondrial helicase Hmi1p in *Candida albicans* and *Saccharomyces cerevisia*. Tartu, 2006. 113 p.
124. **Kersti Lilleväli.** Gata3 and Gata2 in inner ear development. Tartu, 2007. 123 p.
125. **Kai Rünk.** Comparative ecology of three fern species: *Dryopteris carthusiana* (Vill.) H.P. Fuchs, *D. expansa* (C. Presl) Fraser-Jenkins & Jermy and *D. dilatata* (Hoffm.) A. Gray (Dryopteridaceae). Tartu, 2007. 143 p.
126. **Aveliina Helm.** Formation and persistence of dry grassland diversity: role of human history and landscape structure. Tartu, 2007. 89 p.
127. **Leho Tedersoo.** Ectomycorrhizal fungi: diversity and community structure in Estonia, Seychelles and Australia. Tartu, 2007. 233 p.
128. **Marko Mägi.** The habitat-related variation of reproductive performance of great tits in a deciduous-coniferous forest mosaic: looking for causes and consequences. Tartu, 2007. 135 p.
129. **Valeria Lulla.** Replication strategies and applications of Semliki Forest virus. Tartu, 2007. 109 p.
130. **Ülle Reier.** Estonian threatened vascular plant species: causes of rarity and conservation. Tartu, 2007. 79 p.
131. **Inga Jüriado.** Diversity of lichen species in Estonia: influence of regional and local factors. Tartu, 2007. 171 p.
132. **Tatjana Krama.** Mobbing behaviour in birds: costs and reciprocity based cooperation. Tartu, 2007. 112 p.
133. **Signe Saumaa.** The role of DNA mismatch repair and oxidative DNA damage defense systems in avoidance of stationary phase mutations in *Pseudomonas putida*. Tartu, 2007. 172 p.
134. **Reedik Mägi.** The linkage disequilibrium and the selection of genetic markers for association studies in european populations. Tartu, 2007. 96 p.
135. **Priit Kilgas.** Blood parameters as indicators of physiological condition and skeletal development in great tits (*Parus major*): natural variation and application in the reproductive ecology of birds. Tartu, 2007. 129 p.
136. **Anu Albert.** The role of water salinity in structuring eastern Baltic coastal fish communities. Tartu, 2007. 95 p.
137. **Kärt Padari.** Protein transduction mechanisms of transportans. Tartu, 2008. 128 p.
138. **Siiri-Lii Sandre.** Selective forces on larval colouration in a moth. Tartu, 2008. 125 p.
139. **Ülle Jõgar.** Conservation and restoration of semi-natural floodplain meadows and their rare plant species. Tartu, 2008. 99 p.
140. **Lauri Laanisto.** Macroecological approach in vegetation science: generality of ecological relationships at the global scale. Tartu, 2008. 133 p.
141. **Reidar Andreson.** Methods and software for predicting PCR failure rate in large genomes. Tartu, 2008. 105 p.
142. **Birgot Paavel.** Bio-optical properties of turbid lakes. Tartu, 2008. 175 p.
143. **Kaire Torn.** Distribution and ecology of charophytes in the Baltic Sea. Tartu, 2008, 98 p.

144. **Vladimir Vimberg.** Peptide mediated macrolide resistance. Tartu, 2008, 190 p.
145. **Daima Örd.** Studies on the stress-inducible pseudokinase TRB3, a novel inhibitor of transcription factor ATF4. Tartu, 2008, 108 p.
146. **Lauri Saag.** Taxonomic and ecologic problems in the genus *Lepraria* (*Stereocaulaceae*, lichenised *Ascomycota*). Tartu, 2008, 175 p.
147. **Ulvi Karu.** Antioxidant protection, carotenoids and coccidians in green-finches – assessment of the costs of immune activation and mechanisms of parasite resistance in a passerine with carotenoid-based ornaments. Tartu, 2008, 124 p.
148. **Jaanus Remm.** Tree-cavities in forests: density, characteristics and occupancy by animals. Tartu, 2008, 128 p.
149. **Epp Moks.** Tapeworm parasites *Echinococcus multilocularis* and *E. granulosus* in Estonia: phylogenetic relationships and occurrence in wild carnivores and ungulates. Tartu, 2008, 82 p.
150. **Eve Eensalu.** Acclimation of stomatal structure and function in tree canopy: effect of light and CO₂ concentration. Tartu, 2008, 108 p.
151. **Janne Pullat.** Design, functionlization and application of an *in situ* synthesized oligonucleotide microarray. Tartu, 2008, 108 p.
152. **Marta Putrinš.** Responses of *Pseudomonas putida* to phenol-induced metabolic and stress signals. Tartu, 2008, 142 p.
153. **Marina Semtšenko.** Plant root behaviour: responses to neighbours and physical obstructions. Tartu, 2008, 106 p.
154. **Marge Starast.** Influence of cultivation techniques on productivity and fruit quality of some *Vaccinium* and *Rubus* taxa. Tartu, 2008, 154 p.
155. **Age Tats.** Sequence motifs influencing the efficiency of translation. Tartu, 2009, 104 p.
156. **Radi Tegova.** The role of specialized DNA polymerases in mutagenesis in *Pseudomonas putida*. Tartu, 2009, 124 p.
157. **Tsipe Aavik.** Plant species richness, composition and functional trait pattern in agricultural landscapes – the role of land use intensity and landscape structure. Tartu, 2009, 112 p.
158. **Kaja Kiiver.** Semliki forest virus based vectors and cell lines for studying the replication and interactions of alphaviruses and hepaciviruses. Tartu, 2009, 104 p.
159. **Meelis Kadaja.** Papillomavirus Replication Machinery Induces Genomic Instability in its Host Cell. Tartu, 2009, 126 p.
160. **Pille Hallast.** Human and chimpanzee Luteinizing hormone/Chorionic Gonadotropin beta (*LHB/CGB*) gene clusters: diversity and divergence of young duplicated genes. Tartu, 2009, 168 p.
161. **Ain Vellak.** Spatial and temporal aspects of plant species conservation. Tartu, 2009, 86 p.
162. **Triinu Remmel.** Body size evolution in insects with different colouration strategies: the role of predation risk. Tartu, 2009, 168 p.

163. **Jaana Salujõe.** Zooplankton as the indicator of ecological quality and fish predation in lake ecosystems. Tartu, 2009, 129 p.
164. **Ele Vahtmäe.** Mapping benthic habitat with remote sensing in optically complex coastal environments. Tartu, 2009, 109 p.
165. **Liisa Metsamaa.** Model-based assessment to improve the use of remote sensing in recognition and quantitative mapping of cyanobacteria. Tartu, 2009, 114 p.
166. **Pille Säälük.** The role of endocytosis in the protein transduction by cell-penetrating peptides. Tartu, 2009, 155 p.
167. **Lauri Peil.** Ribosome assembly factors in *Escherichia coli*. Tartu, 2009, 147 p.
168. **Lea Hallik.** Generality and specificity in light harvesting, carbon gain capacity and shade tolerance among plant functional groups. Tartu, 2009, 99 p.
169. **Mariliis Tark.** Mutagenic potential of DNA damage repair and tolerance mechanisms under starvation stress. Tartu, 2009, 191 p.
170. **Riinu Rannap.** Impacts of habitat loss and restoration on amphibian populations. Tartu, 2009, 117 p.
171. **Maarja Adojaan.** Molecular variation of HIV-1 and the use of this knowledge in vaccine development. Tartu, 2009, 95 p.
172. **Signe Altmäe.** Genomics and transcriptomics of human induced ovarian folliculogenesis. Tartu, 2010, 179 p.
173. **Triin Suvi.** Mycorrhizal fungi of native and introduced trees in the Seychelles Islands. Tartu, 2010, 107 p.
174. **Velda Lauringson.** Role of suspension feeding in a brackish-water coastal sea. Tartu, 2010, 123 p.
175. **Eero Talts.** Photosynthetic cyclic electron transport – measurement and variably proton-coupled mechanism. Tartu, 2010, 121 p.
176. **Mari Nelis.** Genetic structure of the Estonian population and genetic distance from other populations of European descent. Tartu, 2010, 97 p.
177. **Kaarel Krjutškov.** Arrayed Primer Extension-2 as a multiplex PCR-based method for nucleic acid variation analysis: method and applications. Tartu, 2010, 129 p.
178. **Egle Köster.** Morphological and genetical variation within species complexes: *Anthyllis vulneraria* s. l. and *Alchemilla vulgaris* (coll.). Tartu, 2010, 101 p.
179. **Erki Õunap.** Systematic studies on the subfamily Sterrhinae (Lepidoptera: Geometridae). Tartu, 2010, 111 p.
180. **Merike Jõesaar.** Diversity of key catabolic genes at degradation of phenol and *p*-cresol in pseudomonads. Tartu, 2010, 125 p.
181. **Kristjan Herkül.** Effects of physical disturbance and habitat-modifying species on sediment properties and benthic communities in the northern Baltic Sea. Tartu, 2010, 123 p.
182. **Arto Pulk.** Studies on bacterial ribosomes by chemical modification approaches. Tartu, 2010, 161 p.

183. **Maria Põllupüü.** Ecological relations of cladocerans in a brackish-water ecosystem. Tartu, 2010, 126 p.
184. **Toomas Silla.** Study of the segregation mechanism of the Bovine Papillomavirus Type 1. Tartu, 2010, 188 p.
185. **Gyaneshwer Chaubey.** The demographic history of India: A perspective based on genetic evidence. Tartu, 2010, 184 p.
186. **Katrin Kepp.** Genes involved in cardiovascular traits: detection of genetic variation in Estonian and Czech populations. Tartu, 2010, 164 p.
187. **Virve Sõber.** The role of biotic interactions in plant reproductive performance. Tartu, 2010, 92 p.
188. **Kersti Kangro.** The response of phytoplankton community to the changes in nutrient loading. Tartu, 2010, 144 p.
189. **Joachim M. Gerhold.** Replication and Recombination of mitochondrial DNA in Yeast. Tartu, 2010, 120 p.
190. **Helen Tammert.** Ecological role of physiological and phylogenetic diversity in aquatic bacterial communities. Tartu, 2010, 140 p.
191. **Elle Rajandu.** Factors determining plant and lichen species diversity and composition in Estonian *Calamagrostis* and *Hepatica* site type forests. Tartu, 2010, 123 p.
192. **Paula Ann Kivistik.** ColR-ColS signalling system and transposition of Tn4652 in the adaptation of *Pseudomonas putida*. Tartu, 2010, 118 p.
193. **Siim Sõber.** Blood pressure genetics: from candidate genes to genome-wide association studies. Tartu, 2011, 120 p.
194. **Kalle Kipper.** Studies on the role of helix 69 of 23S rRNA in the factor-dependent stages of translation initiation, elongation, and termination. Tartu, 2011, 178 p.
195. **Triinu Siibak.** Effect of antibiotics on ribosome assembly is indirect. Tartu, 2011, 134 p.
196. **Tambet Tõnissoo.** Identification and molecular analysis of the role of guanine nucleotide exchange factor RIC-8 in mouse development and neural function. Tartu, 2011, 110 p.
197. **Helin Räägel.** Multiple faces of cell-penetrating peptides – their intracellular trafficking, stability and endosomal escape during protein transduction. Tartu, 2011, 161 p.
198. **Andres Jaanus.** Phytoplankton in Estonian coastal waters – variability, trends and response to environmental pressures. Tartu, 2011, 157 p.
199. **Tiit Nikopensius.** Genetic predisposition to nonsyndromic orofacial clefts. Tartu, 2011, 152 p.
200. **Signe Värvi.** Studies on the mechanisms of RNA polymerase II-dependent transcription elongation. Tartu, 2011, 108 p.
201. **Kristjan Välk.** Gene expression profiling and genome-wide association studies of non-small cell lung cancer. Tartu, 2011, 98 p.
202. **Arno Põllumäe.** Spatio-temporal patterns of native and invasive zooplankton species under changing climate and eutrophication conditions. Tartu, 2011, 153 p.

203. **Egle Tammeleht.** Brown bear (*Ursus arctos*) population structure, demographic processes and variations in diet in northern Eurasia. Tartu, 2011, 143 p.
205. **Teele Jairus.** Species composition and host preference among ectomycorrhizal fungi in Australian and African ecosystems. Tartu, 2011, 106 p.
206. **Kessy Abarenkov.** PlutoF – cloud database and computing services supporting biological research. Tartu, 2011, 125 p.
207. **Marina Grigorova.** Fine-scale genetic variation of follicle-stimulating hormone beta-subunit coding gene (*FSHB*) and its association with reproductive health. Tartu, 2011, 184 p.
208. **Anu Tiitsaar.** The effects of predation risk and habitat history on butterfly communities. Tartu, 2011, 97 p.
209. **Elin Sild.** Oxidative defences in immunoecological context: validation and application of assays for nitric oxide production and oxidative burst in a wild passerine. Tartu, 2011, 105 p.
210. **Irja Saar.** The taxonomy and phylogeny of the genera *Cystoderma* and *Cystodermella* (Agaricales, Fungi). Tartu, 2012, 167 p.
211. **Pauli Saag.** Natural variation in plumage bacterial assemblages in two wild breeding passerines. Tartu, 2012, 113 p.
212. **Aleksei Lulla.** Alphaviral nonstructural protease and its polyprotein substrate: arrangements for the perfect marriage. Tartu, 2012, 143 p.
213. **Mari Järve.** Different genetic perspectives on human history in Europe and the Caucasus: the stories told by uniparental and autosomal markers. Tartu, 2012, 119 p.
214. **Ott Scheler.** The application of tmRNA as a marker molecule in bacterial diagnostics using microarray and biosensor technology. Tartu, 2012, 93 p.
215. **Anna Balikova.** Studies on the functions of tumor-associated mucin-like leukosialin (CD43) in human cancer cells. Tartu, 2012, 129 p.
216. **Triinu Kõressaar.** Improvement of PCR primer design for detection of prokaryotic species. Tartu, 2012, 83 p.
217. **Tuul Sepp.** Hematological health state indices of greenfinches: sources of individual variation and responses to immune system manipulation. Tartu, 2012, 117 p.
218. **Rya Ero.** Modifier view of the bacterial ribosome. Tartu, 2012, 146 p.
219. **Mohammad Bahram.** Biogeography of ectomycorrhizal fungi across different spatial scales. Tartu, 2012, 165 p.
220. **Annely Lorents.** Overcoming the plasma membrane barrier: uptake of amphipathic cell-penetrating peptides induces influx of calcium ions and downstream responses. Tartu, 2012, 113 p.
221. **Katrin Männik.** Exploring the genomics of cognitive impairment: whole-genome SNP genotyping experience in Estonian patients and general population. Tartu, 2012, 171 p.
222. **Marko Prous.** Taxonomy and phylogeny of the sawfly genus *Empria* (Hymenoptera, Tenthredinidae). Tartu, 2012, 192 p.

223. **Triinu Visnapuu.** Levansucrases encoded in the genome of *Pseudomonas syringae* pv. tomato DC3000: heterologous expression, biochemical characterization, mutational analysis and spectrum of polymerization products. Tartu, 2012, 160 p.
224. **Nele Tamberg.** Studies on Semliki Forest virus replication and pathogenesis. Tartu, 2012, 109 p.
225. **Tõnu Esko.** Novel applications of SNP array data in the analysis of the genetic structure of Europeans and in genetic association studies. Tartu, 2012, 149 p.
226. **Timo Arula.** Ecology of early life-history stages of herring *Clupea harengus membras* in the northeastern Baltic Sea. Tartu, 2012, 143 p.
227. **Inga Hiiesalu.** Belowground plant diversity and coexistence patterns in grassland ecosystems. Tartu, 2012, 130 p.
228. **Kadri Koorem.** The influence of abiotic and biotic factors on small-scale plant community patterns and regeneration in boreonemoral forest. Tartu, 2012, 114 p.
229. **Liis Andresen.** Regulation of virulence in plant-pathogenic pectobacteria. Tartu, 2012, 122 p.
230. **Kaupo Kohv.** The direct and indirect effects of management on boreal forest structure and field layer vegetation. Tartu, 2012, 124 p.
231. **Mart Jüssi.** Living on an edge: landlocked seals in changing climate. Tartu, 2012, 114 p.
232. **Riina Klais.** Phytoplankton trends in the Baltic Sea. Tartu, 2012, 136 p.
233. **Rauno Veeroja.** Effects of winter weather, population density and timing of reproduction on life-history traits and population dynamics of moose (*Alces alces*) in Estonia. Tartu, 2012, 92 p.
234. **Marju Keis.** Brown bear (*Ursus arctos*) phylogeography in northern Eurasia. Tartu, 2013, 142 p.
235. **Sergei Pölme.** Biogeography and ecology of *alnus*- associated ectomycorrhizal fungi – from regional to global scale. Tartu, 2013, 90 p.
236. **Liis Uusküla.** Placental gene expression in normal and complicated pregnancy. Tartu, 2013, 173 p.
237. **Marko Lõoke.** Studies on DNA replication initiation in *Saccharomyces cerevisiae*. Tartu, 2013, 112 p.
238. **Anne Aan.** Light- and nitrogen-use and biomass allocation along productivity gradients in multilayer plant communities. Tartu, 2013, 127 p.
239. **Heidi Tamm.** Comprehending phylogenetic diversity – case studies in three groups of ascomycetes. Tartu, 2013, 136 p.
240. **Liina Kangur.** High-Pressure Spectroscopy Study of Chromophore-Binding Hydrogen Bonds in Light-Harvesting Complexes of Photosynthetic Bacteria. Tartu, 2013, 150 p.
241. **Margus Leppik.** Substrate specificity of the multisite specific pseudouridine synthase RluD. Tartu, 2013, 111 p.
242. **Lauris Kaplinski.** The application of oligonucleotide hybridization model for PCR and microarray optimization. Tartu, 2013, 103 p.

243. **Merli Pärnoja**. Patterns of macrophyte distribution and productivity in coastal ecosystems: effect of abiotic and biotic forcing. Tartu, 2013, 155 p.
244. **Tõnu Margus**. Distribution and phylogeny of the bacterial translational GTPases and the Mqsr/YgiT regulatory system. Tartu, 2013, 126 p.
245. **Pille Mänd**. Light use capacity and carbon and nitrogen budget of plants: remote assessment and physiological determinants. Tartu, 2013, 128 p.
246. **Mario Plaas**. Animal model of Wolfram Syndrome in mice: behavioural, biochemical and psychopharmacological characterization. Tartu, 2013, 144 p.
247. **Georgi Hudjašov**. Maps of mitochondrial DNA, Y-chromosome and tyrosinase variation in Eurasian and Oceanian populations. Tartu, 2013, 115 p.
248. **Mari Lepik**. Plasticity to light in herbaceous plants and its importance for community structure and diversity. Tartu, 2013, 102 p.
249. **Ede Leppik**. Diversity of lichens in semi-natural habitats of Estonia. Tartu, 2013, 151 p.
250. **Ülle Saks**. Arbuscular mycorrhizal fungal diversity patterns in boreo-nemoral forest ecosystems. Tartu, 2013, 151 p.
251. **Eneli Oitmaa**. Development of arrayed primer extension microarray assays for molecular diagnostic applications. Tartu, 2013, 147 p.
252. **Jekaterina Jutkina**. The horizontal gene pool for aromatics degradation: bacterial catabolic plasmids of the Baltic Sea aquatic system. Tartu, 2013, 121 p.
253. **Helen Vellau**. Reaction norms for size and age at maturity in insects: rules and exceptions. Tartu, 2014, 132 p.
254. **Randel Kreitsberg**. Using biomarkers in assessment of environmental contamination in fish – new perspectives. Tartu, 2014, 107 p.
255. **Krista Takkis**. Changes in plant species richness and population performance in response to habitat loss and fragmentation. Tartu, 2014, 141 p.
256. **Liina Nagirnaja**. Global and fine-scale genetic determinants of recurrent pregnancy loss. Tartu, 2014, 211 p.
257. **Triin Triisberg**. Factors influencing the re-vegetation of abandoned extracted peatlands in Estonia. Tartu, 2014, 133 p.
258. **Villu Soon**. A phylogenetic revision of the *Chrysis ignita* species group (Hymenoptera: Chrysididae) with emphasis on the northern European fauna. Tartu, 2014, 211 p.
259. **Andrei Nikonov**. RNA-Dependent RNA Polymerase Activity as a Basis for the Detection of Positive-Strand RNA Viruses by Vertebrate Host Cells. Tartu, 2014, 207 p.
260. **Eele Õunapuu-Pikas**. Spatio-temporal variability of leaf hydraulic conductance in woody plants: ecophysiological consequences. Tartu, 2014, 135 p.
261. **Marju Männiste**. Physiological ecology of greenfinches: information content of feathers in relation to immune function and behavior. Tartu, 2014, 121 p.

262. **Katre Kets.** Effects of elevated concentrations of CO₂ and O₃ on leaf photosynthetic parameters in *Populus tremuloides*: diurnal, seasonal and interannual patterns. Tartu, 2014, 115 p.
263. **Küllil Lokko.** Seasonal and spatial variability of zooplankton communities in relation to environmental parameters. Tartu, 2014, 129 p.
264. **Olga Žilina.** Chromosomal microarray analysis as diagnostic tool: Estonian experience. Tartu, 2014, 152 p.
265. **Kertu Lõhmus.** Colonisation ecology of forest-dwelling vascular plants and the conservation value of rural manor parks. Tartu, 2014, 111 p.
266. **Anu Aun.** Mitochondria as integral modulators of cellular signaling. Tartu, 2014, 167 p.
267. **Chandana Basu Mallick.** Genetics of adaptive traits and gender-specific demographic processes in South Asian populations. Tartu, 2014, 160 p.
268. **Riin Tamme.** The relationship between small-scale environmental heterogeneity and plant species diversity. Tartu, 2014, 130 p.
269. **Liina Remm.** Impacts of forest drainage on biodiversity and habitat quality: implications for sustainable management and conservation. Tartu, 2015, 126 p.
270. **Tiina Talve.** Genetic diversity and taxonomy within the genus *Rhinanthus*. Tartu, 2015, 106 p.
271. **Mehis Rohtla.** Otolith sclerochronological studies on migrations, spawning habitat preferences and age of freshwater fishes inhabiting the Baltic Sea. Tartu, 2015, 137 p.
272. **Alexey Reshchikov.** The world fauna of the genus *Lathrolestes* (Hymenoptera, Ichneumonidae). Tartu, 2015, 247 p.
273. **Martin Pook.** Studies on artificial and extracellular matrix protein-rich surfaces as regulators of cell growth and differentiation. Tartu, 2015, 142 p.
274. **Mai Kukumägi.** Factors affecting soil respiration and its components in silver birch and Norway spruce stands. Tartu, 2015, 155 p.
275. **Helen Karu.** Development of ecosystems under human activity in the North-East Estonian industrial region: forests on post-mining sites and bogs. Tartu, 2015, 152 p.
276. **Hedi Peterson.** Exploiting high-throughput data for establishing relationships between genes. Tartu, 2015, 186 p.
277. **Priit Adler.** Analysis and visualisation of large scale microarray data. Tartu, 2015, 126 p.
278. **Aigar Niglas.** Effects of environmental factors on gas exchange in deciduous trees: focus on photosynthetic water-use efficiency. Tartu, 2015, 152 p.
279. **Silja Laht.** Classification and identification of conopeptides using profile hidden Markov models and position-specific scoring matrices. Tartu, 2015, 100 p.
280. **Martin Kesler.** Biological characteristics and restoration of Atlantic salmon *Salmo salar* populations in the Rivers of Northern Estonia. Tartu, 2015, 97 p.

281. **Pratyush Kumar Das.** Biochemical perspective on alphaviral nonstructural protein 2: a tale from multiple domains to enzymatic profiling. Tartu, 2015, 205 p
282. **Priit Palta.** Computational methods for DNA copy number detection. Tartu, 2015, 130 p.
283. **Julia Sidorenko.** Combating DNA damage and maintenance of genome integrity in pseudomonads. Tartu, 2015, 174 p.
284. **Anastasiia Kovtun-Kante.** Charophytes of Estonian inland and coastal waters: distribution and environmental preferences. Tartu, 2015, 97 p.
285. **Ly Lindman.** The ecology of protected butterfly species in Estonia. Tartu, 2015, 171 p.
286. **Jaanis Lodjak.** Association of Insulin-like Growth Factor I and Corticosterone with Nestling Growth and Fledging Success in Wild Passerines. Tartu, 2016, 113 p.
287. **Ann Kraut.** Conservation of Wood-Inhabiting Biodiversity – Semi-Natural Forests as an Opportunity. Tartu, 2016, 141 p.
288. **Tiit Örd.** Functions and regulation of the mammalian pseudokinase TRIB3. Tartu, 2016, 182. p.
289. **Kairi Käiro.** Biological Quality According to Macroinvertebrates in Streams of Estonia (Baltic Ecoregion of Europe): Effects of Human-induced Hydromorphological Changes. Tartu, 2016, 126 p.
290. **Leidi Laurimaa.** *Echinococcus multilocularis* and other zoonotic parasites in Estonian canids. Tartu, 2016, 144 p.